Wind Turbine Tower Structure Analysis According to Wind Load in Terms of Cost

Selcuk SAHIN

Master Thesis

Presented in partial fulfillment of the requirements for the double degree:
"Advanced Master in Naval Architecture" conferred by University of Liege
"Master of Sciences in Applied Mechanics, specialization in Hydrodynamics, Energetics and Propulsion" conferred by Ecole Centrale de Nantes
Developed at West Pomeranian University of Technology, Szczecin, Poland and Pusan National University, Pusan, Korea in the framework of the

"EMSHIP"
Erasmus Mundus Master Course in
"Integrated Advanced Ship Design"

Ref. 159652-1-2009-1-BE-ERA MUNDUS-EMMC

Supervisor: Prof. Maciej Taczała, West Pomeranian University of Technology, Szczecin
Prof. Jeom Kee Paik, Pusan National University, Busan

Reviewer: Dr. Hervé LE SOURNE, L'Institut Catholique d'Arts et Métiers (ICAM), Nantes

Szczecin, February 2016

CONTENTS

LIST OF FIGURES

ABBREVIATIONS

AWEA	American Wind Energy Association
ASTM	American Society for Testing and Materials
DEL	Damage Equivalent Load
DIN	German Instute for Standardization
EC	Eurocode
EC3	Eurocode 3: Design of Steel Structures
EC3-1-1	Eurocode 3: Part 1-1: General Rules
EC3-1-4	Eurocode 3: Part 1-4: Supplementary Rules for Stainless Steel
EC3-1-5	Eurocode 3: Part 1-5: Plated Structural Elements
EC3-1-6	Eurocode 3: Part 1-6: Strength and Stability of Shell Structures
EC3-1-9	Eurocode 3: Part 1-9: Fatigue
EN	European Standards
EU	European Union
FEM	Finite Element Method
GWEC	Global Wind Energy Council
HAWT	Horizontal-Axis Wind Turbine
IEC	International Electrotechnical Commision
SRF	Stress Reserve Factor
UK	United Kingdom
VAWT	Vertical-Axis Wind Turbine

ACKNOWLEDGEMENTS

I want to thank all the people who shared their knowledge with me for the development of this work. First of all, I would like to express my cordial thankfulness to my advisors Prof. Maciej Taczała from West Pomeranian University, Prof. J.K. Paik from Pusan National University and Prof. Philippe Rigo from the University of Liege.

Also, I would like to thank the master thesis examination committee.

In additional, I would like to give special thanks to Dr. Young Il Park and Sang-Eui Lee who guided me in wind turbine industry with their knowledge and comments.

I would also like to thank my friends and classmates: S. Oy, J. D. Benther, A. Selamoglu for their supports and aids in order to finish my final thesis.

Finally, I would like to thank my family for their support throughout my life.

DECLARATION OF AUTHORSHIP

I declare that this thesis and the work presented in it are my own and have been generated by me as the result of my own original research.

Where I have consulted the published work of others, this is always clearly attributed.

Where I have quoted from the work of others, the source is always given. With the exception of such quotations, this thesis is entirely my own work.

I have acknowledged all main sources of help.

Where the thesis is based on work done by myself jointly with others, I have made clear exactly what was done by others and what I have contributed myself.

This thesis contains no material that has been submitted previously, in whole or in part, for the award of any other academic degree or diploma.

I cede copyright of the thesis in favor of the University of …..

Date: Signature

ABSTRACT

The development of wind energy is drastically increasing as a result of the energy need in the world. The main concerns about the design is to make a safe and economically feasible wind turbines. The design of the wind turbine tower must be strong and stiff enough to endure the varying wind and wave loads.

In this study, a site specific 3MW monopile type wind turbine tower was designed and analysed according to European Standards considering wind loads. The standard analysis procedure of the tower is respectively buckling, fatigue and dynamic analyses were done analytically and optimum door opening geometry was found and FEM analyses examined. Basic cost optimization of the tower was also done.

The objectives of this thesis help to producers (1) how to design wind turbine towers in structural aspect, (2) identify which kind of standards must be followed, (3) follow the standards and (4) show idealization and FEM analyses of door opening of wind tower.

The analytic results of the designed tower were found in interval that is wanted to reach. The importance of the tower door opening was observed. Considering to other door opening geometries, the geometry that was chosen for this thesis was one of the good result.

Keywords (Standards, Wind Turbine, Tower, Door Opening, Analyses)

1. INTRODUCTION

1.1. Why Wind Energy

In the world, a big percentage of our energy is provided from fossil fuels. These are basically coal, oil and gas. These sources are not sustainable, therefore at the end it will run out. Additionally, as a result of using these sources, the environment is damaged by humans. As a consequent of intensive use of the fossil fuels; global warming, extinction of species and human health problems are increasing.

Nowadays, fossil energy is continually replaced by renewable energy, therefore energy impact magnitude on the environment is lower compared to fossil fuels. Being responsible for nature, many countries have implemented their own renewable energy initiatives into their future energy plans. According to (GWEC 2012), in 2019 cumulative wind capacity will be more than 650 GW as it can be seen in Figure 1,

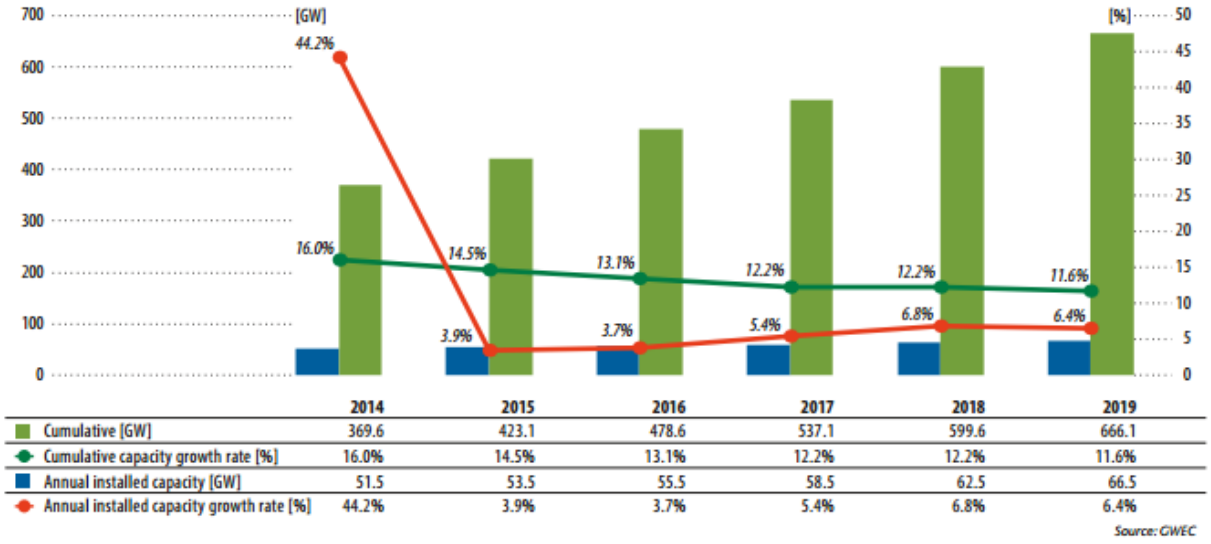

	2014	2015	2016	2017	2018	2019
Cumulative [GW]	369.6	423.1	478.6	537.1	599.6	666.1
Cumulative capacity growth rate [%]	16.0%	14.5%	13.1%	12.2%	12.2%	11.6%
Annual installed capacity [GW]	51.5	53.5	55.5	58.5	62.5	66.5
Annual installed capacity growth rate [%]	44.2%	3.9%	3.7%	5.4%	6.8%	6.4%

Source: GWEC

Figure 1: Market forecast for 2014-2019 (GWEC 2012)

Additionally cost/KW ratio for wind energy gets lower as it can be seen in Figure 2,

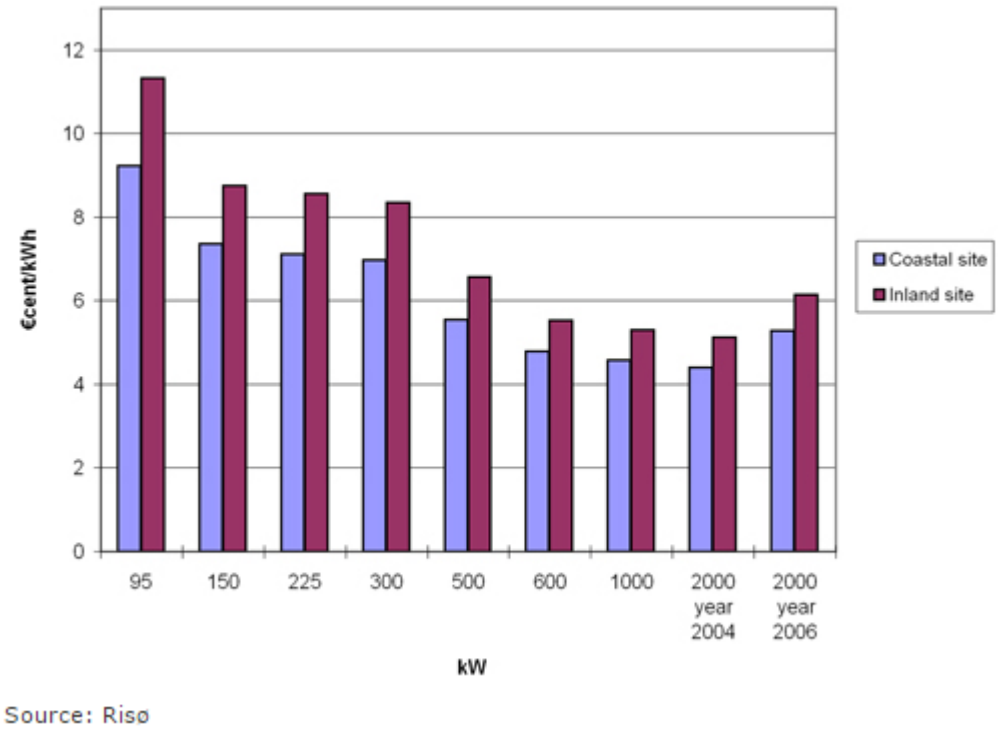

Figure 2: Total wind energy cost per unit of electricity produced ("Development of the Cost of Wind-Generated Power" n.d.)

1.2. Wind Market

Amazingly, wind energy increases its popularity day by day. Nowadays, wind turbine energy is the most developed and commercially viable energy source among the renewable energy resources. Wind power is produced from a useful form of the wind energy using wind turbines or wind mills.

The first windmill was used in Europe in the 12th century. However, the first attempts to produce energy from the wind started in 19th century in Denmark. In 1894, the first energy production from the wind has succeeded. On the other hand, during that period oil and gas sectors developed a lot and because of that, wind energy had to wait until 1973. Between 1973 and 1979 a world oil crises occurred. During that time, people turned their face to another energy sources. Firstly, small turbines were developed such as 20-30 kilowatt. From that time to now, turbines reach to 5-10 megawatt.

Figure 3: Gansu onshore wind farm in China ("New Wind and Solar Sectors Won't Solve China's Water Scarcity | Circle of Blue WaterNews" n.d.)

Because of the technological and material development, the diameter of turbines and length of the tower were increased in order to bring more wind speed. Big wind farms were established that included several wind turbines. Farm's features are flat large areas, mountain or hills top no turbulence. These farms are called onshore wind farm as can be seen in Figure 3. In addition to onshore, engineers developed offshore wind turbines, because finding a convenient place for onshore turbines is not that easy. In contrary, there is a very big opportunity on the sea, as shown in Figure 4. There are some advantages and disadvantages between these two kinds of the wind farm. Advantages of offshore are constant wind speed, more wind potential. Disadvantages of offshore are the foundation, cost, installation, transportation, and maintenance.

Figure 4: The Swedish offshore wind farm Lillgrund in the Øresund between Malmö and Copenhagen ("Wind Turbine Risks to Seabirds: New Tool Maps Birds' Sensitivity to Offshore Farms (Constantine Alexander's Blog)" n.d.)

Power production is one of the most important criteria for all kind of wind farm. Before installation; long-term wind speed measurement, estimation of yearly energy production, turbine selection and cost analyzes must be done. In order to estimate total energy production time/costs, one basic rule can be applied, from the experiences, generally production is 1/3 of the rated turbine out. As a basic example, a 100 MW rated output offshore wind farm (it means 20 number, 5 MW wind turbines) can produce 100*1/3*24*365 = 292000 MWh per year. Considering a house in Europe uses 4000 kWh per year, as a result, energy consumption of 75000 houses will be provided.

According to GWEC's 2014 report, total installed wind capacity is 369.597 MW from 1997 to 2014. Details can be seen in Figure 5,

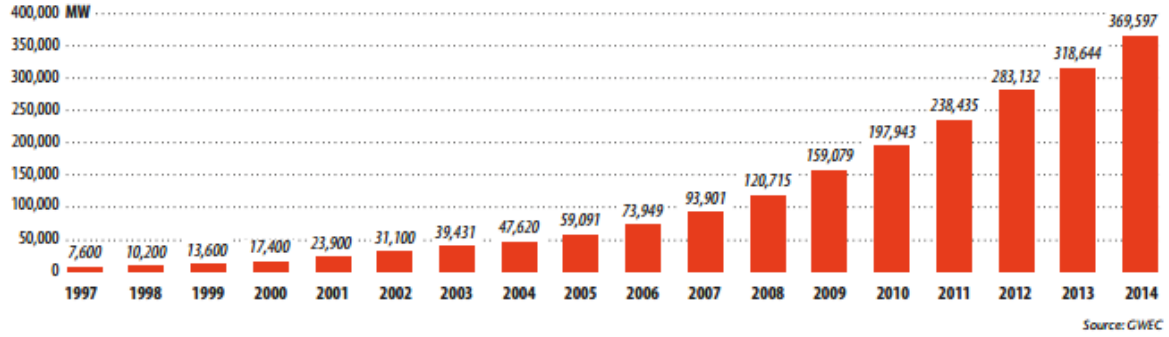

Figure 5: Global cumulative installed wind capacity 1997-2014 (GWEC 2012)

Also, the annual installed wind capacity can be seen in the same report, due to Figure 6, in 2014, turbine companies did record installation for wind energy.

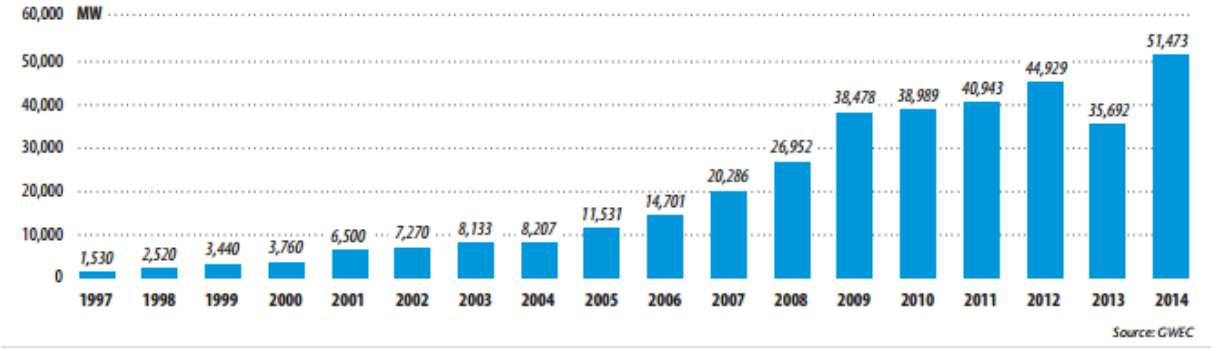

Figure 6: Global annual installed wind capacity 1997-2014 (GWEC 2012)

In order to see the future of the wind turbine sector, one can check the world recently investments country by country in 2014 GWEC data. As it can be seen in Figure 7, China made one of the biggest capacity investment in 2014. Furthermore, China has the biggest wind energy capacity in the world according to the GWEC data. On the other hand, the European zone made the second largest capacity investment in 2014. In particular, Germany is the main actor of the EU. Germany has a second biggest capacity increment in 2014. The USA is still one of the big players in the wind energy industry. After China, USA has the second biggest cumulative capacity in the world.

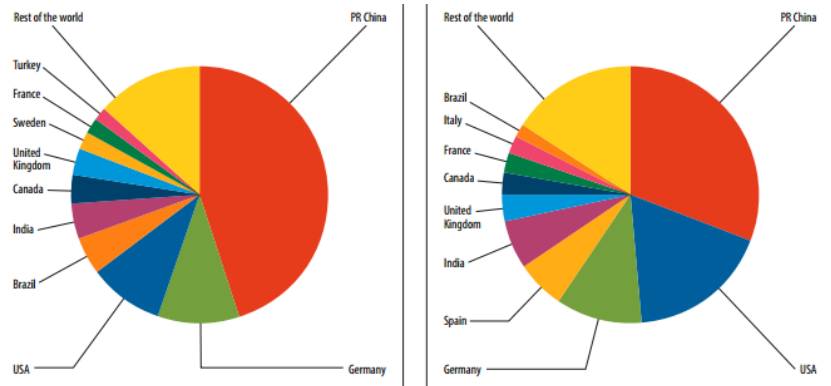

Country	MW	% SHARE
PR China	23,196	45.1
Germany	5,279	10.2
USA	4,854	9.4
Brazil*	2,472	4.8
India	2,315	4.5
Canada	1,871	3.6
United Kingdom	1,736	3.4
Sweden	1,050	2.0
France	1,042	2.0
Turkey	804	1.6
Rest of the world	6,852	13.3
Total TOP 10	**44,620**	**87**
World Total	**51,473**	**100**

** Projects fully commissioned, grid connection pending in some cases* *Source: GWEC*

Country	MW	% SHARE
PR China	114,609	31.0
USA	65,879	17.8
Germany	39,165	10.6
Spain	22,987	6.2
India	22,465	6.1
United Kingdom	12,440	3.4
Canada	9,694	2.6
France	9,285	2.5
Italy	8,663	2.3
Brazil*	5,939	1.6
Rest of the world	58,473	15.8
Total TOP 10	**311,124**	**84.2**
World Total	**369,597**	**100**

** Projects fully commissioned, grid connection pending in some cases* *Source: GWEC*

Figure 7: Top 10 new installed capacity Jan-Dec 2014(Left) & Top 10 cumulative capacity Dec 2014 (Right) (GWEC 2012)

During 2014, 12858 MW of wind power was installed across EU member states accounting for 11,829 MW of the total. For details, Figure 8 can be observed. In 2014, wind energy industry installed more capacity than gas and coal combination. The number of capacity that was added for coal and gas is 3.305 MW and 2.338 MW respectively. The summation of this two capacity almost half of wind energy capacity according to GWEC.

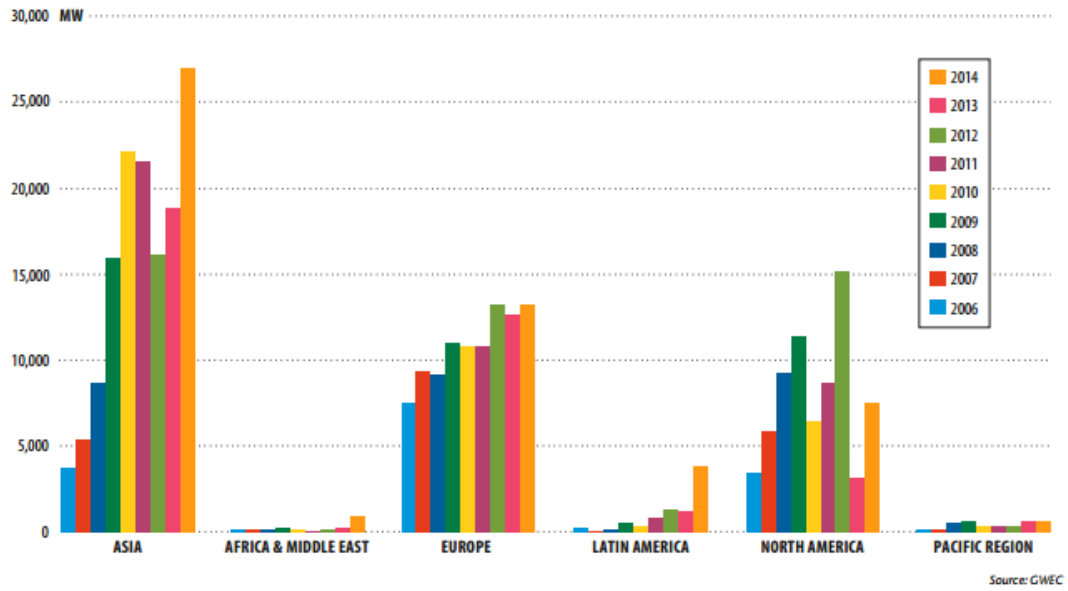

Figure 8: Annual installed capacity by region 2006-2014 (GWEC 2012)

Germany and the United Kingdom (UK) are the two biggest members of EU wind installation 2014. Germany made 5279 MW installation corresponding to UK's 1736 MW capacity installation. It means 59.5% of total EU wind installation. Nevertheless, UK is the largest offshore wind market in the world. Total offshore wind turbine installation is almost 4494 MW. This number equals to over half of the global offshore market. After, these two big players, France and Sweden installed new capacity of more than 2GW.

As it can be observed in Figure 1, all estimations that comes from GWEC shows that wind market will become bigger in the coming years. Furthermore, considering to new technologies and cost reduction in the production, people will benefit from the wind in a better as well as cheaper way. Also due to some politic crises, countries that don't have big fossil sources in their lands, have to diversify their energy sources. The wind is one of the biggest sources in this diversity. Because the wind does not depend on another country.

Moreover, the wind is renewable energy. It produces very low-levels of pollution compared to coal and gas. Especially in China, thermal power stations constitute big threats to human health with respect to air pollution. Also, nuclear energy stations carry a big risk to human life. As an example; in Fukushima, the nuclear matter/material leak has not yet been stopped.

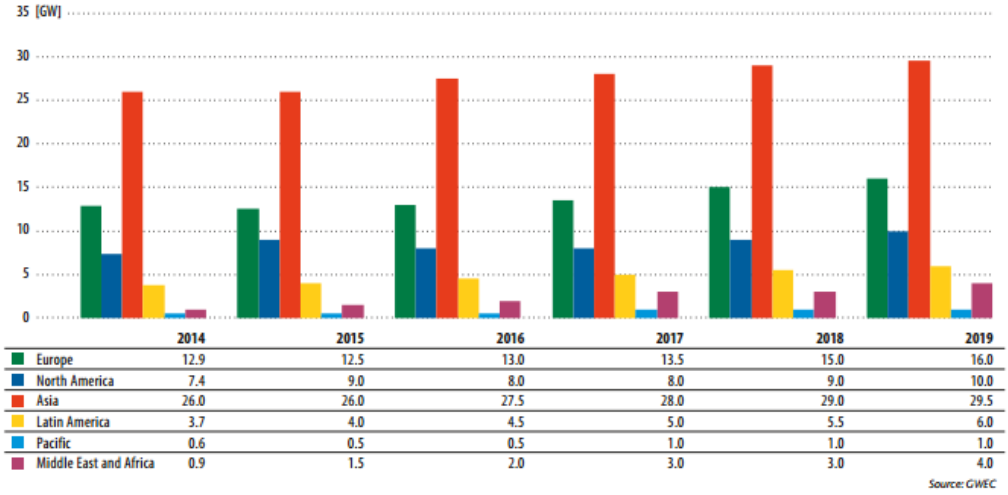

	2014	2015	2016	2017	2018	2019
Europe	12.9	12.5	13.0	13.5	15.0	16.0
North America	7.4	9.0	8.0	8.0	9.0	10.0
Asia	26.0	26.0	27.5	28.0	29.0	29.5
Latin America	3.7	4.0	4.5	5.0	5.5	6.0
Pacific	0.6	0.5	0.5	1.0	1.0	1.0
Middle East and Africa	0.9	1.5	2.0	3.0	3.0	4.0

Source: GWEC

Figure 9: Annual market forecast by region 2014-2019 (GWEC 2012)

Considering to reasons that were mentioned above, the wind energy sector has to grow. As it can be seen in Figure 9 and Figure 10, GWEC's market forecasts for each region, also supports that idea. According to a forecast from 2014 to 2019, Asia will reach 282 GW wind energy power. Europa will follow to Asia and Europa will have 202 GW settled wind energy in 2019.

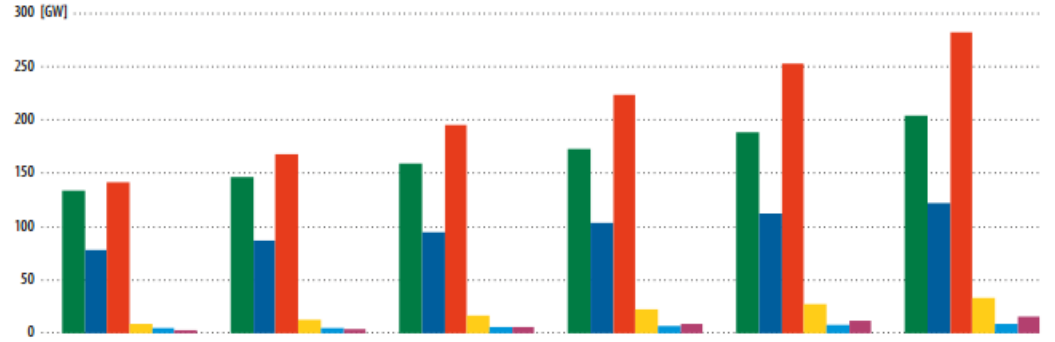

	2014	2015	2016	2017	2018	2019
Europe	134.0	146.5	159.5	173.0	188.0	204.0
North America	78.1	87.1	95.1	103.1	112.1	122.1
Asia	142.0	168.0	195.5	223.5	252.5	282.0
Latin America	8.5	12.5	17.0	22.0	27.5	33.5
Pacific	4.4	4.9	5.4	6.4	7.4	8.4
Middle East and Africa	2.5	4.0	6.0	9.0	12.0	16.0

Source: GWEC

Figure 10: Cumulative market forecast by region 2014-2019 (GWEC 2012)

As observed in Table 1, in the next 5 years, all around the world wind energy markets will reach big numbers. Although the economic crises in EU, the market will become 56.34% bigger than now. On the other hand, Asian wind will dominate the market. They will become almost two times larger than now.

Table 1: Cumulative market forecast for increment of wind energy capacity

	2014-2015	2015-2016	2016-2017	2017-2018	2018-2019	2014-2019
Europe	9.33%	8.87%	8.46%	8.67%	8.51%	52.24%
North America	11.52%	9.64%	7.96%	8.73%	8.92%	56.34%
Asia	18.31%	16.37%	14.32%	12.98%	11.68%	98.59%
Latin America	47.06%	36.00%	29.41%	25.00%	21.82%	294.12%
Pacific	11.36%	10.20%	18.52%	15.63%	13.51%	90.91%
Middle East and Africa	60.00%	50.00%	50.00%	33.33%	33.33%	540.00%

Not only the market but also technology on the turbine has increased. Figure 11 shows alteration of hub-height, generating capacity and rotor length of wind turbines year by year.

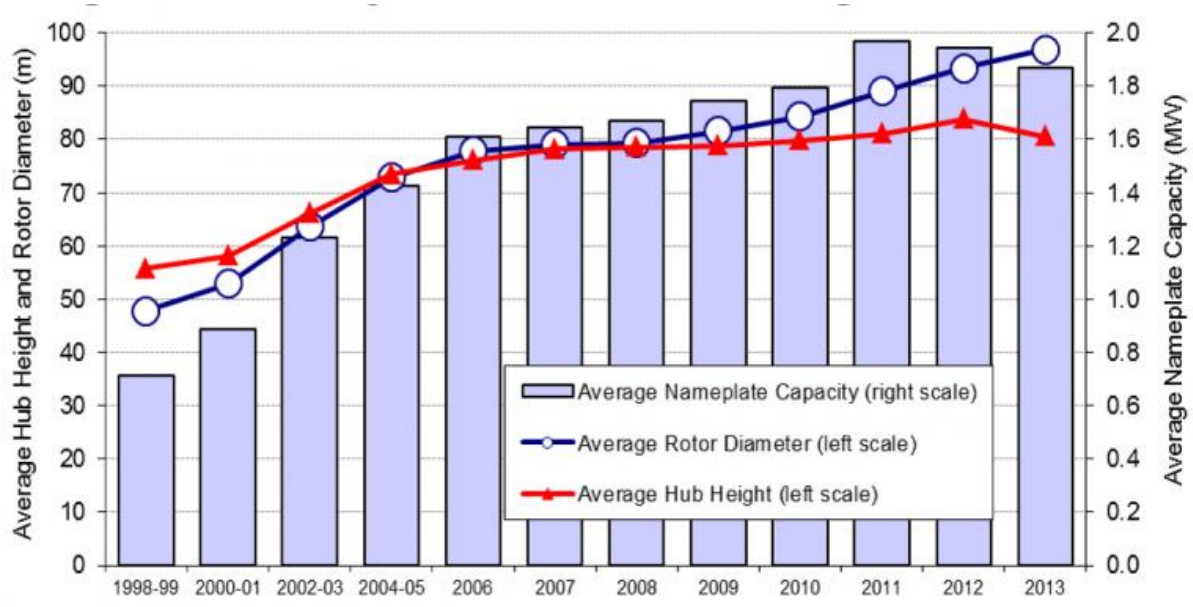

Figure 11: Average hub-height, generating capacity and rotor length of wind turbines, by installation year (US DOE 2014)

The figure above shows that technological and market behavior of wind energy grows in parallel. So, innovation of wind turbine must continue in order to increase markets all over the world. As a result of this innovation, turbines that can work in different conditions can be produced.

1.3. Anatomy of Wind Turbines

Generally, wind turbines can be divided into two parts. These are horizontal-axis wind turbines and vertical axis wind turbines. HAWT have the main rotor shaft at the top of a tower and it turns parallel to wind. In contrary shaft of the VAWT turns vertically. In order to see difference between two types of turbine, Figure 12 might give an idea.
Considering to big percentage of the market, in this thesis, horizontal-axis turbines will be studied.

Figure 12: HAWT and VAWT (“Wind Basics - Hill Country Wind Power” n.d.)

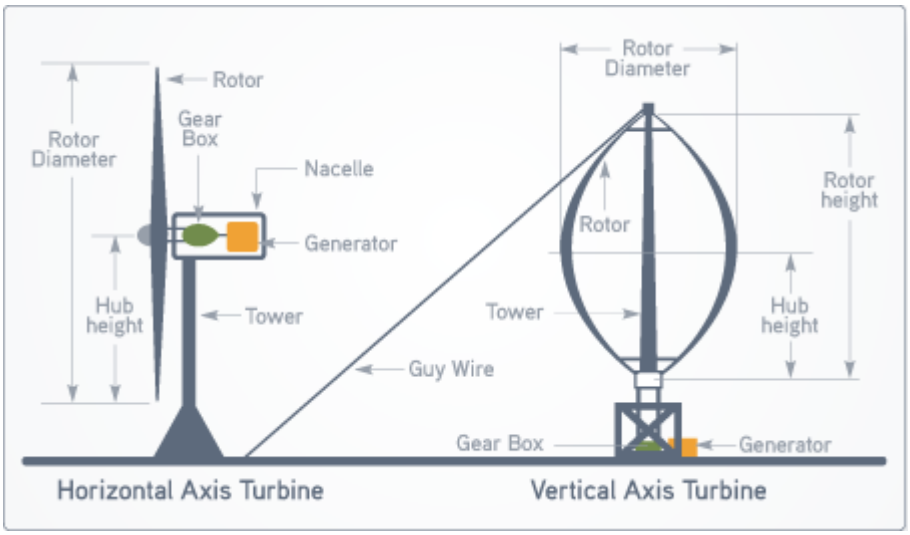

Basically, horizontal-axis wind turbines consist of 5 main parts. These are,

1. Foundation
2. Tower
3. Nacelle
4. Rotor
5. Electricity System Room

And these parts can be seen in Figure 13,

Figure 13: Components of horizontal wind turbine (Kanbur 2014)

1.3.1. Components of a Horizontal Axis Wind Turbine

In this part of the report, part of the wind turbine will be examined.

1.3.1.1. Foundation

Figure 14: Concrete foundation of onshore wind turbine (“Wind Farm | Riley Group” n.d.)

Turbines have to sit in a steel reinforced concrete foundation like Figure 14. Depending on the size of the turbine dimensions, the foundation size should be obtained. The foundation is important for withstanding strong wind conditions. The foundation is generally underground when construction is completed, there is no chance to see this.

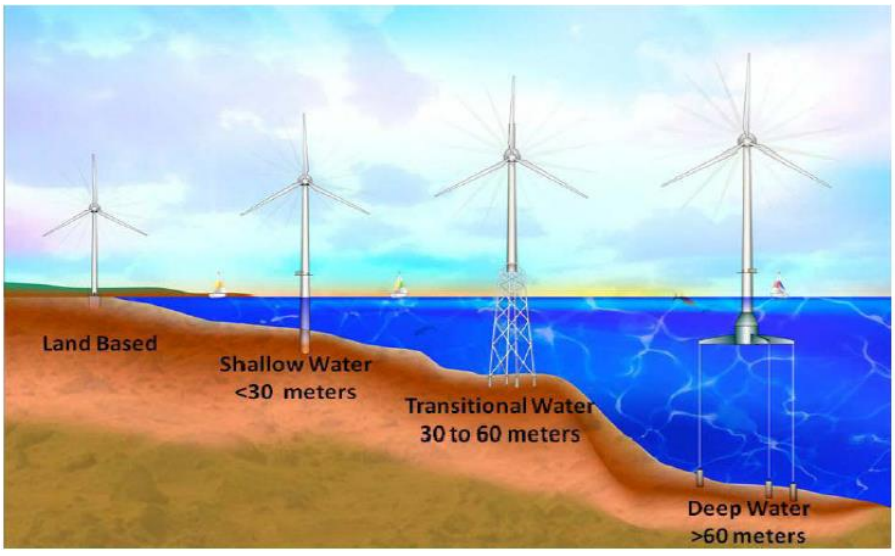

Figure 15: The offshore wind energy development considering to deepness (Aydin 2007)

Figure 15 shows the foundation for offshore wind turbines. According to deepness, subsea foundation types change. Some foundation technologies were given in Figure 16. As it was mentioned before, according to deepness, subsea foundation goes to change.

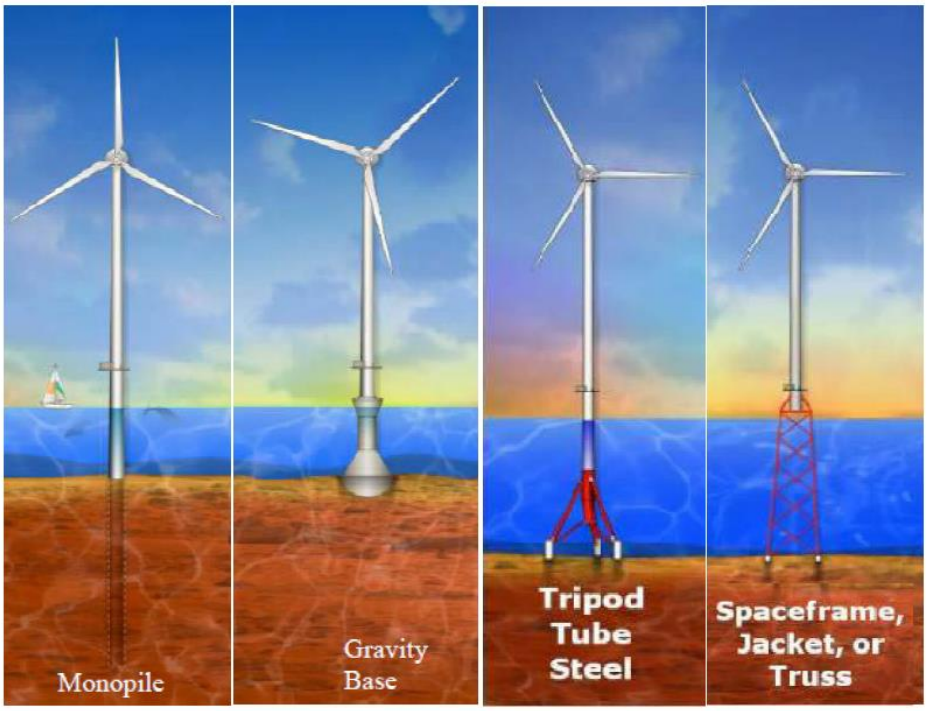

Figure 16: Shallow and deep-water foundation technologies (Aydin 2007)

1.3.1.2. Tower

The mission of the tower is to carry the rotor and nacelle's mass. One ideal design of the tower can transfer loads, which come from wind and rotor to the foundation in order to avoid an accident. The cost of wind turbine tower is around 30-33% of the total investment. In order to avoid the big cost of the tower, minimization of the mass of the tower is very critical work for the last two decades. Nowadays, tubular conical towers are used in the production of modern wind turbines, so very well shape towers can be produced using this method. Tubular conical parts are manufactured in 20-30 meters long welded cans and they are bolted with each other on the site.

Steel tubular conical towers may be manufactured as the tapered steel or concrete. According to production condition, steel tower could be pressed or welded together in each can. This process could be done in a plant or on site. One of the important topics is transportation. Generally, the allowance diameter of tower is 4.4m for transportation. So, some special permissions are required in order to carry towers. Sometimes, using specific methods of assembly in the field can solve transportation problems.

1.3.1.3. Nacelle

According to AWEA, the nacelle is a cover housing that houses all of the generating components in a wind turbine, including the generator, gearbox, drive train and brake assembly. The nacelle of a wind turbine is the box-like component that sits atop the tower and is connected to the rotor. The nacelle contains the majority of the approximately 8000 components of the wind turbine. The nacelle housing is made of fiberglass and protects the internal components from the environment. The nacelle cover is fastened to the main frame, which also supports all the other components inside the nacelle. The main frames are large metal structures that must be able to withstand large fatigue loads. One general view of nacelle can be observed in Figure 17.

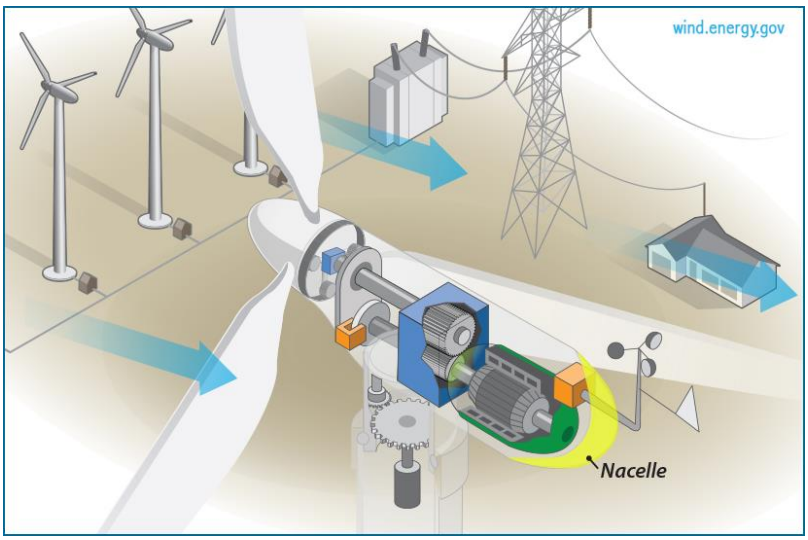

Figure 17: View of nacelle ("The Inside of a Wind Turbine | Department of Energy" n.d.)

1.3.1.4. Rotor

The rotor consist of blades and a hub. Generally, 3 blade systems are most popular. However, there are a few examples of 2 blades systems. Blades are produced by fiberglass and carbon fiber. On the other hand, there can be many kinds of hub type. Such as rigid and joint.

1.3.1.5. Electric System Room

Under the wind turbine, there is a room that is called the electric system room. This room is for some kind of electricity activities. Generally, inside the room, one can see many cables, transformers, converters and power factor correction capacitors.

1.4. Types of Wind Turbine Towers

Nowadays, wind turbine towers can be produced in many types and made of many materials. As a material, towers are made of concrete or constructional steel. In generally, towers can be divided into four categories, lattice towers, cylindrical towers, concrete towers and hybrid towers which are made from both concrete and metal.

1.4.1. Lattice Towers

As it can be seen in Figure 18, lattice tower consists from many pieces of metal stick. The connection between these metal parts is made by bolts. One of the positive aspects of this structure is it is easily accessible. This kind of small parts can be found in all metal producer. Also, according to the shape of the tower, the wind load effect is lower than other structure types. However, this kind of structure cannot carry very heavy nacelles and the main cost is higher than other tower types.

Figure 18: Lattice tower sample ("Everything You Need to Know About Small Wind Turbines" n.d.)

1.4.2. Steel Cylindrical Towers

Nowadays, in the wind energy sector, the most chosen type of wind turbine tower is the steel cylindrical tower. Considering to other towers, these kinds of towers are quite lighter than the others. These are not only lighter but also economic. Actually, the main reason to choose this type of tower is the strength of the structure. Compared with other tower types, cylindrical towers are much stronger.

Generally, these towers' main sections are connected to each other with bolts. But before connection, in order to produce the cylindrical part, bended flap metal must be welded from their vertical welding line. Generally each can is chosen around 2-3 meters. Then these 2-3 meters part are welded horizontally. A sample of a cylindrical tower and flange connections can be seen in Figure 19.

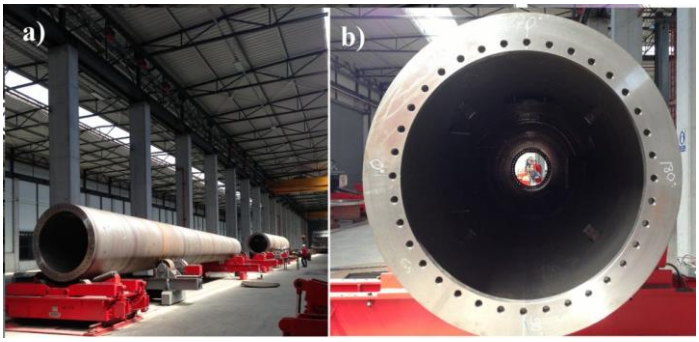

Figure 19: a) Steel cylindrical tower b) Flange connection (Kanbur 2014)

As it mentioned above, the main sections must be connected to each other with flanges and bolts. Before real connection, one technician must apply the pre-stressing process for all bolts in each section. This activity can be seen in following Figure 20,

Figure 20: Pre-Stressing process (Kanbur 2014)

In generally from bottom to top, the diameter of each can gets smaller. Also, the thickness of each can changes according to loads. As mentioned above, steel cylindrical towers are more economical than others. Due to its structural shape, the tower has fewer bolts connections compared with lattice towers, it means that less number of pre-stressing and stressing time. Additionally, cylindrical towers need less maintenance than other types. In safety aspects, cylindrical towers provide more safety climbing space for technicians. The esthetic view is also one positive way for this kind of towers.

As it can be seen in Figure 21, one of the very important issues is transportation. The diameter of sections must be sized according to country regulations. Or else, it causes a big traffic problem. For offshore wind turbines, all production must be managed by the company that is responsible for transportation in a seaway. Day by day, the energy requirement is being increased. The result of this increment towers become higher and larger. So, the problem of transportation becomes a more important issue than in past. One of the solutions is to, divide sections to more small pieces. Nevertheless, dividing by small pieces makes more cost for companies.

Figure 21: Tower and blades transportation for offshore wind turbines ("Heavy Lift Vessel 'Atlantic' Delivered to Her Owners - CONOSHIP" n.d.)

1.4.3. Concrete Towers

Compared with steel towers, concrete towers are not as popular as steel structures. On the other hand, according to energy requirements, the height of tower and rotor diameter are going to increase a lot. The result of this increment, in order to reach more safety structures, investors turn to concrete structures. Especially, dynamic analyzes results of concrete structures are quite impressive.

Generally, concrete towers are assembled in the field, as it can be seen in following Figure 22. Additionally, concrete is used in construction sector a lot, so there is no provider problem. For wind towers, a pre-stressing concrete method is used by companies. As a result of this method, a number of crack on the concrete get decrease. Less crack mean is long life in terms of fatigue. One another good aspect of concrete is local torsions or bending. During assembly, steel structures must be checked very carefully for local torsions or bending.

Figure 22: Concrete towers for wind turbines ("ACCIONA Windpower Inaugurates the First Concrete Tower Production Plant in Mexico" n.d.)

1.4.4. Hybrid Towers

As it can be understood from its name, hybrid towers use steel and concrete together. These tower consist of two main parts. One good sample can be observed in Figure 23. The first part is the concrete foundation and half of the tower, the second part is the cylindrical tower above the concrete. The aim of the hybrid tower is benefitting from both tower types positive aspects. For instance, the concrete tower doesn't have the problem of transportation, and steel structures are lighter than concrete. Using a hybrid tower can give flexibility for companies.

Figure 23: Assembly process for hybrid tower ("Prefabricated DYWIDAG Tendons Secure Innovative ATS Hybrid Wind Tower - DYWIDAG-Systems International" n.d.)

Compared with a fully concrete tower, during the assembly of the hybrid towers, the less strong crane is necessary. It means an easy assembly process and less cost than the fully concrete tower. Furthermore, the top of the hybrid tower is steel, therefore, it's less heavy than fully concrete. This is a positive thing in earthquake conditions.

1.5. Standards

According to (GWEC 2012), wind turbine production is increasing drastically. As a result of this increase, production must be taken under control due to production quality, safety and environmental effects. Therefore, wind turbine producers must follow some standards in order to avoid negative consequences/side effects.

As a result of industrial development, countries/regions have their own standards. Thus, countries can provide better service quality to their citizens. European Standards, American Standards, Japanese Standards might be given as an example. If one wants to control all these standards, one will see they have quite similar approaches. Countries have some different conditions due to climate and production methods, therefore some part of the standard can show some difference according to country.

In this thesis European Standards are going to be used. It means all design calculation, safety numbers, empirical data will be taken from European Standards (Eurocodes EC). European Standards was chosen because:

- This study (thesis) was developed in Europe.
- Europe is one of the big innovation centers in wind energy.
- Thesis advisors were using European Norms.
- Widely accepted in many different countries.

A turbine tower is a steel construction. Therefore during the design process "Eurocode 3: Design of Steel Structures" was used. All structure is designed according to EC3. Details of the calculation can be seen analytical part of the thesis. But basically, design values of geometrical data must be convenient for (CEN (European Commitee for Standardization) 2005a).

According to (CEN (European Commitee for Standardization) 2007b):

1. The thickness of the shell should be taken as defined in the relevant application standard. If no application standard is relevant, the nominal thickness of the wall, reduced by the prescribed value of corrosion loss, should be used.
2. The thickness ranges range within which the rules of this Standard may be applied are defined in the relevant EN1993 application parts.
3. The middle surface of the shell should be taken as the reference surface for loads.
4. The radius r of the shell should be taken as the nominal radius of the middle surface of the shell, measured normal to the axis revolution.
5. The buckling design rules of this Standard should not be applied outside the ranges of the r/t ratio set out in section 8 or Annex D or in the relevant EC3 application parts. (CEN (European Commitee for Standardization) 2007b)

1.6. Gap

The tower of the wind turbine is a topic that has been worked for many years. In scientific and experimental literature, there are many different approaches, proposals and suggestions, some of the tower have been already developed in final thesis such as (Kanbur 2014; Travanty 2001; Verma 2011). Furthermore some studies have already been conducted on the subject by universities and companies. All these sample works can be seen in chapter 8.

However, there are not many published paper focusing on the design of wind turbine tower based specifically on standards. As it was mentioned in previous chapters, standard is the one of the most important criteria. Without standards, turbine cannot be accepted by government for installation. Therefore, all calculations in this report made by standards which will be described in relevant sections throughout the thesis. Another goal of the thesis is to illustrate producers how one steel wind turbine tower can be designed according to standard rules; thus prevent companies from losing money, because of the fact that unsuccessful model that cannot fulfil standard criteria.

Furthermore, there is not many paper about wind turbine door opening. An experimental structural analyses can be seen in (Dimopoulos and Gantes 2012). However even this work, there is nothing about door shape idealization. Chapter 5 will show how to deal with door opening of the tower.

1.7. Objectives

This thesis is aiming to give ideas how to design a wind turbine tower in structural aspects and how to find ideal door opening of turbine tower by using ANSYS based on European Standards.

The study is supervised by Prof. Taczala from West Pomeranian University of Technology, Prof. Philippe Rigo from University of Liege and Prof. J.K. Paik from KOSORI, and will be published in a paper which is called “Ultimate Strength of Cylindrical Towers with Opening in Wind Turbine Structures”, where tower door opening is idealized and analyzed.

Within the framework of the thesis, one site-specific wind turbine tower was designed and an optimal door opening type was found which are the main objectives of the work. As it was mentioned before, all calculations were done according to standards. Furthermore, around one hundred types of door openings were investigated, useful data were collected and sorted. These door types were analyzed by using ANSYS and ideal result was found. Another objective is to provide a sort of guideline for tower producers illustrating how to use standards and how to design a tower that satisfies standards. Last goal is to show people importance of a door opening for wind tower design and how they can idealize their design.

1.8. Structure of the Work

When the thesis was being developed, the flowchart given below was followed. The chart was generated by thesis supervisor at the beginning of the internship.

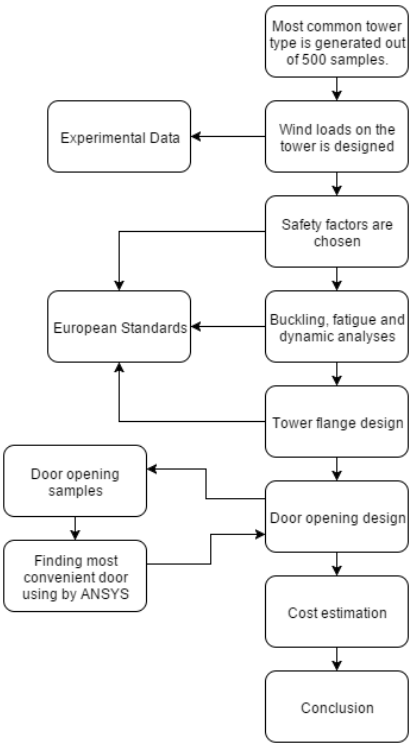

Figure 24: Flowchart of final thesis

2. STATE OF THE ART

Wind turbines have been developed since over than 100 years ago. As a result of this development, nowadays it is becoming one of the biggest energy sources. Therefore, recently many researches have been published regarding the subject.

First of all, there are many projects developed and applied that we can see on the web. All these data were sorted and based on the gathered data, most common tower type was selected. Experimental data showing the loads applying on the structure were taken from the advisor of the thesis and convenient shape and flange size were decided. For material of the tower, (Standard 2004) were the source of the thesis. During all this time, sample thesis and guidelines were followed such as (Det Norske Veritas 2011; Kanbur 2014; Karimirad 2014; Verma 2011)

When preliminary design of the model of tower was completed, analytical calculations were started to be done using (CEN (European Commitee for Standardization) 2005a). For buckling calculations, (CEN (European Commitee for Standardization) 2007a, 2007b) was used. All buckling detail about the shell were given in the standards. Then fatigue calculations were done using (CEN (European Commitee for Standardization) 2005b). During the dynamic calculations (Kanbur 2014; Lanier and Way 2005) were followed. As it was underlined before, standards were critical for the thesis, as you can see above during the calculations standards were used for entire calculations.

Door opening of the tower is one of the crucial part of the report. When opening was being developed, it was seen that there are not many published works on the subject. Therefore, during the analyses stage, opening on the shell structures were studied in general. In order to evaluate the validity of the FEM results of the tower, (Husson 2008) was used. It gives ideas about designing FEM model. FEM model was developed in ANSYS. ANSYS was selected as structural analyses program due to the fact that it is one of the most widely used software and several guidelines and tutorials are present.

Cost estimation was made using (Lanier and Way 2005; Verma 2011). However, cost estimations were done relatively roughly since data related with the calculations are confidential and are not shared by the companies. As a suggestion for future works, it is fair to say that cost estimation part of the work may be improved in many aspects.

3. TURBINE TOWER SELECTION

According to information that was given above; in this report cylindrical steel tower will be examined. This model was chosen because the cylindrical model is the most chosen type of tower by wind energy industry. Also, considering to wind load, very similar model can be used for offshore and onshore conditions. Some similar towers can be seen in Italy and Belgium.

During the thesis probabilistic method was followed. Before start to this research, 495 wind towers data was brought from all over the world by internet. These data was separated according to tower height and divided by 8 groups in each 20 meters interval. After examination of these values, the biggest group is 60-80 meters height group with 37% of total tower number as it can be seen in Figure 25. Therefore model was chosen in that interval. Producer can see most common used tower model according to the data that is collected in the thesis. Based on the suggestions of the thesis advisor, 65 meters model was selected to be the ideal length for further work.

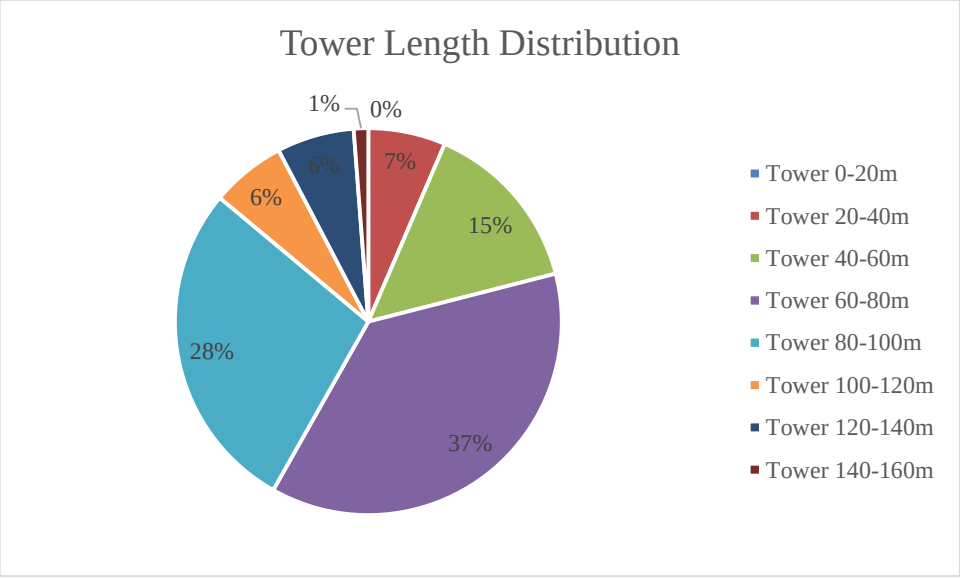

Figure 25: Tower length distribution

The tower is a cylindrical tower which consists of 3 sections that are bolted together through internal flange-bolt connections. In addition to that, the tower is connected to the base by bolts

as well (it can be offshore or onshore foundation). Shape of the tower can be seen in Figure 26. For the details of the geometry, appendix might be seen.

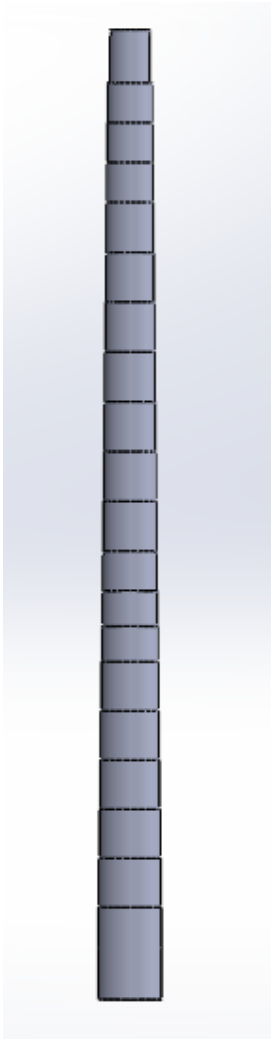

Figure 26: Preliminary designed tower

4. ANALYTICAL ANALYSES

In this part of the report, sample tower that was chosen in previous stage of the work will be evaluated considering EC. All diameter and lengths will be checked under safety regulations. One of the important issues is designing loads. Considering to short time of the master thesis, no possibility for long time wind measurement therefore real experimental wind loads data is

provided by the advisor. In order to figure out wind load engineering, one brief explanation could be read in the following part of the report.

4.1. Wind Load Design

In this part of the thesis loads on the tower will be assessed.

4.1.1. Basic Wind Load Design

According to (Shakya n.d.), theoretically wind load on the tower might be calculated by following formulas:

$$q_z = 0.613 * K_z * K_{zt} * K_d * I * V^2 \quad \textbf{(1)}$$

$$F = q_z * G * C_f * A_f \quad \textbf{(2)}$$

q_z : velocity pressure
K_z : velocity pressure expose coefficient depends on height
K_d : wind directional factor
I : importance factor
V : wind based speed
F : velocity pressure
G : gust effect factor
C_f : force coefficient factor
A_f : projected area normal to wind

4.1.2. Experimental Wind Load Design

In addition to the designed wind load, it can be developed by experiment. In this thesis, experimental load variables were used. As a result of this, it can be said that obtained results are close to reality. However, it is not always possible due to the fact that specific cases are not eligible with ease.

In general, the load input consists of two methods that are currently used popularly. These are sensor load method and the top load method. Basically, the top load method is generated from extrapolation of the top loads throughout the tower. In order to increase estimation accuracy in the loads at desired level, curve shape factor is also given. The sensor method uses rain flow spectra and precise load values that are measured by sensor throughout the tower. Then using with interpolation, loads values are in the desired level can be found as it can be seen in Figure 27. Linear interpolation is enough to reach exact load.

The calculation methods described in this research, design loads for fatigue and extreme loads are given in different levels throughout the tower considering to sensors. It is basically each 10-15 meters. Circumferential welds are very important for strength calculations, therefore, loads that must be calculated in each 2-3 meters. As it was mentioned in the previous passage, loads in each 2-3 meters can be found by interpolation. On the other hand, fatigue calculations are based on rain flow spectra. As it is known from previous experiences, interpolations are essential for fatigue calculations.

Nevertheless, one of the biggest problems of interpolation is accuracy. Results that come from linear interpolation should be compared with interpolation that includes the effect of curvature which bases on bending moment curve in along the tower. However, it is not possible to use of spectra for the fatigue calculation in a short time, equivalent fatigue moment curve will be used for this check. Additionally, in order to calculate fatigue load through the tower, equivalent fatigue bending moment assumption must be accepted. Considering to the assumption, equivalent fatigue bending moment is for Wohler exponent m=4 and $n=10^7$.

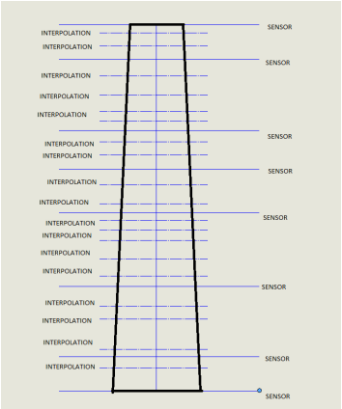

Figure 27: Basic theory of sensor loads and interpolated loads relation

Loads assumptions are must be valid for the specified temperature range in IEC 61400-1. Also, dead weights must be taken into account in accordance with standard DIN 1055 “Design Loads for Buildings”.

Table 2: Extreme load sensor data

Sensor Height	Design Bending Moment	Partial Coefficient	Design Torsion	Design Shear Force	Design Normal Force Tower Top	Wind Speed
-	M_{resd}	γ_f	M_{zd}	$F_{resp,d}$	F_{zc}	V
[m]	[kNm]	[-]	[kNm]	[kN]	[kN]	[m/s]
0	57898	1.35	-1.069	-98	-1284.6	56.5
0.2	57702	1.35	-1.069	-98	-1284.6	56.5
7.4	50667	1.35	-1.069	-98	-1284.7	56.5
12.6	45684	1.35	-1.069	-98	-1283.5	56.6
18.3	40242	1.35	-1.069	-98	-1284.2	56.6
28.8	30562	1.35	-1.069	-98	-1282.1	56.6
33	26818	1.35	-1.069	-98	-1240.8	57.5
41.7	19392	1.35	-1.069	-98	-1470.4	13.8
50.2	13008	1.35	-1.069	-98	-1480.8	13.7
55.4	9418	1.35	-1.069	-98	-1487.7	13.7
63	5539	1.35	-1.015	-44	-1442.6	23.4

Table 2 shows values that are taken from sensors. As it can be seen in Table 2, 11 sensors were used for calculation. According to sensors, maximum design bending moment, maximum design torsion, maximum design shear force, maximum normal force and wind speed can be generated from wind speed. Using these designed bending moments in each sensor, all designed bending moment in tower could be found by linear interpolation simulate like Figure 28,

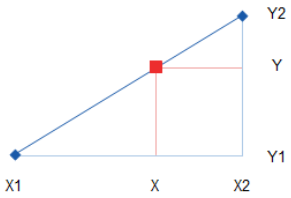

Figure 28: Calculation methodology for linear interpolation ("Excel Interpolation Formulas - Peltier Tech Blog" n.d.)

Interpolation equality:

$$\frac{X - X_1}{X_2 - X_1} = \frac{(Y - Y_1)}{(Y_2 - Y_1)} \quad \textbf{(3)}$$

By changing of variables in the equality, above equation becomes:

$$Y = Y_1 + (X - X_1) * \frac{(Y_2 - Y_1)}{(X_2 - X_1)} \quad \textbf{(4)}$$

In order to see the loads in 38 different levels along the tower, Figure 29 might be evaluated. 38 levels were chosen for interpolation, because of the fact that 38 different cans were planned to be produced.

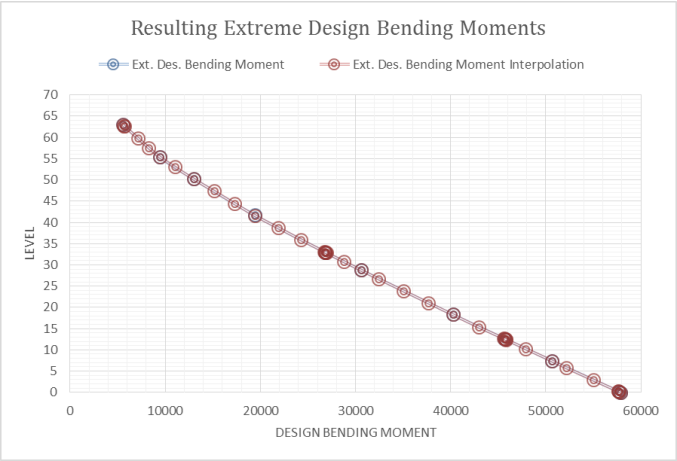

Figure 29: Resulting extreme bending moments along the tower

Sensors help also the estimation of fatigue equivalent bending moments. 11 fatigue bending moments for each sensor can be seen in Table 3,

Table 3: Fatigue load sensor data

Sensor No	Sensor Height	Experimental Fatigue Equivalent Moment	Equivalent Cycles
-	-	$\Delta M_{x'y.eq}$	n_{eq}
[#]	[m]	[kNm]	[#]
1	0	12329	1.00E+07
2	0.2	12281	1.00E+07
3	7.4	10601	1.00E+07
4	12.6	9424	1.00E+07
5	18.3	8181	1.00E+07
6	28.8	6225	1.00E+07
7	33	5536	1.00E+07
8	41.7	4239	1.00E+07
9	50.2	3200	1.00E+07
10	55.4	2886	1.00E+07
11	63	3024	1.00E+07

After using same linear interpolation which is applied in extreme conditions following Figure 30 can be reached.

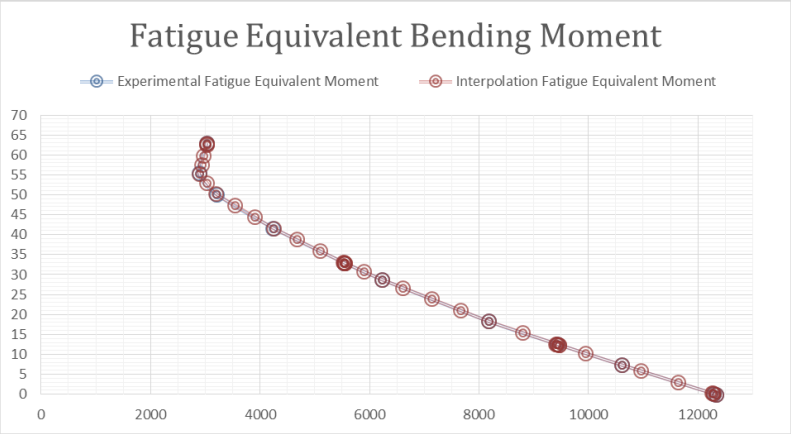

Figure 30: Fatigue bending moments along the tower

4.2. Partial Safety Factors

In order to be economical, instead of only one safety factor, different partial safety factors are applied for each load condition. Safety factor values change from 1.1 to 1.35 depending on the load case.

Like all the industrial sectors, there are many imperfections of production in the wind tower. The producer must make a balance between economic and safety. If best fabrication quality is chosen, the cost of production will increase drastically in contrast to, if worst fabrication quality is chosen, life and quality of tower can decrease. So this is a very important point for tower designer and producer. According to EU regulation of fabrication tolerance quality class, “Class B” was chosen in this thesis. All details about “Class B” can be seen in Table 4.

Table 4: Fabrication tolerance quality classes

Fabrication Tolerance Quality Class	Description	Q
Class A	Excellent	40
Class B	High	25
Class C	Normal	16

Table 5: Partial safety coefficients for extreme conditions according to (CEN (European Commitee for Standardization) 2005a) and (CEN (European Commitee for Standardization) 2007b)

Extreme Conditions			
Name	Symbol	Value	Unit
Fabrication Tolerance Quality Cl.	Q	25	-
Fabrication Tolerance Quality Cl.	a_0	0.65	-
Fabrication Tolerance Quality Cl.	a_τ	0.65	-
Buckling	γ_m	1.2	-
Yielding (sheets & flanges)	γ_m	1.1	-
Yielding (bolts)	$\gamma_{mb,y}$	1.1	-
Tensile strength (bolts)	$\gamma_{mb,u}$	1.25	-
Rolled thread - yield str.	$\gamma_{m,yr}$	1	-
Rolled thread - tensile str.	$\gamma_{m,tr}$	0.9	-
Gravity Load - unfavorable	$\gamma_{f,gu}$	1.1	-
Gravity Load - favorable	$\gamma_{f,gf}$	0.9	-

Table 5 shows partial safeties that were chosen according to EC. During calculation, not only extreme situations but also fatigue must be considered. In order to see fatigue safety numbers, following Table 6 could be observed.

Table 6: Partial safety coefficients for fatigue conditions according to (CEN (European Commitee for Standardization) 2005b)

Fatigue			
Name	Symbol	Value	Unit
Load	γ_f	1	-
Material (sheets)	γ_{mf}	1.265	-
Material (bolts)	γ_{mf}	1.265	-
Calibration factor	C_t	1	-
Air density	ρ_{air}	1.225	kg/m3
Water density	ρ_{water}	1025	kg/m3

4.3. Tower and Shell Analyses

Materials of wind tower shell must provide some properties. This material property can be seen in EC3-1-6. According to EU standards,

1. The material properties of steel should be obtained from the relevant application standard.
2. Where materials with nonlinear stress-strain curves are involved and a buckling analysis is carried out under stress design, the initial tangent value of Young's modulus E should be replaced by a reduced value. If no better method is available, the secant modulus at the 0.2% proof stress should be used when assessing the elastic critical load or elastic critical stress.
3. In the global numerical analysis using material nonlinearity, the 0.2% proof stress should be used to represent the yield stress f_x in all relevant expressions. The stress-strain curve should be obtained from EC3-1-5 Annex C for carbon steels and EC3-1-4 Annex C for stainless steels. (CEN (European Commitee for Standardization) 2007b)

In order to figure out yield and strength behavior of materials, stress-strain relations must be known. Relation could be observed in Figure 31,

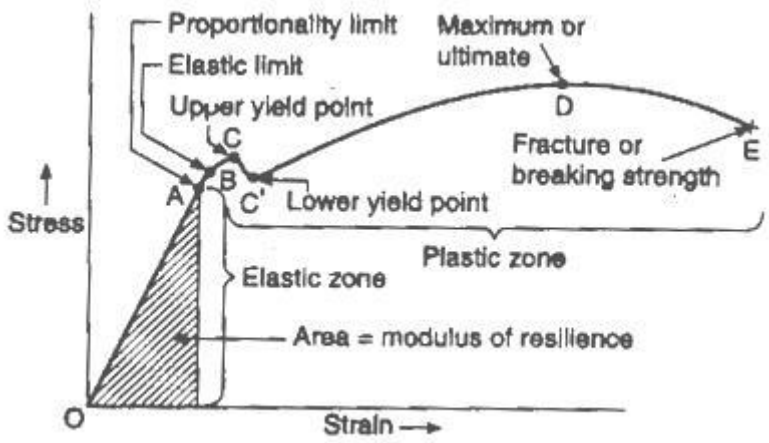

Figure 31: Stress-Strain relation ("Stress Strain Diagram For Ductile And Brittle Materials - Transtutors" n.d.)

Before start to analytical analyzes, materials that are chosen for tower must be mentioned. 65-meter wind turbine shell material yield details can be seen in below for EN and ASTM,

Table 7: Tower shell material quality according to standards in normal temperature (minimum operational temperature is -20°C and minimum stand-still temperature of -30°C)

Tower Shell	
Material Quality According to EN	S355J0 EN 100205
Material Quality According to ASTM	S355K2 EN 100025, ASTM A709

As it can be seen in Table 7 and Table 8, according to conditions and temperatures, different material limits have to be considered. Materials were chosen due to advisor suggestions and other towers samples.

Table 8: Tower shell material quality according to standards in operational temperature (minimum operational temperature is -30°C and minimum stand-still temperature of -40°C)

Tower Shell	
Material Quality According to EN	for shell thickness t<=25mm
	S355J0 EN 100205
	for shell thickness t>25mm
	S355J2 EN 100205
Material Quality According to ASTM	S355K2 EN 10025, ASTM A709

4.3.1. Yield Data

Following Table 9 was prepared according to EN and ASTM standards. One can see nominal strength values of steel for the tower.

Table 9: Yield and tensile strength for sheets (Standard 2004; "Steel Grades according to American Standards - A36, A572, A588, A709, A913, A992" n.d.)

	Sheet Thickness	t	16≥	> 16 ≤40	> 40 ≤63	> 63 ≤80	> 80 ≤100	> 100 ≤150	> 150 ≤200	> 200 ≤250	mm
S355	Yield Strength	f_{yk}	355	345	335	325	315	295	285	275	N/mm^2
	Tensile Strength	f_{uk}	470	470	470	470	470	450	450	450	N/mm^2
A709	Yield Strength	f_{yk}	345	345	345	345	345	345	345	345	N/mm^2
	Tensile Strength	f_{uk}	450	450	450	450	450	450	450	450	N/mm^2

All tower cans are designed for both EN and ASTM. In order to be sure for safety, EN and ASTM properties are combined and the minimum values are used for a given thickness. Final strength values can be seen in Table 10,

Table 10: Minumum yield and tensile strength for sheets (Standard 2004; “Steel Grades according to American Standards - A36, A572, A588, A709, A913, A992” n.d.)

Sheet thickness	t	16≥	> 16 ≤40	> 40 ≤63	> 63 ≤80	> 80 ≤100	> 100 ≤150	> 150 ≤200	> 200 ≤250	mm
Yield Strength	f_{yk}	345	345	335	325	315	295	285	275	N/mm^2
Tensile Strength	f_{uk}	450	450	450	450	450	450	450	450	N/mm^2

4.3.2. Buckling Strength

In this part of the report, buckling will be criticized. All calculations will be done according to EC3-1-6. Formulation and assumptions will be explained. Firstly, basic geometrical calculations will be done then stress calculations will be conducted. Same steps will be repeated for each can of the tower. A sample of can might be seen in Figure 32 and Figure 33,

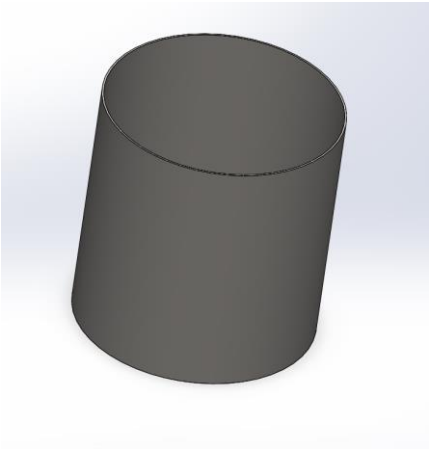

Figure 32: Can sample for tower

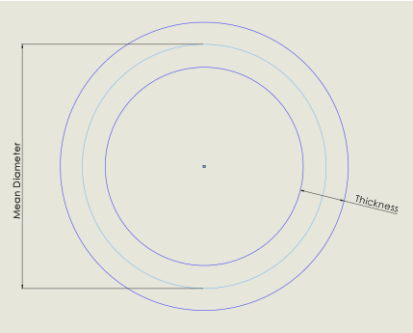

Figure 33: Top view for tower can

Calculation of cross-sectional area:

$$A = \pi * ((r_{mi} + t)^2 - (r_{mi} - t)^2) \quad \textbf{(5)}$$

$$r_{mi} = \frac{D_{mi}}{2} \quad \textbf{(6)}$$

A : cross-sectional area

r_{mi} : mean radius

D_{mi} : mean diameter

t : thickness

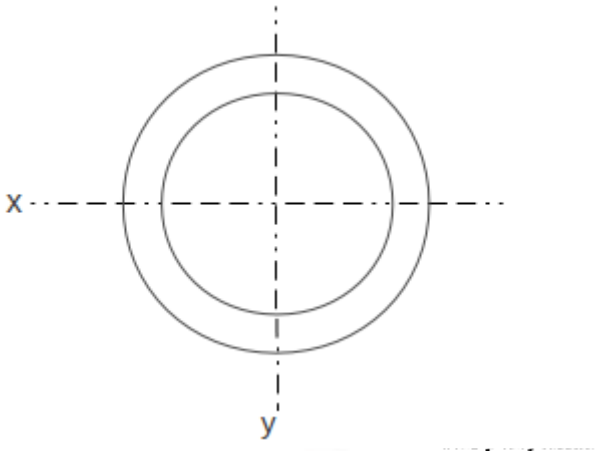

Figure 34: Hollow cylindirical cross section

As it can be seen in Figure 34, moment of inertia for hollow cylindrical cross section can be calculated by the following formula:

$$I = \frac{\pi * ((r_{mi} + t)^4 - (r_{mi} - t)^4)}{4} \quad \textbf{(7)}$$

Throughout the tower boundary condition for each can may change. Boundary condition is relevant the connection type of can. Table 11 shows different boundary conditions that will be used in this report,

Table 11: Boundary conditions for shells (CEN (European Commitee for Standardization) 2007b)

Boundary Condition Code	Simple Term	Description	Normal Displacement	Vertical Displacement	Meridional Rotation
BC1r	Clamped	radially restrained meridionally restrained rotation restrained	w=0	u=0	$\beta_\Phi=0$
BC1f		radially restrained meridionally restrained rotation free	w=0	u=0	$\beta_\Phi\neq0$
BC2r		radially restrained meridionally free rotation restrained	w=0	u≠0	$\beta_\Phi=0$
BC2f	Pinned	radially restrained meridionally free rotation free	w=0	u≠0	$\beta_\Phi\neq0$
BC3	Free edge	radially free meridionally free rotation free	w≠0	u≠0	βΦ≠0

Buckling will be evaluated under calculated loads in terms of sensor data, meridional buckling stress, hoop buckling stress and shear buckling stress. In order to figure out directions of stress, Figure 35 may be observed.

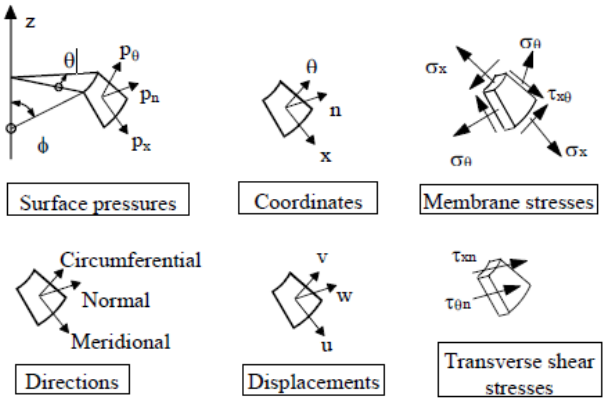

Figure 35: Symbols in shells of revolution (CEN (European Commitee for Standardization) 2007b)

4.3.2.1. Buckling Calculation Stress Data

Calculation of buckling stresses will be divided into four parts, these are direct, bending, shear torsion, shear force stress. Basic stress calculations will be used in following parts of the thesis. In order to understand, fundamental of this calculation the following Figure 36 can give an idea.

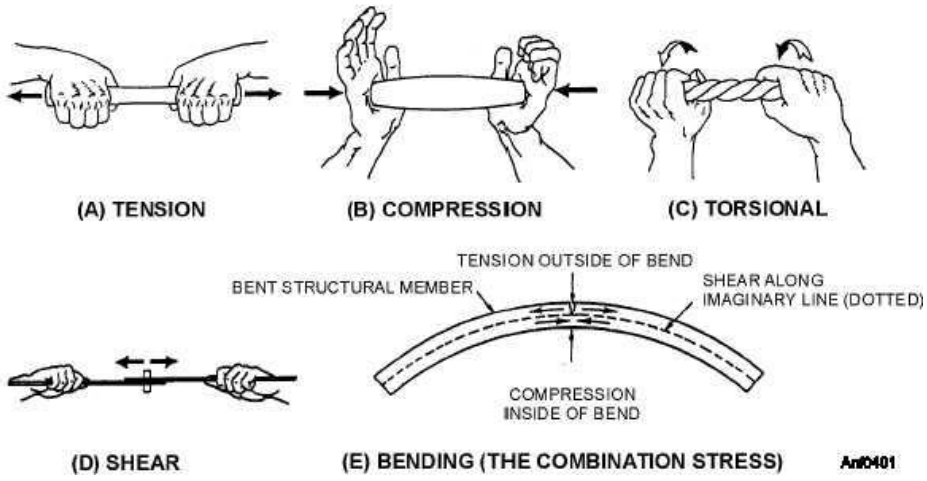

Figure 36: Five different stresses can be seen on tower ("SPECIFIC ACTION OF STRESSES - 14014_74" n.d.)

In order to imagine direct stress on the shell, Figure 37 can give an idea,

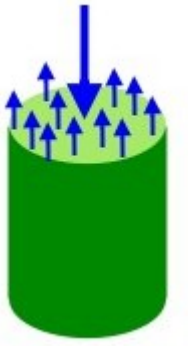

Figure 37: Direct stress ("Force and Strength" n.d.)

Formula of direct stress:

$$\sigma_n = \frac{F_{zd}}{A} \quad \textbf{(8)}$$

σ_n : direct stress

F_{zd} : designed normal force

A : cross-sectional area

Normal design force is obtained from interpolation of sensor loads. At the end of the calculation, 38 different stress data were obtained for each cross section.

Similar to direct stress, basic bending moment formula is applicable. Bending stress formula is:

$$\sigma_b = \frac{M_{resd}}{I} * (r_{mi} + t) \quad \textbf{(9)}$$

σ_b : bending stress

M_{resd} : designed bending moment

I : inertia

r_{mi} : mean radius

t : thickness

Torsion can be figured out from Figure 38, in the field of solid mechanics, torsion is the twisting of an object due to an applied torque. It is expressed in newton meters.

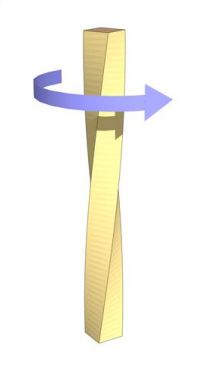

Figure 38: Tube element under torsion (“Torsion (mechanics) - Wikipedia, the Free Encyclopedia” n.d.)

For calculation of shear stress torsion, following formulas and Figure 39 can be examined,

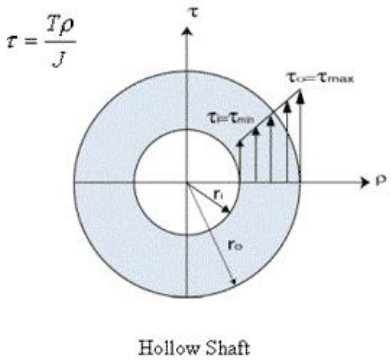

Figure 39: In circular shaft stress varies from the center (“Theory -8” n.d.)

Firstly, polar moment of inertia might be calculated:

$$J = \frac{\pi}{2}(r_o^4 - r_i^4) \quad \textbf{(10)}$$

Then,

$$\tau_{torsion} = \tau_{max} = \tau_2 = \frac{T * r_0}{J} \quad \textbf{(11)}$$

$\tau_{torsion}$: torsion shear stress

J : polar moment of inertia

r_o : outside radius

r_i : inside radius

T : torque

Finally, force shear stress will be examined in the following formula:

$$\tau_{shear} = \frac{F_{resp,d}}{A} \quad \textbf{(12)}$$

τ_{shear} : force shear stress

$F_{resp,d}$: designed shear force

A : cross-sectional area

Geometry of can is assumed shafts with circular sections, therefore deplanation of section is not seen. Total direct stress and total shear stress can be found by following formulas:

$$\sigma_z = \sigma_n + \sigma_b \quad \textbf{(13)}$$

σ_z : total direct stress

σ_n : direct stress

σ_b : bending stress

$$\sigma_{z\vartheta} = \tau_{shear} + \tau_{torsion} \quad \textbf{(14)}$$

$\sigma_{z\vartheta}$: total shear stress

τ_{shear} : force shear stress

$\tau_{torsion}$: torsion shear stress

Hoop stress because of the wind pressure on the structure must be calculated as it can be seen in Figure 40.

Figure 40: Hoop stress on the structure ("EngrApps: Burst and Collapse - Pressure Vessel Design" n.d.)

Hoop stress depends on pressure. Basically, pressure on the tower is resulted from wind. Using wind data that is taken from the sensors, pressure on the tower can be estimated. Initially, EC3-1-6 says that, cylinders must satisfy circumferential shell buckling conditions by following formula,

$$\frac{r}{t} \leq 0.21 * \sqrt{\frac{E}{f_{yk}}} \quad \textbf{(15)}$$

r : radius

t : thickness

E : modulus of elasticity

f_{yk} : characteristic yielding stress

Firstly, wind pressure distribution on the tower should be known. According to EC3-1-6, wind distribution on the tower could be seen in the following Figure 41,

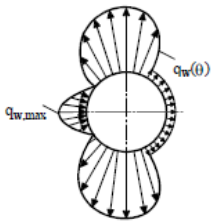

Figure 41: Wind pressure distribution around shell circumference (CEN (European Commitee for Standardization) 2007b)

Because of the complex shape of the pressure distribution on the above figure, calculation is not that easy. According to EC3-1-6, wind pressure on the tower should be converted to a symmetrical condition which is presented in Figure 42,

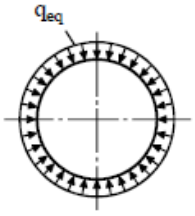

Figure 42: Equivalent axisymmetric pressure distribution (CEN (European Commitee for Standardization) 2007b)

Transformation and wind pressure calculation will be done by following formulas according to EC3-1-6,

Firstly, drag coefficient can be found by:

$$k_\omega = 0.46 * \left(1 + 0.1\sqrt{\frac{C_\theta}{\omega} * \frac{r}{t}}\right) \quad \textbf{(16)}$$

k_w : drag coefficient

C_θ : buckling factor

ω : dimensionless length parameter

r : radius

t : thickness

When the drag coefficient value is between 0.65 and 1, buckling factor can be taken from Table 12 considering to the boundary conditions.

Table 12: External pressure buckling factors for medium-length cylinders C_θ

Case	Cylinder End	Boundary Condition	C_θ
1	end 1 end 2	BC1 BC1	1.5
2	end 1 end 2	BC1 BC2	1.25
3	end 1 end 2	BC2 BC2	1
4	end 1 end 2	BC1 BC3	0.6
5	end 1 end 2	BC2 BC3	0
6	end 1 end 2	BC3 BC3	0

Non-symmetric maximum wind pressure is determined by:

$$q_{wmax} = 0.5 * \rho_{air} * V_{wind}{}^2 \quad \textbf{(17)}$$

q_{wmax} : non-symmetric maximum wind pressure

ρ_{air} : density of air which is 1.225 kg/m^3

V_{wind} : velocity of wind (comes from sensor data interpolations)

Equivalent axisymmetric pressure is defined:

$$q_{eq} = k_w * q_{wmax} \quad \textbf{(18)}$$

q_{eq} : axisymmetric maximum wind pressure

k_w : drag coefficient

q_{wmax} : non-symmetric maximum wind pressure

The hoop stress is defined as:

$$\sigma_\theta = \frac{q_{eq} * r_{mi}}{t} \quad \textbf{(19)}$$

σ_θ : hoop stress

q_{eq} : axisymmetric maximum wind pressure

r_{mi} : main radius

t : thickness

After the completion of all stress calculations, reference stress that consists of all stress such as direct, hoop and shear can be found. The Von Misses stress (total reference stress) of each can of tower can be expressed by:

$$\sigma_{ref} = \sqrt{\sigma_z{}^2 + \sigma_\theta{}^2 - \sigma_z * \sigma_\theta + 3 * \sigma_{z\theta}{}^2} \quad \textbf{(20)}$$

σ_{ref} : Von Misses stress (total reference stress)

σ_z : total direct stress

σ_θ : hoop stress

$\sigma_{z\theta}$: total shear stress

4.3.2.2. Meridional Buckling Stress

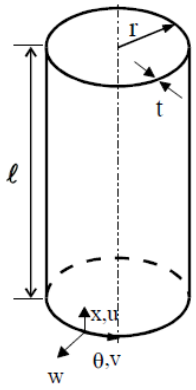

Figure 43: Cylinder geometry (CEN (European Commitee for Standardization) 2007b)

The symbolic geometry of shell can be seen in Figure 43. According to EC-1-6, the length of the shell must be characterized. The length of the shell segment is characterized in terms of the dimensionless length parameter by the following formula:

$$\omega = \frac{l}{r} * \sqrt{\frac{r}{t}} \quad \textbf{(21)}$$

Then:

$$\omega = \frac{l}{\sqrt{rt}} \quad \textbf{(22)}$$

ω : dimensionless length parameter

l : cylinder length between defined boundaries

r : radius of cylinder middle surface

t : thickness

According to dimensionless length parameter, correction factor can be determined by:

For medium-length cylinders, could be defined by:

$$1.7 \leq \omega \leq 0.5 * \left(\frac{r}{t}\right) \quad \textbf{(23)}$$

$$C_x = 1.0 \quad \textbf{(24)}$$

For medium short cylinders, could be determined by:

$$\omega \leq 1.7 \quad \textbf{(25)}$$

$$C_x = 1.36 - \frac{1.83}{\omega} + \frac{2.07}{\omega^2} \quad \textbf{(26)}$$

For medium long cylinders, could be expressed by:

$$\omega > 0.5 * \left(\frac{r}{t}\right) \quad \textbf{(27)}$$

$$C_x = C_{x,N} \tag{28}$$

$$C_{x,N} = 1 + \frac{0.2}{C_{xb}} * \left[1 - 2 * \omega \frac{t}{r}\right] \tag{29}$$

C_{xb} can be obtain from below Table 13,

Table 13: Parameter C_{xb} for the effect of boundary conditions on the elastic critical meridional buckling stress in long cylinders

Case	Cylinder end	Boundary Conditions	C_{xb}
1	end 1 end 2	BC1 BC1	6
2	end 1 end 2	BC1 BC2	3
3	end 1 end 2	BC2 BC2	1

ω : dimensionless length parameter

r : radius of cylinder middle surface

t : thickness

C_x : correction factor

$C_{x,N}$: normal correction factor

C_{xb} : effect of boundary conditions on the elastic critical meridional buckling stress in long cylinders

After all these calculations, the elastic critical meridional buckling stress, using a value of correction factor, may be obtained from:

$$\sigma_{x,Rcr} = 0.605 * E * C_x * \left(\frac{t}{r}\right) \tag{30}$$

$\sigma_{x,Rcr}$: elastic critical meridional buckling stress

E : modulus of elasticity

C_x : correction factor

t : thickness

r : radius of cylinder middle surface

Following the EC3-1-6, characteristic imperfection amplitude determined by:

$$\Delta w_k = \frac{1}{Q} * \sqrt{\frac{r}{t}} * t \quad \textbf{(31)}$$

Δw_k : characteristic imperfection amplitude

Q : fabrication quality parameter from Table 4

r : radius of cylinder middle surface

t : thickness

The meridional elastic imperfection reduction factor is expressed by:

$$a_x = \frac{0.62}{1 + 1.91\left(\frac{\Delta w_k}{t}\right)^{1.44}} \quad \textbf{(32)}$$

a_x : meridional elastic imperfection reduction factor

Δw_k : characteristic imperfection amplitude

t : thickness

Basically cylinders need not be checked against meridional shell buckling if they satisfy:

$$\frac{r}{t} \leq 0.03 \frac{E}{f_{yk}} \quad \textbf{(33)}$$

r : radius of cylinder middle surface

t : thickness

E : modulus of elasticity

f_{yk} : characteristic yielding stress

If cylinders don't satisfy above equation, the meridional squash limit slenderness, the plastic range factor and the interaction exponent should be taken as:

$$\overline{\lambda_{x0}} = 0.20 \quad \textbf{(34)}$$

$$\beta = 0.60 \quad \textbf{(35)}$$

$$\eta = 1.0 \quad \textbf{(36)}$$

For long cylinders, there is one special condition in order to calculate meridional squash limit slenderness, according to EC3-1-6:

$$\overline{\lambda_{x0}} = 0.20 + 0.10 * \left(\frac{\sigma_{xE}}{\sigma_{xE,M}}\right) \quad \textbf{(37)}$$

λ_{x0} : meridional squash limit slenderness

β : plastic range factor

$\boldsymbol{\eta}$: interaction exponent

σ_{xE} : design value of the meridional stress $\sigma_{x,Ed}$

$\sigma_{xE,M}$: the component of $\sigma_{x,Ed}$ that derives from tubular global bending

The value of the plastic limit relative slenderness could be found by:

$$\overline{\lambda_p} = \sqrt{\frac{a}{1-\beta}} \quad \textbf{(38)}$$

λ_p : plastic limit relative slenderness

a : elastic imperfection reduction factor

β : plastic range factor

The relative shell slenderness for meridional buckling stresses should be expressed by:

$$\overline{\lambda_x} = \sqrt{\frac{f_{yk}}{\sigma_{x,Rcr}}} \quad \textbf{(39)}$$

λ_x : relative shell slenderness for meridional buckling

f_{yk} : characteristic yielding stress

$\sigma_{x,Rcr}$: elastic critical meridional buckling stress

The meridional buckling reduction factors could be determined by following formula, according to relative slenderness of the shell:

$$\chi_x = 1 \; for \; \overline{\lambda} \leq \overline{\lambda_0} \quad \textbf{(40)}$$

$$\chi_x = 1 - \beta * \left(\frac{\overline{\lambda} - \overline{\lambda_0}}{\overline{\lambda_p} - \overline{\lambda_0}} \right)^{\eta} \; for \; \overline{\lambda_0} < \overline{\lambda} < \overline{\lambda_p} \quad \textbf{(41)}$$

$$\chi_x = \frac{a}{\overline{\lambda}^2} \; for \; \overline{\lambda_p} \leq \overline{\lambda} \tag{42}$$

χ_x : meridional buckling reduction factor

λ : relative shell slenderness for meridional buckling

λ_0 : meridional squash limit slenderness

β : plastic range factor

λ_p : plastic limit relative slenderness

$\boldsymbol{\eta}$: interaction exponent

a : elastic imperfection reduction factor

Then characteristic buckling stresses can be found for each tower can by following formula:

$$\sigma_{x,Rk} = \chi_x * f_{yk} \tag{43}$$

$\sigma_{x,Rk}$: characteristic buckling stresses

χ_x : meridional buckling reduction factor

f_{yk} : characteristic yielding stress

Finally designed buckling resistance could be determined by:

$$\sigma_{x,Rd} = \sigma_{x,Rk} * \gamma_{M1} \tag{44}$$

$\sigma_{x,Rd}$: design buckling resistance

$\sigma_{x,Rk}$: characteristic buckling stresses

γ_{M1} : partial factor

For partial factor doesn't have standard rule. Therefor value can be taken according to country and sector. However, basically it shouldn't be taken as smaller than 1.1, in this work it is taken 1.2

4.3.2.3. Circumferential Buckling Stress

Dimensionless length parameter can be seen in formula 21st then according to dimensionless length parameter, segment can be determined.

Depend on the boundary condition the factor of C_θ might be taken from Table 12,

For medium-length cylinders, could be defined by:

$$20 \leq \left(\frac{\omega}{C_\theta}\right) \leq 1.63 * \left(\frac{r}{t}\right) \quad \textbf{(45)}$$

Later, the elastic critical circumferential buckling stress for medium cylinder, could be found from:

$$\sigma_{\theta,Rcr} = 0{,}92 * E * \left(\frac{C_\theta}{\omega}\right) * \left(\frac{t}{r}\right) \quad \textbf{(46)}$$

$\sigma_{\theta,Rcr}$: elastic critical meridional buckling stress
E : modulus of elasticity
C_θ : correction factor
ω : dimensionless length parameter
t : thickness
r : radius of cylinder middle surface

For short cylinders, could be defined by:

$$\frac{\omega}{C_\theta} \leq 20 \quad \textbf{(47)}$$

$C_{\theta s}$ can be taken in Table 14,

Table 14: External pressure buckling factors for short cylinders $C_{\theta s}$

Case	Cylinder end	Boundary Condition	$C_{\theta s}$
1	end 1 end 2	BC1 BC1	$1.5+(10/\omega^2)-(5/\omega^3)$
2	end 1 end 2	BC1 BC2	$1.25+(8/\omega^2)-(4/\omega^3)$
3	end 1 end 2	BC2 BC2	$1.0+(3/\omega^{1.35})$
4	end 1 end 2	BC1 BC3	$0.6+(1/\omega^2)-(0.3/\omega^3)$

The elastic critical circumferential buckling stress for short cylinder, may be found from:

$$\sigma_{\theta,Rcr} = 0{,}92 * E * \left(\frac{C_\theta}{\omega}\right) * \left(\frac{t}{r}\right) \quad \textbf{(48)}$$

$\sigma_{\theta,Rcr}$: elastic critical meridional buckling stress

E : modulus of elasticity

C_θ : correction factor

ω : dimensionless length parameter

t : thickness

r : radius of cylinder middle surface

For long cylinders, could be defined by:

$$\frac{\omega}{C_\theta} > 1.63 * \left(\frac{r}{t}\right) \quad \textbf{(49)}$$

Then, the elastic critical circumferential buckling stress for long cylinders, is found by:

$$\sigma_{\theta,Rcr} = E * \left(\frac{t}{r}\right)^2 \left[0.275 + 2.03 * \left(\frac{C_\theta}{\omega} * \frac{r}{t}\right)^4\right] \quad \textbf{(50)}$$

$\sigma_{\theta,Rcr}$: elastic critical meridional buckling stress

E : modulus of elasticity

t : thickness

r : radius of cylinder middle surface

C_θ : correction factor

ω : dimensionless length parameter

Circumferential buckling parameters can be determined from fabrication quality, according to EC3-1-6, fabrication quality can be seen in Table 15,

Table 15: Values of a_θ based on fabrication quality

Fabrication Tolerance Quality Class	Description	a_θ
Class A	Excellent	0.75
Class B	High	0.65
Class C	Normal	0.5

The circumferential squash limit slenderness, the plastic range factor and the interaction exponent should be taken as:

$$\overline{\lambda_{\theta 0}} = 0.40 \quad \textbf{(51)}$$

$$\beta = 0.60 \quad \textbf{(52)}$$

$$\eta = 1.0 \tag{53}$$

Cylinders need not be checked against circumferential shell buckling if they satisfy:

$$\frac{r}{t} \leq 0.21\sqrt{\frac{E}{f_{yk}}} \tag{54}$$

$\lambda_{\theta 0}$: circumferential squash limit slenderness

β : plastic range factor

$\boldsymbol{\eta}$: interaction exponent

r : radius of cylinder middle surface

t : thickness

E : modulus of elasticity

The value of the plastic limit relative slenderness could be found from:

$$\overline{\lambda_p} = \sqrt{\frac{a}{1-\beta}} \tag{55}$$

λ_p : plastic limit relative slenderness

a : elastic imperfection reduction factor

β : plastic range factor

The relative shell slenderness for circumferential buckling stresses may be determined from:

$$\overline{\lambda_\theta} = \sqrt{\frac{f_{yk}}{\sigma_{\theta,Rcr}}} \quad \textbf{(56)}$$

λ_θ : relative shell slenderness for circumferential buckling

f_{yk} : characteristic yielding stress

$\sigma_{\theta,Rcr}$: elastic critical circumferential buckling stress

The circumferential buckling reduction factors could be determined according to relative slenderness of the shell:

$$\chi_\theta = 1 \; for \; \overline{\lambda} \leq \overline{\lambda_0} \quad \textbf{(57)}$$

$$\chi_\theta = 1 - \beta * \left(\frac{\overline{\lambda} - \overline{\lambda_0}}{\overline{\lambda_p} - \overline{\lambda_0}} \right)^\eta \; for \; \overline{\lambda_0} < \overline{\lambda} < \overline{\lambda_p} \quad \textbf{(58)}$$

$$\chi_\theta = \frac{a}{\overline{\lambda}^2} \; for \; \overline{\lambda_p} \leq \overline{\lambda} \quad \textbf{(59)}$$

χ_θ : circumferential buckling reduction factor

λ : relative shell slenderness for circumferential buckling

λ_0 : circumferential squash limit slenderness

β : plastic range factor

λ_p : plastic limit relative slenderness

$\boldsymbol{\eta}$: interaction exponent

a : elastic imperfection reduction factor

Then characteristic buckling stresses can be found for each tower can by following formula:

$$\sigma_{\theta,Rk} = \chi_{\theta} * f_{yk} \quad \textbf{(60)}$$

$\sigma_{x,Rk}$: characteristic buckling stresses

χ_x : circumferential buckling reduction factor

f_{yk} : characteristic yielding stress

Finally designed buckling resistance could be determined by:

$$\sigma_{\theta,Rd} = \sigma_{\theta,Rk} * \gamma_{M1} \quad \textbf{(61)}$$

$\sigma_{\theta,Rd}$: design buckling resistance

$\sigma_{\theta,Rk}$: characteristic buckling stresses

γ_{M1} : partial factor

4.3.2.4. Shear Buckling Stress

Dimensionless length parameter can be seen in formula 21st.

For medium-length cylinders, which are defined by:

$$10 \leq \omega \leq 8.7 * \left(\frac{r}{t}\right) \quad \textbf{(62)}$$

Correction factor may be found:

$$C_{\tau} = 1.0 \quad \textbf{(63)}$$

ω : dimensionless length parameter

r : radius of cylinder middle surface

t : thickness

C_τ : correction factor

For short cylinders, could be defined by:

$$\omega < 10 \quad \textbf{(64)}$$

Correction factor may be found:

$$C_\tau = \sqrt{1 + \frac{42}{\omega^3}} \quad \textbf{(65)}$$

ω : dimensionless length parameter

C_τ : correction factor

For long cylinders, which are defined by:

$$\omega > 8.7 * \left(\frac{r}{t}\right) \quad \textbf{(66)}$$

Correction factor may be found:

$$C_\tau = \frac{1}{3} * \sqrt{\omega * \frac{t}{r}} \quad \textbf{(67)}$$

ω : dimensionless length parameter

r : radius of cylinder middle surface

t : thickness

C_τ : correction factor

Shear buckling parameters can be determined by fabrication quality, according to EC3-1-6, fabrication quality can be seen in Table 15,

The shear squash limit slenderness, the plastic range factor and the interaction exponent should be taken as:

$$\overline{\lambda_{\tau 0}} = 0.40 \quad \textbf{(68)}$$

$$\beta = 0.60 \quad \textbf{(69)}$$

$$\eta = 1.0 \quad \textbf{(70)}$$

Cylinders need not be checked against circumferential shell buckling if they satisfy:

$$\frac{r}{t} \leq 0.16 \left[\sqrt{\frac{E}{f_{yk}}} \right]^{0.67} \quad \textbf{(71)}$$

$\lambda_{\tau 0}$: shear squash limit slenderness

β : plastic range factor

$\boldsymbol{\eta}$: interaction exponent

r : radius of cylinder middle surface

t : thickness

E : modulus of elasticity

f_{yk} : characteristic yielding stress

$$\overline{\lambda_p} = \sqrt{\frac{a}{1-\beta}} \tag{72}$$

λ_p : plastic limit relative slenderness

a : elastic imperfection reduction factor

β : plastic range factor

The relative shell slenderness for shear buckling stresses should be determined by:

$$\overline{\lambda_\tau} = \sqrt{\frac{f_{yk}}{\tau_{x\theta,Rcr}}} \tag{73}$$

λ_θ : relative shell slenderness for shear buckling

f_{yk} : characteristic yielding stress

$\sigma_{x\tau,Rcr}$: elastic critical shear buckling stress

The shear buckling reduction factors could be determined according to relative slenderness of the shell:

$$\chi_\tau = 1 \; for \; \overline{\lambda} \leq \overline{\lambda_0} \tag{74}$$

$$\chi_\tau = 1 - \beta * \left(\frac{\overline{\lambda} - \overline{\lambda_0}}{\overline{\lambda_p} - \overline{\lambda_0}} \right)^\eta \; for \; \overline{\lambda_0} < \overline{\lambda} < \overline{\lambda_p} \tag{75}$$

$$\chi_\tau = \frac{a}{\overline{\lambda}^2} \; for \; \overline{\lambda_p} \leq \overline{\lambda} \tag{76}$$

χ_τ : shear buckling reduction factor

λ : relative shell slenderness for circumferential buckling

λ_0 : shear squash limit slenderness

β : plastic range factor

λ_p : plastic limit relative slenderness

$\boldsymbol{\eta}$: interaction exponent

a : elastic imperfection reduction factor

Then characteristic buckling stresses might be found for each tower can by following formula:

$$\tau_{x\theta,Rk} = \frac{\chi_\theta * f_{yk}}{\sqrt{3}} \tag{77}$$

$\tau_{x\theta,Rk}$: characteristic buckling stresses

χ_x : circumferential buckling reduction factor

f_{yk} : characteristic yielding stress

Finally designed buckling resistance could be determined by:

$$\tau_{x\theta,Rd} = \tau_{x\theta,Rk} * \gamma_{M1} \tag{78}$$

$\tau_{x\theta,Rd}$: design buckling resistance

$\tau_{x\theta,Rk}$: characteristic buckling stresses

γ_{M1} : partial factor

4.3.2.5. Buckling Stress Reserve Factor Calculations

The stress reserve factor is the ratio between experimental data and European standards. The SRF must be greater than "1" for each buckling condition. In order to obtain exact SRF following formulas can be used:

SRF for yielding:

$$f_{yd} = \frac{f_{yk}}{1.2} \tag{79}$$

$$SRF_y = \frac{\sigma_{ref}}{f_{yd}} \tag{80}$$

f_{yd} : yielding strength design
f_{yk} : characteristic yielding stress
SRF_y : stress reserve factor for yielding
σ_{ref} : Von Misses stress (total reference stress)

SRF for meridional buckling:

$$SRF_m = \frac{\sigma_{x,Rd}}{\sigma_z} \tag{81}$$

SRF_m : stress reserve factor for meridional buckling
$\sigma_{x,Rd}$: meridional design buckling stress
σ_z : total normal stress

SRF for circumferential buckling:

$$SRF_c = \frac{\sigma_{\theta,Rd}}{\sigma_a} \quad \textbf{(82)}$$

SRF_m : stress reserve factor for meridional buckling

$\sigma_{\theta,Rd}$: circumferential design buckling stress

σ_a : hoop stress

SRF for shear buckling:

$$SRF_s = \frac{\tau_{\theta,Rd}}{\tau_{z\theta}} \quad \textbf{(83)}$$

SRF_s : stress reserve factor for shear buckling

$\tau_{\theta,Rd}$: shear design buckling stress

$\tau_{z\theta}$: total shear stress

Interaction Parameters:

$$k_x = 1 + x_x^2 \quad \textbf{(84)}$$

$$k_\tau = 1.5 + 0.5 * x_\tau^2 \quad \textbf{(85)}$$

$$Interact\ Utility = \left(\frac{\sigma_z}{\sigma_{x,Rd}}\right)^{k_x} + \left(\frac{\tau_{z\theta}}{\tau_{x\theta,Rd}}\right)^{k_\tau} \quad \textbf{(86)}$$

$$SRF_I = \frac{1}{Interact\ Utility} \quad \textbf{(87)}$$

k_x : buckling interaction parameter

x_x : meridional buckling reduction factor

k_τ : shear interaction parameter

x_τ : shear buckling reduction factor

σ_a : hoop stress

$\sigma_{x,Rd}$: meridional design buckling stress

$\tau_{z\theta}$: total shear stress

$\tau_{\theta,Rd}$: shear design buckling stress

SRF_I : stress reserve factor for interaction

These five SRF is the critical ratios for each buckling condition. In order to figure out tower is safety or not, minimum SRF value for each can must be evaluated. The value that is below than one, cannot be approved. Critical SRF values for this tower may be seen in following Figure 44,

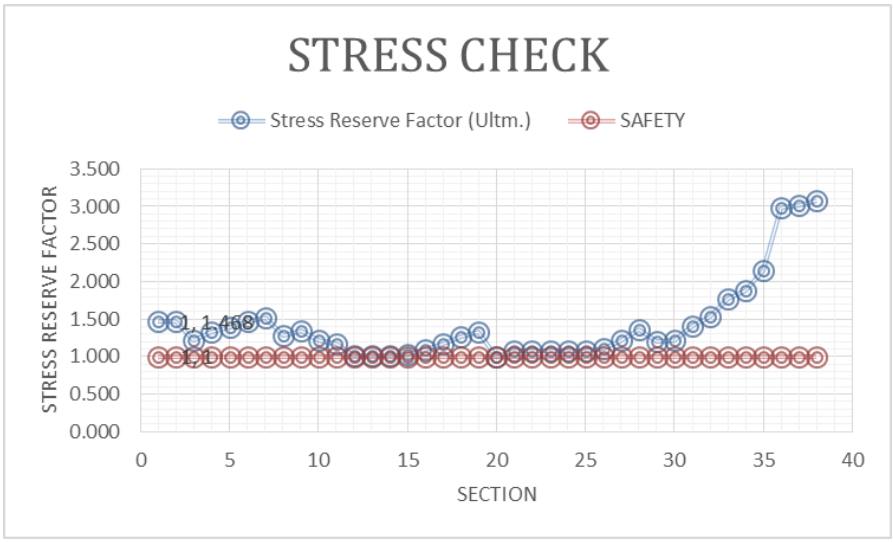

Figure 44: Stress reserve factor each can

For these tower minimum SRF value is 1.003 in the SRF Interaction at 20th can.

4.3.3. Fatigue Strength

In steel construction, structure is exposed continious load during all of the life such as wave, wind. Because of these continious loads there will be some small cracks. These cracks will increase day by day, it might be risk for collapse. Therefore, during design of the tower, not only buckling but also fatigue calculation must be done. Fatigue is very important in the joint areas such as welding or flanges. Two important parameters for fatigue is number of cycles and stress interval.

Basically, welding is applied on the tower in three main parts. These are welding for being cylinder, welding between two cans and welding between flange and section. Details can be seen in Figure 45,

Figure 45: Welding connections in the tower (Kanbur 2014)

Fatigue loads is critical in the weld between two cans also weld between sections and flanges, typical weld in a tubular tower can be seen in Figure 46,

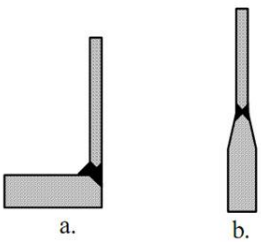

Figure 46: Typical weld details in a tubular tower a) weld at flange b) weld between two cans (Verma 2011)

Wind loading on the tower is the main reason of fatigue cracking. Fatigue design can be carried out depend on the S-N curves that are made in the laboratory. In the calculation of the fatigue Palmgren-Miner's is the key factor.

Before start to talk about S-N curve, detail categories of joints may be figured out. According to their notch effect, welded joints are classified into detail categories. The detail category is values that reference to fatigue stress. Basically detail category shows fatigue value at $2*10^6$ number of cycles. It depend on the geometry and fabrication. The given detail categories assume 100% controlled in a penetration aspect. Not only the detail categories of welding but also surface of welding is very important. Weld should provide a stress flow as smooth as possible without major internal or external notches, discontinuities in rigidity and obstructions to strains. In order to prevent stress concentration, the wall thickness must be tapered with a slope not to be greater than 1:4.

Table 16: Detail categories for common welds in a tubular tower

Weld	Categories ($\Delta\sigma_R$)
Can to Can	80-90
Can to Flange	71

All part of wind turbines are exposed to different stress ranges. This stress variation can be illustrated like Figure 47,

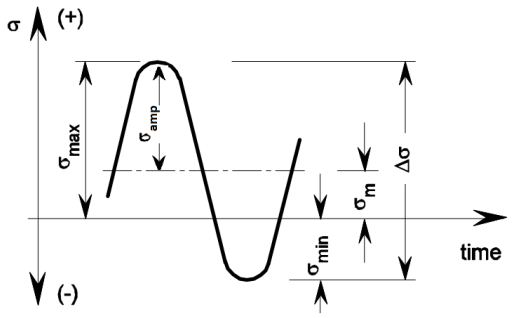

Figure 47: The stress cycle (Germanischer Lloyd Industrial Services GmbH 2010)

According to Figure 47, stresses can be expressed by,

$$\sigma_m = \frac{(\sigma_{max} + \sigma_{min})}{2} \quad \textbf{(88)}$$

$$\sigma_{amp} = \frac{|\sigma_{max} - \sigma_{min}|}{2} \quad \textbf{(89)}$$

$$R = \frac{\sigma_{min}}{\sigma_{max}} \quad \textbf{(90)}$$

σ_{max} : maximum upper stress

σ_{min} : minimum upper stress

σ_{amp} : amplitude of the stress cycle

R : ratio between minumum and maximum stress

4.3.3.1. S-N Curve

In order to perform fatigue analysis, the S-N curve for the weld must be followed from EC3-1-9 as it can be seen in Figure 48. Basically, S-N curve can be calculated by following formulas:

$$\log(N) = 6.69897 + m * Q \quad \textbf{(91)}$$

$$Q = log\left(\frac{\Delta\sigma_R}{\Delta\sigma}\right) - \frac{0.39794}{m_o} \quad \textbf{(92)}$$

m : inverse slope of S-N curve

m_o : inverse slope in the range $N \leq 5*10^6$

$\Delta\sigma_R$: fatigue strength reference value of S-N curve at $2*10^6$ cycles of stress range

$\Delta\sigma$: stress range [N/mm^2]

N : number of endured stress cycless according to S-N curve

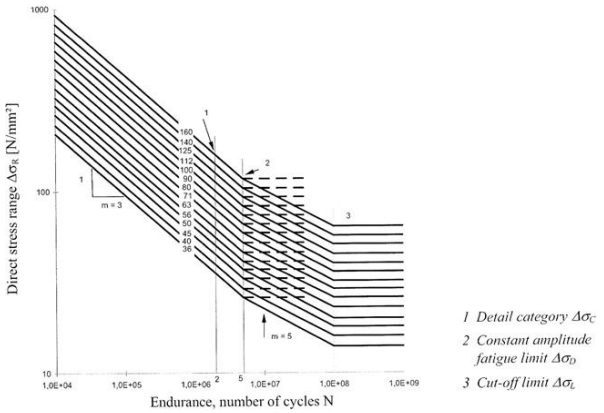

Figure 48: Fatigue strength curves for direct stress ranges (CEN (European Commitee for Standardization) 2005b)

4.3.3.2. Palmgren-Miner's Rule

The fatigue is the process that is cumulative damage, different varies of loads could be estimated by using S-N curve considering to Palmgren-Miner's cumulative damage approach. The total damage that is on the tower, can help to estimate design life of the tower. It can be expressed as the summation of the damage from each stress levels at each load cycle. According to Palmgren-Miner's rule, the accumulated damage can be expressed by:

$$D = \sum_i \frac{n_i}{N_i} \quad \textbf{(93)}$$

D : accumulated fatigue damage

n_i : stress cycles of the i^{th} stress range

N_i : corresponding number of cycles to failure

Failure may happen when the accumulated fatigue damage is higher than 1.0. In order to withstand, D must be smaller or equal to 1.0.

4.3.3.3. Safety Factors

Safety factors must be considered during the design of structure. These safety factors are obtained by country standards. Each tower producer must follow these standards in order to avoid some fatigue accident. All these safety numbers come from empirical experiences.

For the towers, main safety strategies and numbers can be seen in Table 17 and Table 18,

Table 17: Safety strategies for structures

Partial Safety γ_{mf} Factor Consequence of Failure	Fail Safe and Damage Tolerant Strategy	Safe Life and Infinite Life Strategy
Loss of secondary structural parts	1.00	1.15
Loss of entire structure	1.15	1.30
Loss of human life	1.30	1.40

Table 18: Safety factors for structures

Material Factor	Load Safety Factor	Total Safety Factor	Design Fatigue Life
γ_{mf}	γ_{Ff}	γ_{Mf}	Year
1.1	1	1.265	20

As it can be seen above tables, total safety number may be determined by:

$$\gamma_{Mf} = \gamma_{mf} * \gamma_{Ff} * Safe\ Life\ \&\ Infinite\ Life\ Str. \quad \textbf{(94)}$$

γ_{Mf} : total safety factor

γ_{mf} : material factor

γ_{Ff} : load safety factor

4.3.3.4. Fatigue Damage Calculation

In this section, fatigue calculation of wind tower will be presented. Calculation will be shown step by step. However, in order to provide EC3-1-9 standards, shape and fatigue detail category were modified during the calculation as it can be seen in Figure 49. Basically, the calculation loop was repeated twice, because in the first calculation, tower couldn't provide the standards. Then design was improved, and it satisfied European Norms.

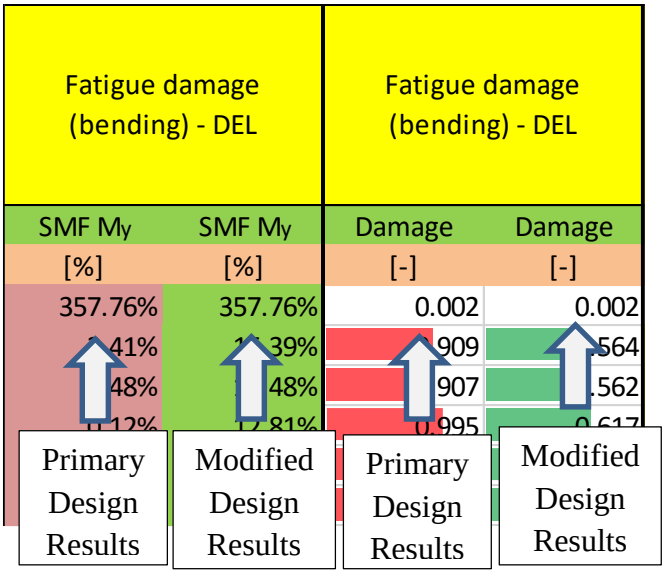

Figure 49: Chancing tower details in order to provide European Standards

First of all geometrical calculations are done for shape of the tower. Section modulus for each can could be determined by:

$$W_{ben} = \frac{\pi * \left({D_{outer}}^4 - {D_{inner}}^4\right)}{32 * D_{outer}} \quad \textbf{(95)}$$

$$W_{tor} = W_{ben} * 2 \quad \textbf{(96)}$$

$$c_{red} = \left(\frac{25}{t}\right)^{0.2} \quad \textbf{(97)}$$

$$For\ t \leq 25\ mm : c_{red} = 1 \quad \textbf{(98)}$$

W_{ben} : section modulus of bending

W_{tor} : section modulus of torsion

c_{red} : thickness reduction factor

t : thickness

As it was mentioned above, in this tower 71, 80 and 90 fatigue class material were used. Considering these classes, constant amplitude fatigue limit and cut-off limit can be expressed by:

$$\Delta\sigma_D = \left(\frac{2}{5}\right)^{\frac{1}{3}} * \Delta\sigma_C \quad \textbf{(99)}$$

$$\Delta\sigma_L = \left(\frac{5}{100}\right)^{\frac{1}{5}} * \Delta\sigma_D \quad \textbf{(100)}$$

$\Delta\sigma_D$: constant amplitude fatigue limit

$\Delta\sigma_C$: detail category fatigue limit

$\Delta\sigma_L$: cut-off fatigue limit

As it was mentioned at the beginning of the fatigue part, fatigue load on the tower is real life loads that is taken from a similar sample. Therefore, fatigue equivalent moments are taken from experimental data provided by supervisor. As a result of using real life data, final result will be closer to the real life condition.

$$\Delta\sigma_i = \frac{\Delta M_y}{W_{ben}} * SCF \quad \textbf{(101)}$$

$\Delta\sigma_i$: bending stress range

ΔM_y : fatigue equivalent moment

W_{ben} : section modulus for the tower wall at the specific tower level

SCF : stress concentration factor, usually determined by FEA

$$\Delta\sigma_{i,d} = \Delta\sigma_i * \gamma_{Mf} \quad \textbf{(102)}$$

$\Delta\sigma_{i,d}$: design bending stress range

$\Delta\sigma_i$: bending stress range

γ_{Mf} : total safety factor

The torsional stress range is determined by following expression:

$$\Delta\tau_i = \frac{\Delta M_z}{2 * W_{tor}} \quad \textbf{(103)}$$

$$\Delta\tau_{i,d} = \Delta\tau_i * \gamma_{Mf} \quad \textbf{(104)}$$

$\Delta\tau_{i,d}$: design torsion stress range

$\Delta\tau_i$: torsion stress range

γ_{Mf} : total safety factor

According to EC3-1-9, wohler exponent could be found by:

$$if\ \ \Delta\sigma_{i,d} \geq C_{rd} * \Delta\sigma_D \tag{105}$$

$$N = \frac{\sigma_C^m}{\left(\sigma_{i,d}/C_{red}\right)^m} * 2 * 10^6, m = 3 \tag{106}$$

$$if\ \ \Delta\sigma_{i,d} < C_{red} * \Delta\sigma_D \tag{107}$$

$$N = \frac{\sigma_D^m}{\left(\sigma_{i,d}/C_{red}\right)^m} * 2 * 10^6, m = 5 \tag{108}$$

$$if\ \ \Delta\sigma_{i,d} \leq C_{red} * \Delta\sigma_L,\ \ N = \infty \tag{109}$$

$\Delta\sigma_{i,d}$: design bending stress range

c_{red} : thickness reduction factor

$\Delta\sigma_D$: constant amplitude fatigue limit

$\Delta\sigma_C$: detail category fatigue limit

N : number of cycles to failure with design stress range $\sigma_{i,d}$

m : wohler exponent

$\Delta\sigma_L$: cut-off fatigue limit

In order to estimate structure life torsional calculation might be done. Torsional stress range can be determined by:

$$\Delta\tau_L = \left(\frac{2}{100}\right)^{\frac{1}{5}} * \Delta\tau_C \quad \textbf{(110)}$$

$$if \ \ \Delta\tau_{i,d} > \Delta\tau_L \quad \textbf{(111)}$$

$$N = \frac{\Delta\tau_C^m}{\Delta\tau_{i,d}{}^m} * 2 * 10^6, m = 5 \quad \textbf{(112)}$$

$$if \ \ \Delta\tau_{i,d} \leq \Delta\tau_L, \ \ N = \infty \quad \textbf{(113)}$$

$\Delta\tau_{i,d}$: torsion bending stress range

c_{red} : thickness reduction factor

$\Delta\tau_C$: detail category fatigue limit

N : number of cycles to failure with torsion stress range $\tau_{i,d}$

m : wohler exponent

$\Delta\tau_L$: cut-off fatigue limit

According to Miner's summation, the fatigue data for a given tower is expressed by,

$$D_{d,\sigma} + D_{d,\tau} \leq 1 \quad \textbf{(114)}$$

$$D_d = \sum_i \frac{n_i}{N_i} = \sum \frac{n_i}{N(\sigma_{i,d})} \ or \sum \frac{n_i}{N(\tau_{i,d})} \quad \textbf{(115)}$$

$D_{d,\sigma}$: bending stress summation

$D_{d,\tau}$: torsion stress summation

D_d : accumulated fatigue damage

n_i : stress cycles of the i^{th} stress range

N_i : corresponding number of cycles to failure

Additionally, fatigue must be checked by damage equivalent load method. Method uses Miner's summation. By using DEL method fatigue life also can be estimated. Fatigue life might be determined by:

$$SMF_{My} = \frac{1}{\left(\gamma_{Mf}*\left(\frac{10^7}{10^{\log(2*10^6)}}+4*log(\Delta\sigma_C)-4*log\left(\frac{\Delta M_y}{W_{ben}*C_{red}}\right)^{0.25}\right)\right)} - 1 \quad \textbf{(116)}$$

$$DEL = \left(\frac{1}{1+SMF_{My}}\right)^4 \quad \textbf{(117)}$$

SMF_{My}: DEL percentage

γ_{Mf} : total safety factor

$\Delta\sigma_C$: detail category fatigue limit

ΔM_y : fatigue equivalent moment

W_{ben} : section modulus for the tower wall at the specific tower level

c_{red} : thickness reduction factor

DEL : damage equivalent load

Finally fatigue life can be estimated by:

$$Fatigue\ Life = \frac{Design\ Fatigue\ Life(20\ years)}{DEL} \quad \textbf{(118)}$$

Based on the calculations done so far, SRF must be checked. As a result of this check, one can guess, whether the structure is resistant enough. If it is not, as it was mentioned above, design should be modified until whole SRF exceed or equal to “1.0”.

SRF can be obtained by:

$$\Delta\sigma_R = \left(\frac{a}{N_R}\right)^{\left(\frac{1}{m}\right)} \quad \textbf{(119)}$$

$$\Delta\sigma_{lim} = \Delta\sigma_R * \gamma_{Mf} \quad \textbf{(120)}$$

$$SRF = \frac{\Delta\sigma_{lim}}{\Delta\sigma_i} \quad \textbf{(121)}$$

$\Delta\sigma_R$: design stress range
a : constant comes from m
N_R : number cycles assumed as a reference value
m : wohler exponent
$\Delta\sigma_{lim}$: allowable stress
γ_{Mf} : safety factor
SRF : stress reserve factor
$\Delta\sigma_i$: bending stress range

To sum up, after one modification, the tower provided all necessities which were obtained by EC3. Results for SRF and DEL can be seen in Figure 50,

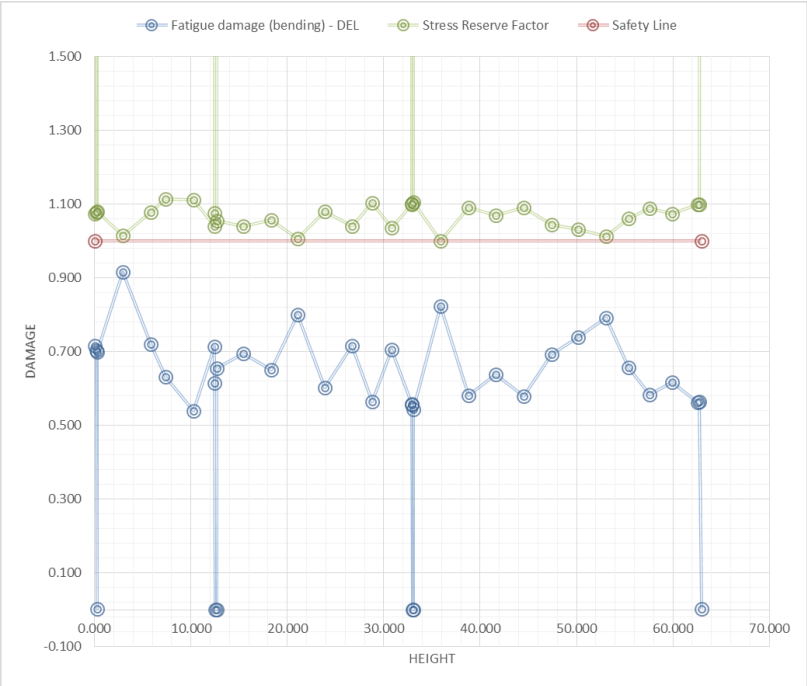

Figure 50: DEL and SRF corresponding to tower height

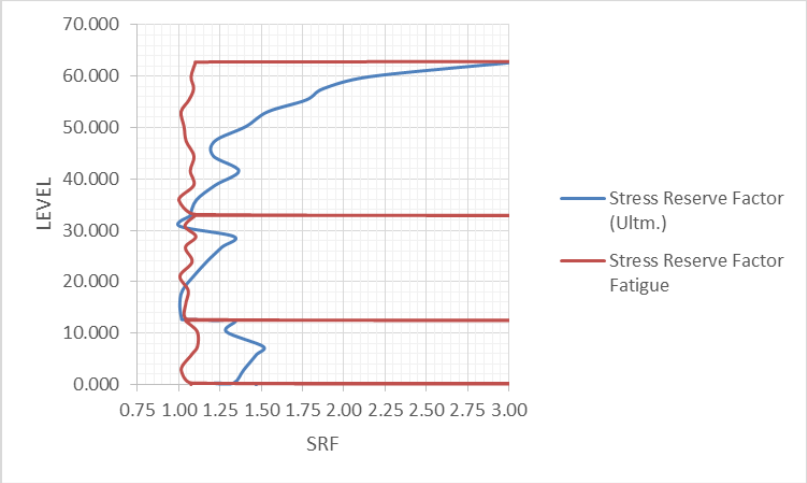

Figure 51: SRF for fatigue and buckling

Figure 51 summarizes all the results obtained from fatigue and ultimate buckling calculations. For each can and connection, stress reserve factor is equal or greater than “1”. Basically, this figure shows that all sections of the tower satisfy ultimate and fatigue conditions according to (CEN (European Commitee for Standardization) 2005a).

4.3.4. Dynamic

During the wind turbine design, main dynamic characteristic of turbine must be obtained. In order to avoid resonance, natural frequency value of the tower should be further from the turbine operating frequency (1P and 3P). In following subtitles, dynamic character of the tower will be checked.

4.3.4.1. Determining Tower Natural Frequency

According to (Amirouche 2006), Baumeister's natural frequency for a simple straight cylindrical steel tower can be found by following formula:

In order to see importance of the tower mass in natural frequency, Baumeister's natural frequency value corresponding to mass can be seen in Figure 52,

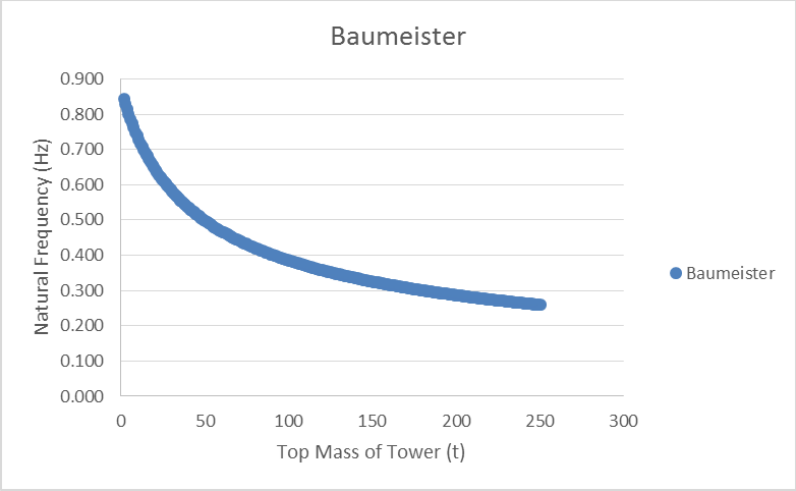

Figure 52: Baumeister frequency value corresponding to tower mass

Table 19: Characteristic data of turbine

E	2.10E+08	kN/m^2
I_{ave}	0.318	m^4
m_{tower}	105.157	t
m_{rotor}	112.671	t
L	65.000	m

Table 19 illustrates data of turbine that is necessary for calculation.

$$f_n = \frac{1}{2\pi} * \sqrt{\frac{3 * E * I}{h^3 * (0.23 * m_{tower} + m_{rotor})}} \quad \textbf{(122)}$$

f_n : estimated natural frequency of the tower

h : height of the tower

E : elastic modulus

I_{ave} : moment of inertia (average inertia of all the cans)

m_{rotor} : weight of rotor mass

m_{tower} : tower mass

As a result of these calculations, f_n = 0.684 Hz

Due to production defect and different conditions, natural frequency can be changed ±%5.

4.3.4.2. Determining Operation Frequency and Working Frequency

Firstly operation speed of the turbine must be provided by nacelle producer. In this thesis, a specific nacelle was not chosen, therefore (Lanier and Way 2005)'s samples were interpolated for further calculations. Samples for interpolation can be seen in Table 20. At the end operation frequency was found approximately 16 rpm.

Table 20: Nacelle operation speed for 1.5 and 3.6 MW wind turbines

Turbine	Operation Speed	
	rpm	Hz
1.5 MW(EQ)	20.5	0.342
1.5 MW(Wind)	20.5	0.342
3.6 MW(EQ)	13.2	0.220
3.6 MW(Wind)	13.2	0.220
5.0 MW(EQ)	11.2	0.187
5.0 MW(Wind)	11.2	0.187

Frequency limits can be calculated by:

$$1P_{Hz} = \frac{1P_{rpm}}{60} \quad \textbf{(123)}$$

$$3P_{Hz} = 3 * 1P_{Hz} \quad \textbf{(124)}$$

$$1.1P_{Hz} = 1.1 * 1P_{Hz} \quad \textbf{(125)}$$

$$2.7P_{Hz} = 2.7 * 1P_{Hz} \quad \textbf{(126)}$$

$1P_{Hz}$: block frequency in Hz

$1P_{rpm}$: block frequency in rpm

$3P_{Hz}$: 3 blades block frequency in Hz

$1.1P_{Hz}$: min. working frequency in Hz

$2.7P_{Hz}$: max. working frequency in Hz

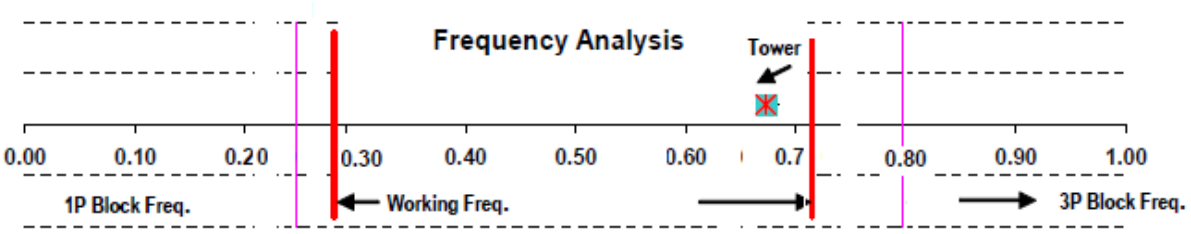

Figure 53: Frequency analyses of the tower

As it can be seen in Figure 53, $1P_{Hz}$ = 0.26, $3P_{Hz}$ = 0.80, $1.1P_{Hz}$ = 0.29 and $2.7P_{Hz}$ = 0.72 Hertz. Tower frequency was stated above as an f_n = 0.684 Hz. To sum up, tower is in safe region. Additionally, f_n is in between $1.1P_{Hz}$ and $2.7P_{Hz}$, it means, the tower that is stated in this thesis is "soft" class wind tower.

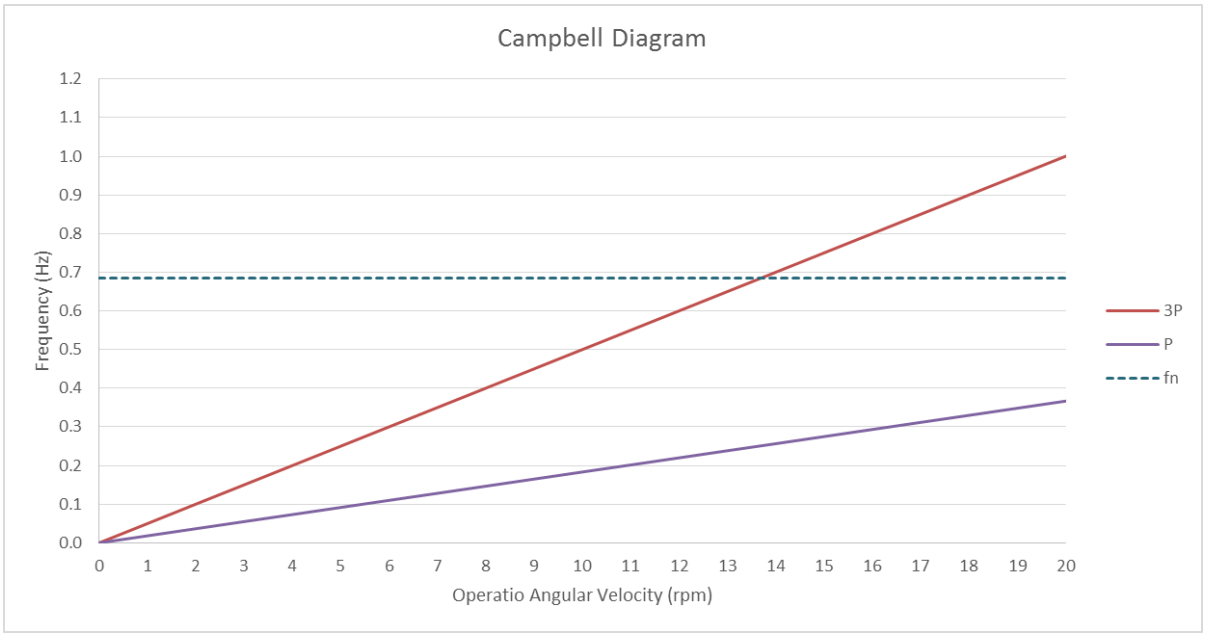

Figure 54: Campbell Diagram

Figure 54 illustrates to f_n value is in between $1P_{Hz}$ and $3P_{Hz}$. According to (Lanier and Way 2005), soft wind turbine frequency value should be inside to this range when turbine is working.

4.4. Tower Flange Design

In order to connect each segment in the cylindrical tower, flange connection might be used. Circular flanges is welded two segments. There are holes on the flanges. Using these holes and bolts, connection might be satisfied.

For three main segments tower, one segment connection between nacelle and tower, two middle level segment connections among the cans and one bottom level segment connection between tower and foundation might be used.

Due to load differences in the each level of the tower, accident scenarios on the flanges can be different. Basically, one cannot expect same ultimate flange behavior on the top and bottom. Therefore, for each condition different formula will be used considering geometry and level.

Loads on the flange also very important factor. Estimation of the load can be seen in following passage.

Loads on the flange can be calculated by:

$$F_{z,fl} = \left(\frac{F_{z,top}}{\gamma_f} + \frac{F_{z,tower}(h)}{\gamma_{fe,u}} \right) * 0.9 \qquad \textbf{(127)}$$

$F_{z,fl}$: normal force – Design
$F_{z,top}$: design Load on the top
$F_{z,top}$: design Load on the h level
γ_f : safety factor
$\gamma_{fe,u}$: safety factor in the level

In order to simplified solution, only one flange connection will be discussed as it can be seen in Figure 55,

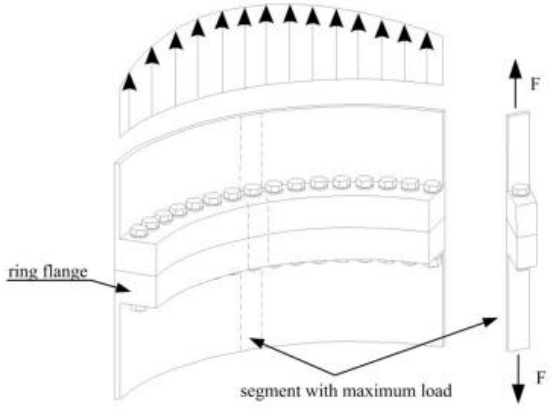

Figure 55: Segment approach for design of ring flange connection (Achmus et al. n.d.)

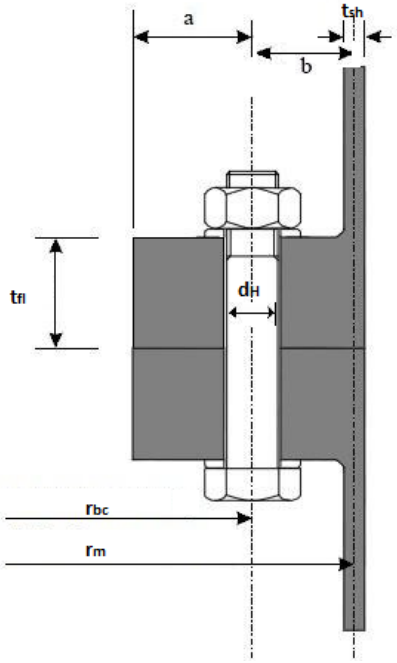

Figure 56: Section view of connection (Kanbur 2014)

Geometrical values that will be used in the calculation can be seen in Figure 56. The yielding stress of the flange material is depend on thickness. Basically thickness is defined as the smallest value of the nominal height of the final machined flange that is measured on the outer diameter side, also nominal width of the finished machined surface might be considered.

The ultimate limit state condition of the flange connection is performed based on both Petersen and Seidel sections. The bolt pretension is disregarded. This is for simplification of the problem.

This approach is quite conservative, due to opening of the flange connection and accompanying plastic deformation will lead to some redistribution of forces and thereby decreased bolt stresses.

In order to solve flange problems, some simplification were done. Therefore, basically 3 different failure mode assumptions were developed until now by Petersen. These failure modes may be examined in Figure 57,

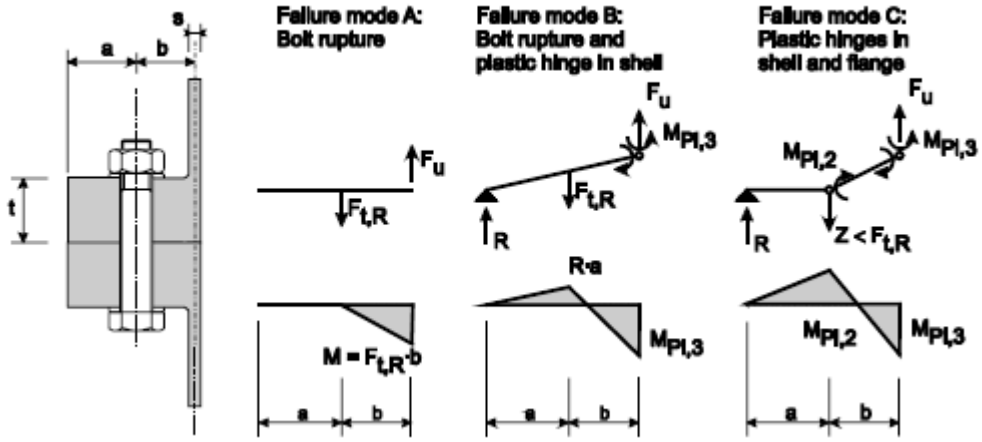

Figure 57: Failure modes of the simlified calculation method acc. to Petersen (Schaumann and Seidel 2000)

Figure 57 shows there are three main failure modes. These are shown by A, B and C. In mode A; the bolt is yielding, in mode B; the bold and tower is yielding and in mode C; the flange is yielding and the tower is yielding. In the following calculation method mode C is changed with failure mode D and E. Mode D and E were developed by Seidel.

As it can be seen in Figure 58, L-flange (single sided) and T-flange (double sided) have different geometries as well as conditions. As a result of these, same formulas cannot be applied to foundation. Therefore, following calculations will be examined in two different conditions.

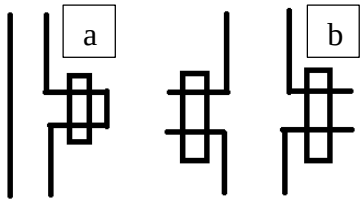

Figure 58: a) L-flange b) T-flange

Using EC3, allowable tension force for the bolt:

$$F_{t,Rd} = \frac{f_{y,k} * A_s}{1.1} \quad \textbf{(128)}$$

$F_{t,Rd}$: allowable tension force

$f_{y,k}$: characteristic yielding stress

A_s : stress area

$$Z = \frac{2 * M_{res}}{n * r_m} - \frac{F_{z,fl}}{n} \quad \textbf{(129)}$$

Z : actual tension force in the shell segment

M_{res} : max. design bending moment

n : number of equally distributed bolts

r_m : mean radious

$F_{z,fl}$: normal design force

The ultimate strength criteria must be fulfilled:

$$Z \leq Z_{U,min} = Min\left(Z_{U,A}, Z_{U,B}, Z_{U,D}, Z_{U,E}\right) \quad \textbf{(130)}$$

The calculation of $Z_{U,min}$ is thus an iterative process as the calculation of $M_{PL,3M/N}$ depend on $Z_{U,min}$..

Arc length between bolts could be determined by:

$$c_m = \frac{2 * \pi * r_m}{n} \quad \textbf{(131)}$$

c_m : arc length between bolts
r_m : mean radious
n : number of equally distributed bolts

Plastic shear force resistance might be determined by:

$$N_{PL,3} = f_{y,d,fl} * c_m * t_{neck} \quad \textbf{(132)}$$

$N_{PL,3}$: plastic shear force resistance
$f_{y,d,fl}$: flange design yielding stress
c_m : arc length between bolts
t_{neck} : flange neck thickness

Plastic moment resistance can be obtained by:

$$M_{PL,3,L} = \frac{f_{y,k,fl}}{\gamma_M} * \frac{c_m * t_{neck}^2}{4} \quad \textbf{(133)}$$

$M_{PL,3,L}$: plastic moment resistance (without shear)
$f_{y,k,fl}$: flange characteristic yielding stress
γ_M : yielding safety factor

c_m : arc length between bolts

t_{neck} : flange neck thickness

Plastic moment resistance could be expressed by:

$$M_{PL,3,M/N} = \left(1 - \left(\frac{Z_{U,min}}{N_{PL,3}}\right)^2\right) * M_{PL,3L} \quad \textbf{(134)}$$

$M_{PL,3,M/N}$: plastic moment resistance

$Z_{U,min}$: minimum allowable segment force

$N_{PL,3}$: plastic shear force resistance

$M_{PL,3,L}$: plastic moment resistance (without shear)

Arc length between bolt center might be determined by:

$$c = \frac{2 * \pi * r_{BC}}{n} \quad \textbf{(135)}$$

c : arc length between bolts

r_{BC} : radious from bolt center

n : number of equally distributed bolts

Plastic moment resistance could be expressed by:

$$M'_{PL,2} = f_{y,d,fl} * \frac{(c - d_H) * t_{fl}^2}{4} \quad \textbf{(136)}$$

$M'_{PL,2}$: plastic moment resistance

$f_{y,d,fl}$: flange design yielding stress

c : arc length between bolts

d_H : hole size

t_{fl} : flange thickness

$$\Delta M_{PL,2} = \frac{F_{t,Rd}}{2} * \frac{D_w + d_H}{4} \quad \textbf{(137)}$$

$\Delta M_{PL,2}$: permutation of plastic moment resistance

$F_{t,Rd}$: allowable tension force

D_w : washer outer diameter

d_H : hole size

t_{fl} : flange thickness

Plastic moment resistance could be expressed by:

$$M_{PL,2} = \frac{c * t_{fl}^2}{2} * f_{y,d,fl} \quad \textbf{(138)}$$

$M_{PL,2}$: plastic moment resistance

c : arc length between bolts

t_{fl} : flange thickness

$f_{y,d,fl}$: flange design yielding stress

Correction factor resistance:

$$b'_E = b - \frac{D_w + d_H}{4} \quad \textbf{(139)}$$

b'_E : correction factor

b : distance from bolt center to mean radious of shell

D_w : washer outer diameter

d_H : hole size

$$V_{PL,3} = \frac{f_{y,d,fl}}{\sqrt{3}} * c_m * t_{fl} \quad \textbf{(140)}$$

$V_{PL,3}$: plastic shear force resistance

$f_{y,d,fl}$: flange design yielding stress

c_m : arc length between bolts

t_{fl} : flange thickness

$$M_{PL,3,T} = \frac{f_{y,k,fl}}{\gamma_M} * \frac{c_m * t_{fl}^2}{4} \quad \textbf{(141)}$$

$M_{PL,3,T}$: plastic moment resistance (without shear)

$f_{y,k,fl}$: flange characteristic yielding stress

γ_M : yielding safety factor

c_m : arc length between bolts

t_{fl} : flange thickness

Plastic moment resistance could be expressed by:

$$M_{PL,3,M/V} = \left(1 - \left(\frac{Z_{U,min}}{2 * V_{PL,3}}\right)^2\right) * M_{PL,3T} \quad \textbf{(142)}$$

$M_{PL,3,M/V}$: plastic moment resistance

$Z_{U,min}$: minimum allowable segment force

$V_{PL,3}$: plastic shear force resistance

$M_{PL,3,T}$: plastic moment resistance (without shear)

4.4.1. L-flange (Single Sided) Calculations

Failure mode A, bolt rupture can be determined by:

$$Z_{U,A} = F_{r,Rd} \tag{143}$$

Failure mode B, bolt rupture and plastic "hinges" in shell can be determined by:

$$Z_{U,B} = \frac{F_{r,Rd} * a + M_{PL,3M/N}}{b} \tag{144}$$

Failure mode D, plastic "hinges" in shell and flange can be determined by:

$$Z_{U,D} = \frac{M'_{PL,2} + \Delta M_{PL,2} * a + M_{PL,3M/N}}{b} \tag{145}$$

Failure mode E, plastic "hinges" in shell and flange can be determined by:

$$Z_{U,E} = \frac{M_{PL,2} + M_{PL,3M/N}}{b'_E} \tag{146}$$

$Z_{U,A}$: allowable segment force mode A

$Z_{U,B}$: allowable segment force mode B

$Z_{U,D}$: allowable segment force mode D

$Z_{U,E}$: allowable segment force mode E

$F_{t,Rd}$: allowable tension force

a : distance between bolt center and inner diameter of section

$M_{PL,3,M/N}$: plastic moment resistance

b : distance from bolt center to mean radious of shell

$M'_{PL,2}$: plastic moment resistance

$\Delta M_{PL,2}$: permutation of plastic moment resistance

b'_E : correction factor

4.4.2. T-flange (Double Sided) Calculations

As it may observed in Figure 59, T-flange failure behavior has some similarity with L-flange however there are some different also. Therefore failure modes formulas have to be modified. Calculations can be seen in below.

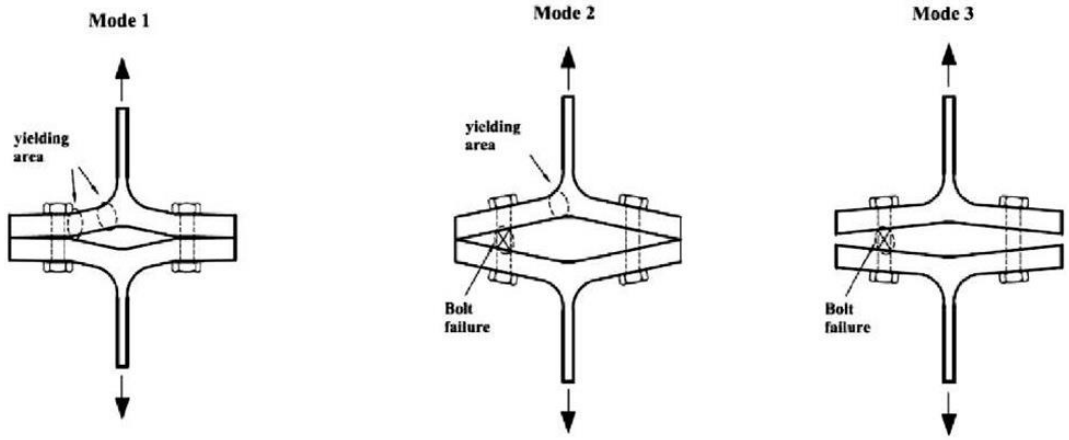

Figure 59: T-flange failure modes (CEN (European Commitee for Standardization) 2007b)

Failure mode A, bolt rupture can be determined by:

$$Z_{U,A} = 2 * F_{r,Rd} \quad \textbf{(147)}$$

Failure mode B, bolt rupture and plastic “hinges” in flange can be determined by:

$$Z_{U,B} = 2 * \frac{F_{r,Rd} * a + M_{PL,3M/V}}{a + b} \quad \textbf{(148)}$$

Failure mode D, plastic “hinges” in flange can be determined by:

$$Z_{U,D} = 2 * \frac{M'_{PL,2} + \Delta M_{PL,2} + M_{PL,3M/V}}{b} \quad \textbf{(149)}$$

Failure mode E, plastic “hinges” in flange can be determined by:

$$Z_{U,E} = \frac{M_{PL,2} + M_{PL,3M/V}}{b'_E} \quad \textbf{(150)}$$

$Z_{U,A}$: allowable segment force mode A

$Z_{U,B}$: allowable segment force mode B

$Z_{U,D}$: allowable segment force mode D

$Z_{U,E}$: allowable segment force mode E

$F_{t,Rd}$: allowable tension force

a : distance between bolt center and inner diameter of section

$M_{PL,3,M/V}$: plastic moment resistance

b : distance from bolt center to mean radious of shell

$M'_{PL,2}$: plastic moment resistance

$\Delta M_{PL,2}$: permutation of plastic moment resistance

b'_E : correction factor

4.4.3. Geometric Restrictions

Geometric restrictions which were developed by Seidel must be satisfied. Therefore, each bolt design must fulfill following criteria.

Characteristic yield strength of the bolt could be determined by:

$$F_{t,R} = f_{y,k} * A_s \quad \textbf{(151)}$$

$F_{t,R}$: characteristic yielding stress of the bolt
$f_{y,k}$: characteristic yielding stress
A_s : stress area

Resistance for L-flange:

$$M_{pl,3} = f_{y,k,fl} * \frac{c_m * t_{neck}^2}{4} \quad \textbf{(152)}$$

Resistance for T-flange:

$$M_{pl,3} = f_{y,k,fl} * \frac{c_m * t_{fl}^2}{4} \quad \textbf{(153)}$$

$M_{pl,3}$: plastic moment resistance
$f_{y,k,fl}$: flange characteristic yielding stress
c_m : arc length between bolts
t_{neck} : flange neck thickness

$$t_{fl,min} = t_B * \sqrt{\frac{a}{1.25 * b}} \quad \textbf{(154)}$$

$$t_B \geq \sqrt{\frac{\frac{F_{t,R} * M_{pl,3}}{a+b} * 8 * b - F_{t,R} * (D_w + d_H) - 8 * M_{pl,3}}{2 * (c - d_H) * f_{y,k,fl}}} \quad \textbf{(155)}$$

Maximum flange width must be:

$$a \leq 3 * b \quad \textbf{(156)}$$

$t_{fl,min}$: minimum flange thickness

t_B : bolt ratio

a : distance between bolt center and inner diameter of section

b : distance from bolt center to mean radious of shell

$F_{t,R}$: characteristic yielding stress of the bolt

$M_{pl,3}$: plastic moment resistance

D_w : washer outer diameter

d_H : hole size

c : arc length between bolts

$f_{y,k,fl}$: flange characteristic yielding stress

If below condition is satisfied, above restrictions have not need to provided:

$$Z_{U,A} \leq Z_{U,B} \leq Z_{U,D} \leq Z_{U,E} \quad \textbf{(157)}$$

4.4.4. Results

Regarding all these restrictions and rules presented above, following table was generated. Minimum forces for different failure modes can be seen in Table 21,

Table 21: Failure mode calculation results

			Bottom	Bottom Middle	Top Middle	
	Min. Allow. Force Failure Mode	A	1176	588	588	[kN]
	Min. Allow. Force Failure Mode	B	1072	425	378	[kN]
	Min. Allow. Force Failure Mode	C	-	-	-	[kN]
	Min. Allow. Force Failure Mode	D	416	450	671	[kN]
	Min. Allow. Force Failure Mode	E	735	1657	1993	[kN]
ZU,min	Minimum Allowable Seg. Force	Min. ZU	416	425	378	[kN]
	Eurocode Restriction 1		ok	ok	ok	
	Eurocode Restriction 2		ok	ok	ok	

Using Table 21, stress reserve factors might be drawn like Figure 60,

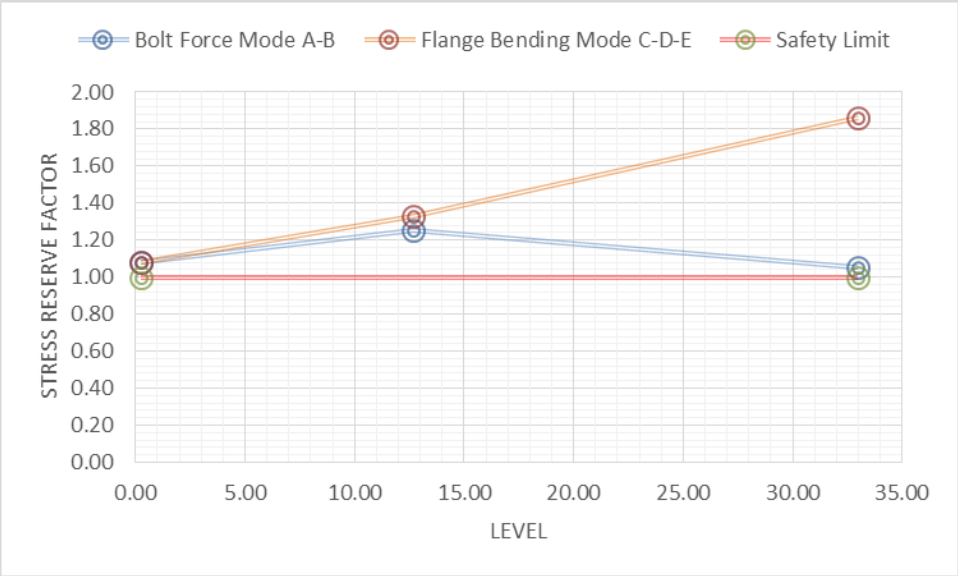

Figure 60: SRF's for bolt and flange

5. ULTIMATE STRENGTH OF CYLINDRICAL TOWERS WITH OPENING IN WIND TURBINE STRUCTURES

Door opening is one of the most critical aspects of the tower. Lack of proper estimation for door openings may lead to severe accidents that may result in huge damages. It can be stated that when a tower is considered to be a tube, an opening is the gap on the tower. The analyses were done based on the assumption that a door opening is a hole on the tower. The importance of the door opening on a tower can be understand clearly from Figure 61.

Figure 61: Wind tower accident due to wrong door opening estimatiıon (“WindAction | Wind Turbines and Public Safety: Setbacks Matter” n.d.)

The aims of this study are to numerically evaluate the effect of design parameters such as door shape, height, width, with or without stiffeners on the ultimate strength of cylindrical wind turbine structures and to efficiently find ideal dimensions of door openings.

The findings of the research have the potential to enhance the structural design and safety assessment of wind turbine structures with door openings.

5.1. Structure Features of Wind Turbine Structures and Openings

5.1.1. Definition of Geometrical Parameters

The geometrical attributes of a typical wind turbine with a door opening are defined as in Figure 62. The following 6 parameters are considered: (a) height to minimum diameter ratio of wind turbine (H/D_{MIN}); (b) height to maximum diameter ratio of wind turbine (H/D_{MAX}); (c) minimum diameter to minimum thickness ratio of wind turbine (D_{MIN}/T_{MIN}); (d) maximum diameter to maximum thickness ratio of wind turbine (D_{MAX}/T_{MAX}); (e) height to width ratio of door opening (h/b); (f) width to thickness ratio of door opening (b/t).

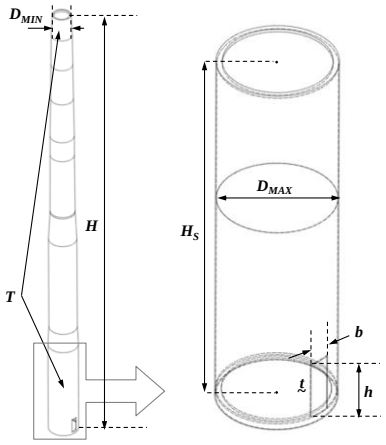

Figure 62: A schematic representation of typical wind turbine with a door opening

5.1.2. Geometrical Feature of Wind Turbine Structures

Data on 102 wind turbines with door opening were collected. The geometrical parameters defined in 5.1.1, were then calculated for the 102 wind turbines. Figure 63 and Figure 64 represent the statistical distribution of the parameters, and Table 22 and Table 23 summarizes results of the analysis. These findings were used to identify the geometrical parameters of a standard wind turbine with a door opening, as follows:

$H = 65{,}000\,\text{mm},\ D_{MAX} = 3750\,\text{mm},\ T_{MAX} = 30\,\text{mm},\ h = 1900\,\text{mm},\ b = 700\,\text{mm}$ and $t = 30\,\text{mm}$.

Figure 63 and Figure 64 illustrate data management, one can figure out how values are managed.

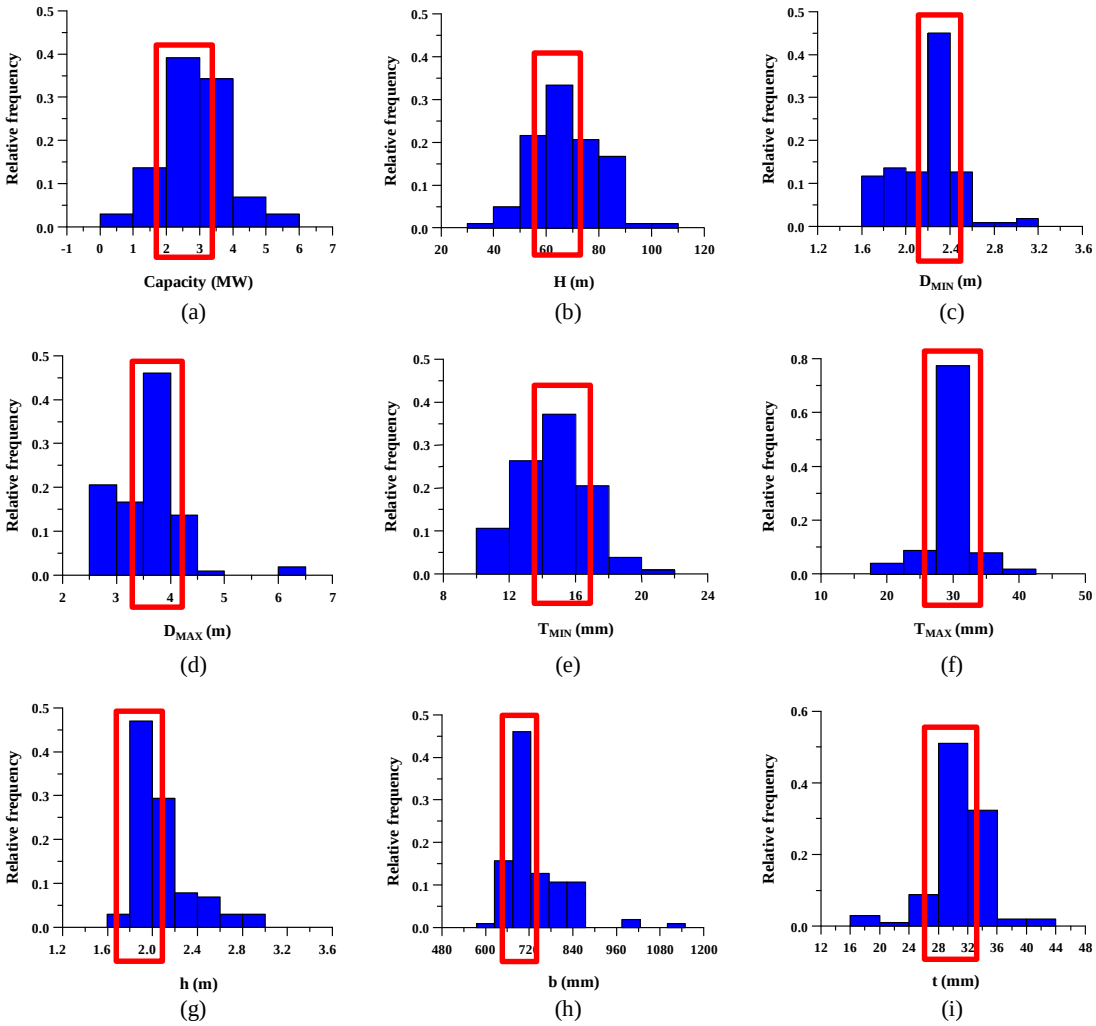

Figure 63: Geometrical characteristics of wind turbine and door opening: (a) capacity; (b) height of wind turbine; (c) maximum diameter of wind turbine; (d) minimum diameter of wind turbine; (e) minimum thickness of wind turbine; (f) maximum thickness of wind turbine; (g) height of door opening; (h) width of door opening; (i) thickness of door opening

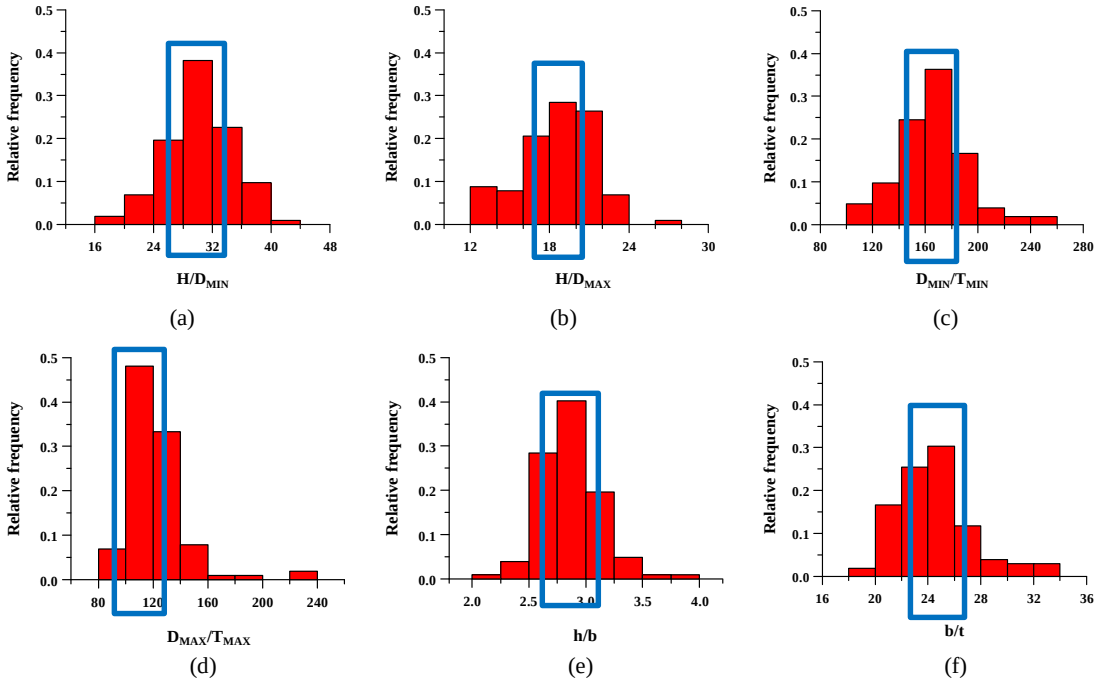

Figure 64: Geometrical characteristics of wind turbine and door opening: (a) height to minimum diameter ratio of wind turbine; (b) height to maximum diameter ratio of wind turbine; (c) minimum diameter to minimum thickness ratio of wind turbine; (d) maximum diameter to maximum thickness ratio of wind turbine; (e) height to width ratio of door opening; (f) width to thickness ratio of door opening

Most probable results of turbine and door opening can be observed in Table 22 and Table 23,

Table 22: Actual range and the most probable dimensions of wind turbine and door opening

Variable	Range	Most probable
Capacity (MW)	0.5~5.0	2.5
H (mm)	37,000~100,000	65,000
D_{MIN} (mm)	1,600~3,000	2,300
D_{MAX} (mm)	2,610~6,000	3,750
T_{MIN} (mm)	10~20	15
T_{MAX} (mm)	16~40	30

h (mm)	1,640~2,900	1,900
b (mm)	620~1,100	700
t (mm)	16~40	30.0

Table 23: Actual range and the most probable ratio of wind turbine and door opening

Variable	Range	Most probable
H / D_{MIN}	17.5~42.1	30.0
H / D_{MAX}	12.0~27.7	19.0
D_{MIN} / T_{MIN}	100.0~250.0	170.0
D_{MAX} / T_{MAX}	95.7~222.2	110.0
h / b	2.2~3.8	2.875
b / t	19.1~43.8	25.0

5.2. Nonlinear Finite Element Modelling

In this part of the report, door opening analyses of the tower will be investigated. During the analyses, welded parts are neglected therefore strength of the connection is more than normal. However, lifetime decreases.

5.2.1. Finite Element Model

A wind turbine with the door opening detailed in section 5.1.2 is regarded as subjected to bending moment in x-axis as shown in Figure 65,

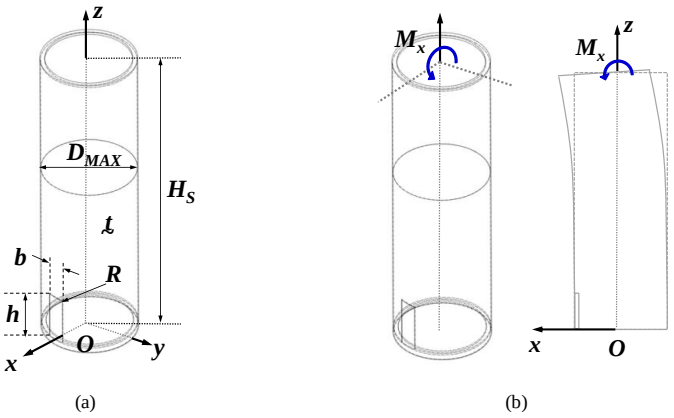

(a) (b)

Figure 65: A schematic representations of typical and applied geometries for the standard turbine with the door opening: (a) nomenclature; (b) typical geometry and applied loading.

Nonlinear finite element analysis is performed using ANSYS (2015), to accommodate both geometrical and material nonlinearities. The SOLID185 element, which has eight nodes with three degrees of freedom at each node, is used to model the wind turbine. The wind turbine is modelled based on the result of quasi-static material test as shown in Figure 65. The material is mild steel with an elastic modulus E of 205.8 GPa; a Poisson's ratio of ν 0.3; and a yield strength σ_Y of 299 MPa.

The maximum magnitude of initial deflection w_0 is assumed to be 30% of the thickness of the wind turbine; that is, the eigenvalue buckling mode is used to determine the shape of the initial deflection. Figure 66 provides an example of the smallest buckling mode near the door opening obtained from the eigenvalue buckling analysis.

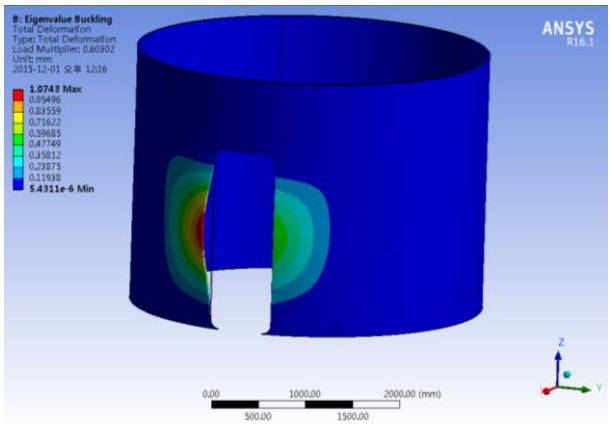

Figure 66: An example of 1st buckling mode under pure bending moment in x-axis

In order to validation of o material Figure 67 might be observed, all further works will be done by assuming following figure,

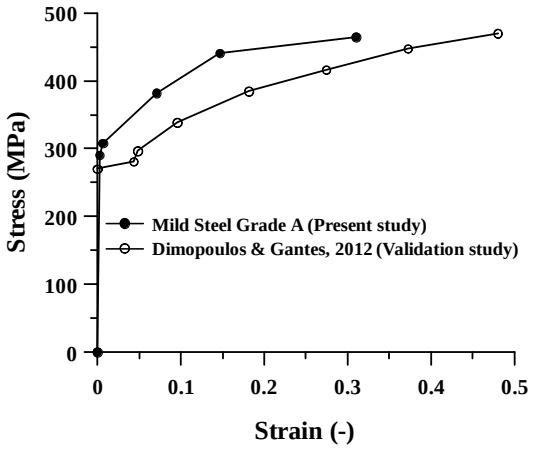

Figure 67: Applied material model for the present and validation studies

5.2.2. Boundary Conditions

The boundary conditions investigated in this study are described in Figure 68. The coordinate system used for their measurement is shown in Figure 68(a). The restraints are described in detail below. Fixed boundary condition, as shown in Figure 68(b),

Bottom surface: translational restraints in the x-, y- and z-directions, $u_x = u_y = u_z = 0$ rotational restraint in the x-, y- and z-direction, $\theta_x = \theta_y = \theta_z = 0$.

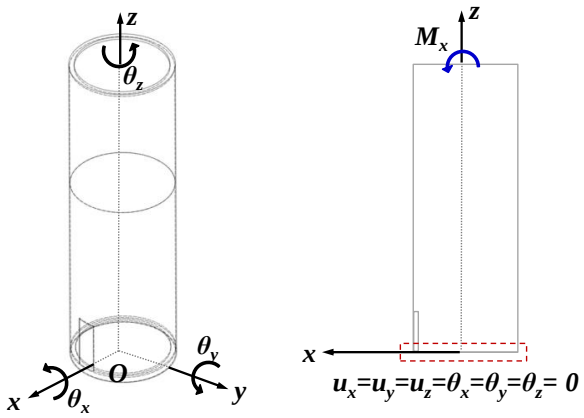

Figure 68: Coordinate system and applied boundary conditions of the wind turbine: (a) coordinate system; (b) fixed.

5.2.3. Mesh-Convergence Study

This section presents the results of mesh-convergence analysis of the wind turbine for 6-type of element sizes when σ_Y = 299 MPa and W_0 = 0.3tb, as shown in Figure 69. The ultimate bending moments about each element size are summarized in Figure 70. Approximately 35,000 elements are sufficient to estimate the ultimate bending moment of the wind turbine.

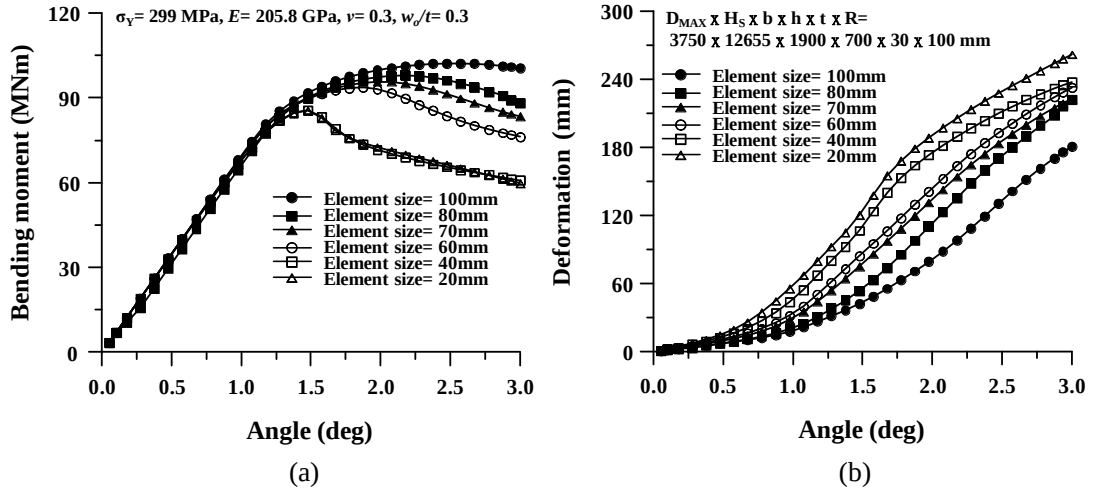

Figure 69: Results of mesh-convergence study for D_{MAX} x H_S = 3750 x 12655 mm, h x b x t x R = 1950 x 700 x 30 x 100 mm, σ_Y = 299 MPa, w_0 = 0.3t : (a) bending moment; (b) deformation

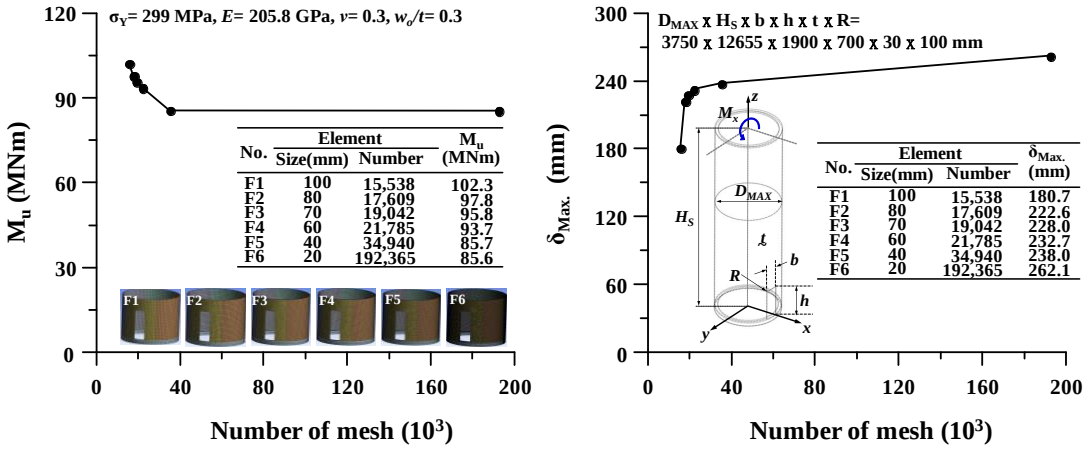

(a) (b)

Figure 70: Results of mesh-convergence study for D_{MAX} x H_S = 3750 x 12655 mm, h x b x t x R = 1950 x 700 x 30 x 100 mm, σ_Y = 299 MPa, w_0 = 0.3t : (a) bending moment; (b) deformation

5.2.4. Validation with Experiment

The FE modeling technique developed in the present study was validated with the experimental result (Dimopoulos and Gantes 2012). Figure 72 shows the result of validation study for the model as shown in Figure 71. It is confirmed that the developed FE modelling technique is effective for simulating ultimate strength of the wind turbine.

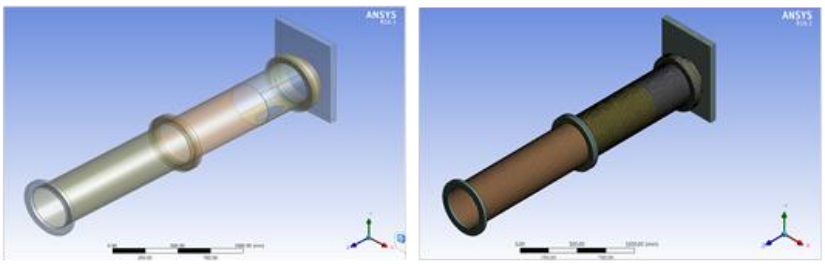

(a) (b)

Figure 71: Geometry information for validation study: (a) applied geometry model; (b) applied mesh model.

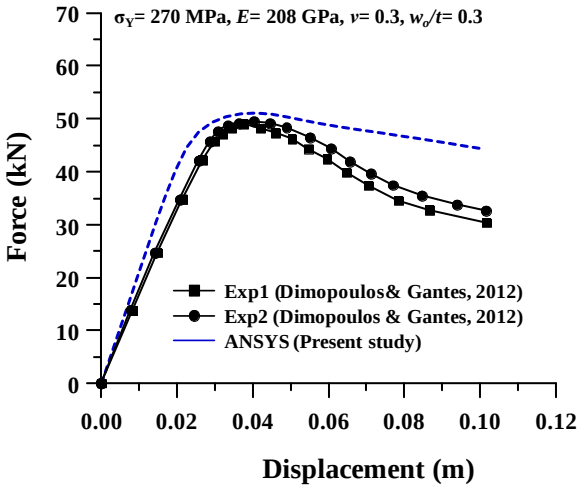

Figure 72: Validation study on developed FE modelling technique (Dimopoulos and Gantes 2012)

5.3. Effect of Opening Shapes

To investigate the effect of opening shape on the ultimate strength of the wind turbine, four-type of shapes including no opening, rectangular, elliptical and combination of half-rectangular and half-elliptical were considered. To examine accurate comparison, the shape varied from dimensions of the standard door opening, h x b x t = 30 mm. Applied geometries are presented in Figure 73.

Figure 74 illustrates the numerical results for four-type of the door opening shapes in terms of 1st buckling mode, stress distribution and total deformation. Figure 75 describes the comparison of the bending moment against the no opening model. It is found that the reduction rate of ultimate strength occurs significantly and the elliptical shape appears the lowest reduction rate. However, it is surmised that the half-rectangular and elliptical model is more proper for considering practical purposes.

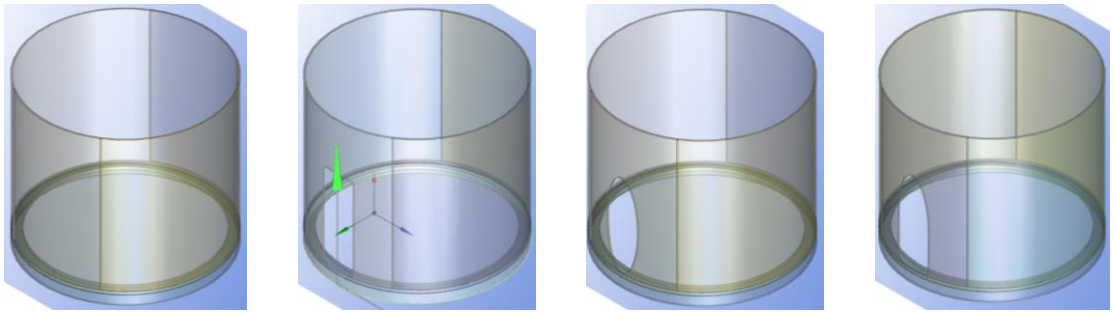

(a) (b) (c) (d)

Figure 73: Applies geometries of the door opening: (a) no opening; (b) rectangular; (c) elliptical; (d) half-rectangular and -elliptical.

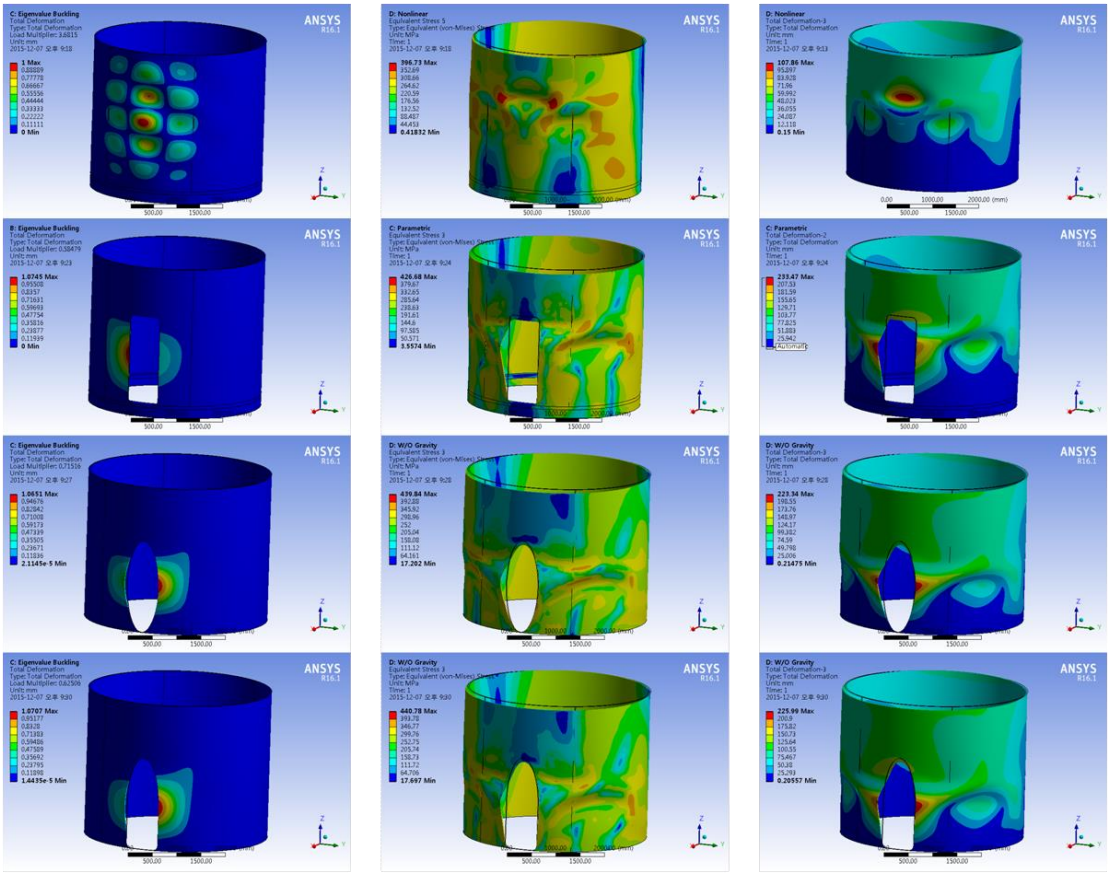

Figure 74: Comparisons of numerical computations for different door opening shapes: (a) 1st buckling mode; (b) stress distribution at rotation angle 3 degrees; (c) deformation at rotation angle 3 degrees.

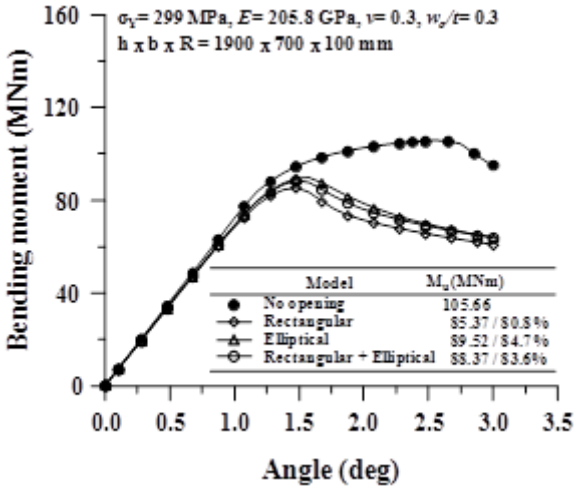

Figure 75: Comparisons of bending moment for different shapes of the door opening.

5.4. Effect of Stiffeners

To identity the effect of stiffener on the ultimate strength of half-rectangular and -elliptical door opening, three-type of stiffeners including edge stiffener, flat bar stiffener and door-shaped stiffener were considered. Applied geometries are presented in Figure 76. For simplicity, the cross section of the stiffener is assumed as a flat-bar and its dimension is h_w x t_w = 50 x 30 mm.

Figure 77 illustrates the numerical results for three-type of the door opening shapes with different stiffeners in terms of 1st buckling mode, stress distribution and total deformation. Figure 78 describes the comparison of the bending moment against the no opening model. It is found that the reduction rate of ultimate strength could be decreased by adding stiffeners. It is observed that approximately, 10% of ultimate strength has been enhanced in case of edge-stiffener and flat-bar stiffener.

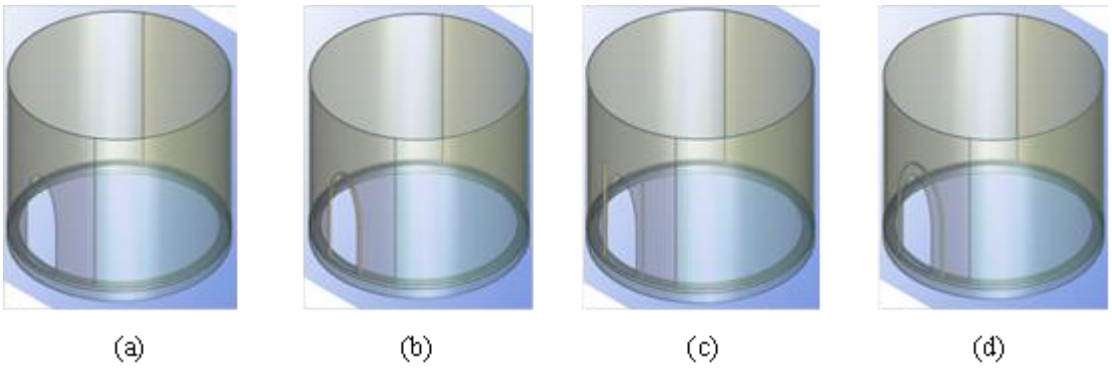

Figure 76: Applied stiffener geometries of the door opening: (a) no stiffener; (b) edge stiffener; (c) flat-bar stiffener; (d) door-shaped stiffener

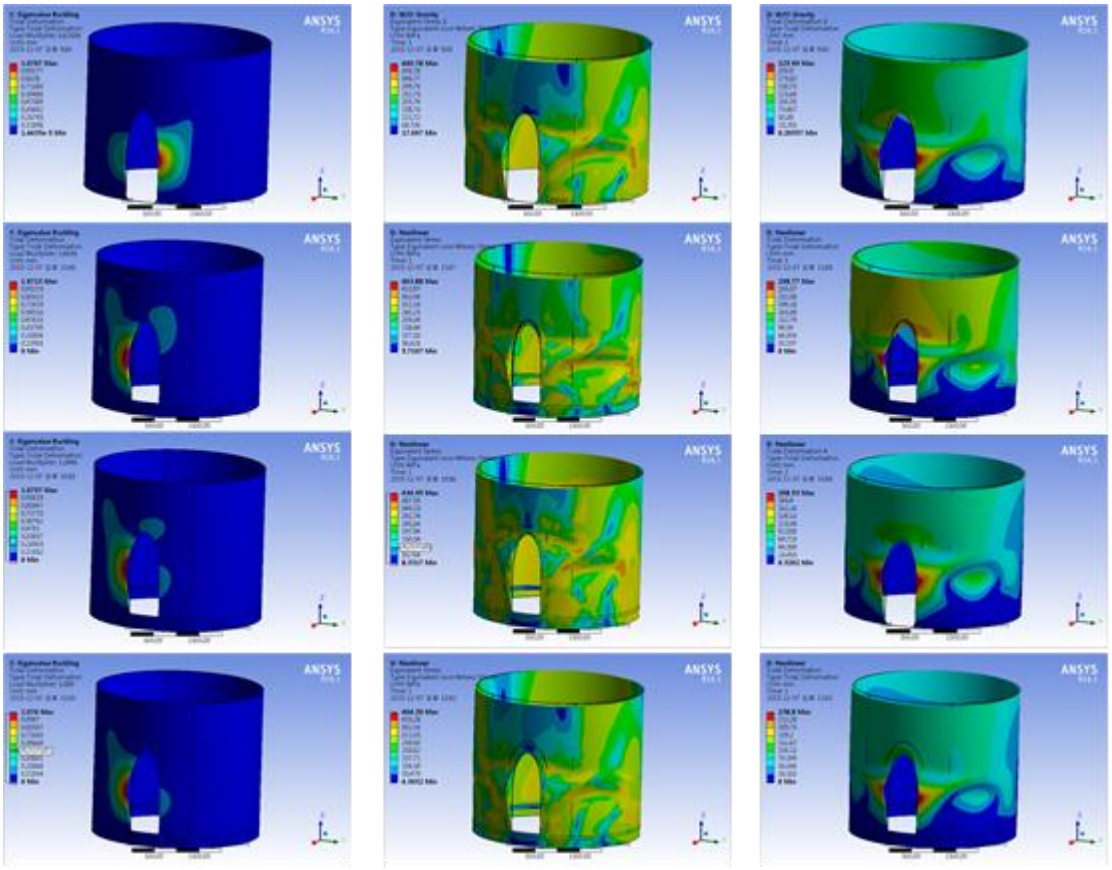

Figure 77: Comparisons of numerical computations for different stiffeners: (a) 1st buckling mode; (b) stress distribution at rotation angle 3 degrees; (c) deformation at rotation angle 3 degrees

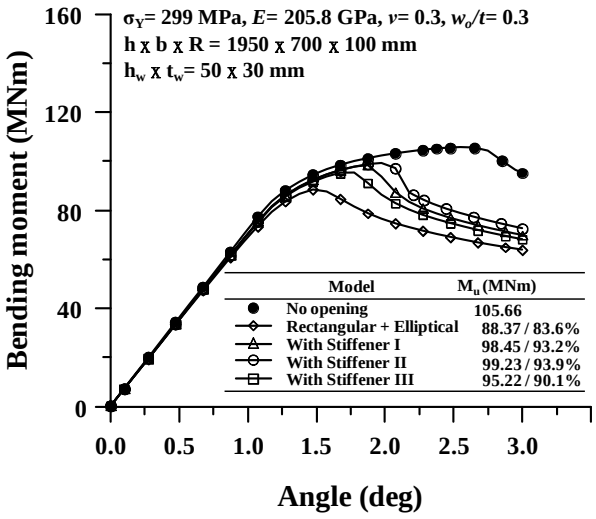

Figure 78: Comparisons of bending moment for different stiffeners of the door opening

5.5. Ideal Door Opening

As a result of all these FEM analysis, ideal door shape of the tower has been decided and it can be seen in Figure 79. As it was mentioned above the geometrical parameters of a standard wind turbine with a door opening, as follows:

$H = 65{,}000\,\text{mm},\ D_{MAX} = 3750\,\text{mm},\ T_{MAX} = 30\,\text{mm},\ h = 1900\,\text{mm},\ b = 700\,\text{mm}$ and $t = 30\,\text{mm}.$

These values were chosen because of the Figure 63 and Figure 64. For details Table 22 and Table 23 might be seen. As it can be seen above, total length of the tower is too high. Therefore, meshing is quite important. In Figure 70, converged mesh size has been found and it is around 35000 elements. In order to understand, results that was found is acceptable and applicable, validation was done. Figure 72 illustrates that tower values are strong enough compare with real cases. Then effect of the door opening was examined. As it is shown in Figure 73, four different types of door opening were examined. As a result of this evaluation, “elliptical” and “half rectangular and half elliptical” models gave best two results. For details, Figure 75 might be seen. Considering to accessibility of door opening and production “half rectangular and half elliptical” model was the most satisfied model. In order to improve door strength, stiffeners should be applied on the door opening. Figure 76 illustrates stiffener types that were being

planned to apply. Figure 78 shows that most considerable result is stiffener II. This model also easiest applicable model. Chosen model can be seen in Figure 79.

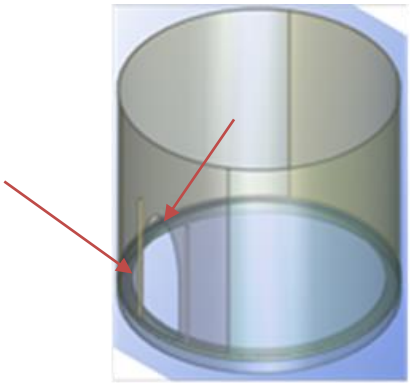

Figure 79: Final door model

6. COST ANALYSIS

This section of thesis covers cost analysis. However it should be stated that calculations and estimations were done rather roughly. This fact is resulted from the time limitation of the work and strict confidentiality policies of the companies. Despite the fact that several companies were contacted, internal regulations and market condition, the companies were reluctant to share these information. Therefore estimations and analysis presented in this section were done theoretically. Also final results were obtained based on a similar wind tower which has similar dimensions and features. It is fair to state that results may be misleading, further research is required for more valid outcomes.

According to (Lanier and Way 2005), main costs for wind turbine:

- Construction of a road to the tower locations
- Construction of site construction offices and furnishings
- Recruitment of management personnel and labor for the tower construction effort
- Design of any special construction equipment needed
- Mobilization, monthly rental, and operating costs for cranes
- Equipment move-in costs

- Construction project mobilization costs
- Foundation construction
- Steel tube tower fabrication, shipping, site assembly, and erection
- Precast concrete fabrication, shipping, site erection, and integration
- Semi-self-erection of hybrid steel/concrete tower
- Erection and installation of turbine nacelle, hub and rotor (but not the procurement cost for these elements)
- Final installation and touch up.

As it can be seen above, many different aspects make sense on the cost. Therefore, there is no chance to talk about only one cost. This situation effects market in a competitive way. As a result of this, companies are not open to share their cost approach so much. On the other hand, prices for articles that might be seen above, it may illustrate big different due to location. For instance, labor cost in Germany and labor cost in Kenya has big difference.

6.1. Fabrication Cost

According to (Jármai and Farkas 1999), fabrication cost of welded structures can be estimated by following method.

$$K = K_m + K_f = k_m * \rho * V + k_f \sum_i T_i \quad \textbf{(158)}$$

Where,

K : cost function
K_m : material cost
K_f : fabrication cost
k_m : material cost factor
k_f : fabrication cost factor
ρ : density of the material
V : volume of the structure

T_i : production times

Production time can be divided into 7 different parts. These are preparation time, time of welding, time of additional fabrication actions, time for flattening plates, surface preparation time, painting time and cutting and edge grinding times.

Considering all these assumptions flange fabrication cost calculation might be seen in following title.

6.1.1. Flange Fabrication Cost

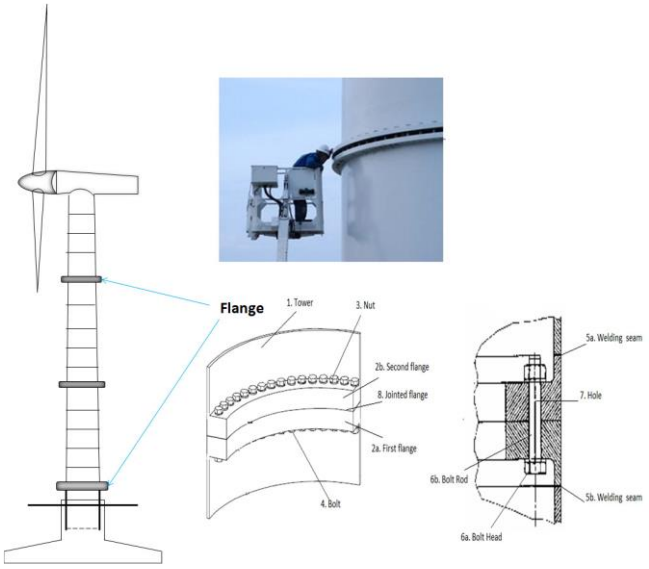

Figure 80: Bolted ring flange connection (Verma 2011)

Basic view of bolted tower can be seen in Figure 80, in order to estimate material cost better, (Husson 2008) was used as a reference. The material costs for flanges and bolts were taken from (Husson 2008). Additionally fabrication cost should be added. Especially drilling and machining are critic and costly. (Lanier and Way 2005) estimate cost around 3000 Dollars (2736 Euros) per piece. In addition to fabrication, assembly for bolting cost is also added. Reference values are taken from (Verma 2011). Final results for these calculation can be seen in Table 24,

Table 24: Foundation cost of flange connection

Component	Unit Price [€]	Amount	Total Price [€]
Flange	4395.00	3.00	13185.00
Bolt (M36x10.9)	11.40	400.00	4560.00
Machining and Drilling	2736.00	3.00	8208.00
Welding Assembly Cost	24235.61	1.00	24235.61
Bolt Assembly Cost	752.00	1.00	752.00
		Total	50940.61

Two conical sections/flanges is welded by using submerged arc welding technique. This technique can be used for different part of the tower. Circumferential weld for wind tower can be calculated by following formula:

$$V_{total} = 2 * \pi * R * t * L_{wi} \quad \textbf{(159)}$$

$$K_{cir} = k_F * \left(\theta_w * \sqrt{K\rho V_{total}} + (1.3 * 0.1559 * 10^{-3} * t^2 * (K-1) * L_{wi})\right) \quad \textbf{(160)}$$

K : number of element to be assembled which in this case is 2

θ_W : difficulty factor in this case is 2

ρ : density of the material

$L_{w,i}$: circumference of the can

t : wall thickness

R : radius of the conical tower

V_{total} : total volume of two sections getting welded

K_{cir} : longitudinal weld cost

k_F : labour cost factor

6.2. Final Cost Estimation

As it was mentioned above, due to company regulations enough data for cost wasn't provided. Because of this, some already installed tower prices were checked. One of the example in (Lanier and Way 2005) carries on similar characteristic. Therefore, cost is being expected around 2150000 € as it can be seen in Table 25 and Figure 81.

Table 25: Tower cost breakdown for 3.6-MW (Lanier and Way 2005)

	3.6 MW All Tubular Steel Wind Design	
	Cost	% of Total
Mobilization & Site Development	262466 $	11%
Foundation Construction	200056 $	9%
Shop Fabrication of Steel Tube and Flange Rings	1138083 $	50%
Field Erection of Steel Tube	127070 $	6%
Tower Concrete Fabrication	0 $	0%
Field Erection of Precast and Post Tensioning	0 $	0%
Jack-Up of Steel Tube within Hybrid Tower	16354 $	1%
Complete Concrete To Steel Connection and install Nacelle and Rotor	20400 $	23%
General Contractor Mark-ups	529330 $	100%
Total Cost	2293759 $	

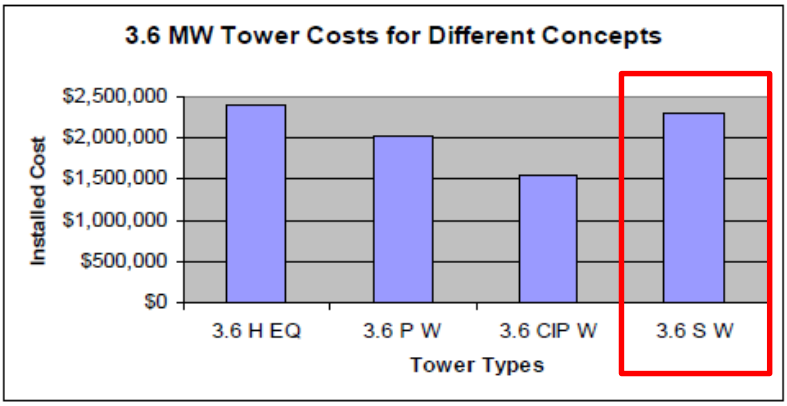

Figure 81: Wind turbine tower cost comparisons for 3.6-MW (Lanier and Way 2005)

7. CONCLUSION AND DISCUSSION

The presented work covers the design of wind turbine tower and its door opening based on standards and present models in the market. The calculations and results are already presented in the thesis and appendices. As a summary, it can be stated that data is gathered and based on the conducted research, the most common tower was selected. The selected tower is modelled and modified based on the standards. Calculations based on previous experimental measurements were carried out on yielding, buckling, dynamic and fatigue providing the standards. The most critical location of the tower was assumed to be door opening. FEM calculation was done for the most widely used types used in market. The ideal one was decided. Finally a rough cost estimation was conducted and presented within the context of thesis.

Several notes can be mentioned regarding the work. First of all, number of initial data might be more. Also it might be gathered directly from the companies for better accuracy of information. However due to limited time of the internship and overall preparation of the thesis, it is fair to state that current data is quite acceptable. Furthermore, initial research covered data from first applications of this technology. Therefore recent trend is not fully represented in the selection of the most common wind turbine tower. The selected height was between 60 to 80 meters, however in current applications higher towers are seen, which are around 100 meters.

It may be noted regarding the wind turbine tower selection that Class B type was selected as production technology. As it is already present in the 4.2 section, selection of Class B reduced the costs of production. However it also resulted in the lower quality of structure. Still all the standards were satisfied and this fact resulted in no problems.

The calculations were done based on experimental results instead of theoretical calculations. This fact results in more valid and realistic design of the tower. The calculations for foundation of the structure were done based on the assumption that both on-shore and off-shore structures have the same characteristics. Based on this assumption, all calculations were done according to on-shore foundation.

The door opening selection was done in a similar fashion with tower selection. Data was gathered and the most common ones were selected. Still it should be noted that in recent applications several other types of door openings are present in the market due to development of production technologies.

Cost estimation part was already briefly criticized in respective section. It can be mentioned that due to limited time and confidentiality policies of companies, the results presented should be evaluated as roughly made for the initial state of the work. Therefore for better estimation of cost, this part should be covered with more data.

Overall, despite the assumptions made, it can be clearly stated that the calculations and designs presented within the work are valid and acceptable. The objectives that were presented initially were satisfied mainly, except the cost estimation part.

As it was mentioned before, the first objective fulfilled was to design a wind turbine tower and an ideal door opening satisfying the standards. In the recent part, with door and without door analyses were done and big strength difference can be observed, further researchers can figure out that door opening important subject for towers. Furthermore it was aimed to create a work that can be used as a guideline for future works in the same filed. It can be suggested that steps of designing a tower are clearly presented within the thesis and it may be used as stepping stone with certain developments. The other goal was to underline the importance of the subject. It can be clearly seen from the literature search and detailed calculations and design steps presented that the subject of wind turbine tower is highly important in recent years and will draw more attention in future.

7.1. Future Research

The thesis aimed to show producers, how to design a wind tower by using standards in order to avoid costly production resulting from non-standard-satisfactory production. The second purpose is to prove the importance of the door opening in wind turbine tower design. Fundamentals of these two goals were completed within the thesis. However some parts of the report still needs further improvement.

Firstly, instead of the probabilistic design of the tower, some optimization program could be used such as “EOLOS”. Therefore, according to the loads, better geometry of the tower can be found. It would also take less time compared to probabilistic design.

During the calculation flanges was assumed same as cans. Then failure modes of flanges was calculated. For buckling, flanges can be evaluated individually.

Number of experimental data may be increased which will eventually lead to generation of other tower types. In this case, the analysis approach presented in the thesis may be implemented for these types as well. Especially, fatigue data may be improved. Furthermore, not only wind loads but also wave loads may be considered in the offshore wind towers. One sample can be developed by using wave loads on the foundation.

In this thesis bolts-flanges fatigue calculations were not done. Fatigue values for bolt and flange must be evaluated. It is also another crucial point of view, which is neglected in this work.

3 types of door openings and 3 types of stiffeners were examined in this thesis. In reality, one can see more than 3 types, therefore data of door opening and stiffeners may be increased to have results for several types. As a result of that, most ideal opening can be found. Also considering fatigue connections, door fatigue calculation can be done.

Cost estimation should be studied in details. A basic software may be developed in EXCEL, then cost can be estimated clearly. Nevertheless, confidentiality problem is still an obstacle for this work.

8. REFERENCES

"ACCIONA Windpower Inaugurates the First Concrete Tower Production Plant in Mexico." http://www.acciona.com/news/acciona-windpower-inaugurates-first-concrete-tower-production-plant-mexico (October 19, 2015).

Achmus, Prof M et al. "Work Package 2 : Ocean Energy System Test – Standardisation and Best Practice Testing D2 . 6 : Report on Offshore Wind System Monitoring Practice and Normalisation Procedures."

Amirouche, Farid. 2006. Mark's Standard Handbook for Mechanical Engineers *Introduction to the Finite-Element Method*.

Aydin, Can. 2007. "Analysis and Optimization of Monopile Type Offshore Wind and Wave Loading." Bogazici University.

CEN (European Commitee for Standardization). 2005a. "ENV 1993-1-1: 2005, Design of Steel Structures-Part 1-1." *General Rules and Rules for Buildings,CEN*.

———. 2005b. "ENV 1993-1-9: 2005, Design of Steel Structures-Part 1-9." *Eurocode 3* 9(2005).

———. 2007a. "ENV 1993-1-1: 2005, Design of Steel Structures-Part 1-3."

———. 2007b. "ENV 1993-1-6: 2005, Design of Steel Structures-Part 1-6." *Eurocode 3* 6(2007).

Det Norske Veritas. 2011. "DNV-OS-J101 Design of Offshore Wind Turbine Structures." (September): 213.

"Development of the Cost of Wind-Generated Power." http://www.wind-energy-the-facts.org/development-of-the-cost-of-wind-generated-power.html (December 13, 2015).

Dimopoulos, C. A., and C. J. Gantes. 2012. "Experimental Investigation of Buckling of Wind Turbine Tower Cylindrical Shells with Opening and Stiffening under Bending." *Thin-Walled Structures* 54: 140–55. http://linkinghub.elsevier.com/retrieve/pii/S0263823112000419.

"EngrApps: Burst and Collapse - Pressure Vessel Design." http://engrapps.com/mechanical-systems-and-materials/mechanical-components/pressure-vessels/burst-collapse-

analysis.php (October 23, 2015).

"Everything You Need to Know About Small Wind Turbines." http://greenterrafirma.com/small_turbines.html (October 19, 2015).

"Excel Interpolation Formulas - Peltier Tech Blog." http://peltiertech.com/excel-interpolation-formulas/ (October 20, 2015).

"Force and Strength." http://www.pt.ntu.edu.tw/hmchai/bm02/bm02method/ForceMeasure.htm (October 21, 2015).

Germanischer Lloyd Industrial Services GmbH. 2010. "Guidline for the Certification of Wind Turbines." *Germanischer Lloyd*: 384.

GWEC. 2012. "Global Wind Report." *Wind energy technology*: 72.

"Heavy Lift Vessel 'Atlantic' Delivered to Her Owners - CONOSHIP." http://www.conoship.com/en_heavy-lift-vessel-atlantic-delivered-to-her-owners,120.html (October 19, 2015).

Husson, Wylliam. 2008. "Friction Connections with Slotted Holes for Wind Towers." : 213. http://pure.ltu.se/portal/files/36285679/LTU_LIC_0845_SE.pdf.

Jármai, K., and J. Farkas. 1999. "Cost Calculation and Optimisation of Welded Steel Structures." *Journal of Constructional Steel Research* 50: 115–35.

Kanbur, Faik Alper. 2014. "500 KW Enerji Kapasiteli Bir Ruzgar Turbinin Çelik Kule Tasarimi." Istanbul Technical University.

Karimirad, Madjid. 2014. *Offshore Energy Structures: For Wind Power, Wave Energy and Hybrid Marine Platforms*.

Lanier, M W, and Federal Way. 2005. "LWST Phase I Project Conceptual Design Study : Evaluation of Design and Construction Approaches for Economical Hybrid Steel / Concrete Wind Turbine Towers LWST Phase I Project Conceptual Design Study : Evaluation of Design and Construction Approaches for ." (January).

"New Wind and Solar Sectors Won't Solve China's Water Scarcity | Circle of Blue WaterNews." http://www.circleofblue.org/waternews/2011/world/new-wind-and-solar-sectors-

wont-solve-chinas-water-scarcity/ (October 19, 2015).

"Prefabricated DYWIDAG Tendons Secure Innovative ATS Hybrid Wind Tower - DYWIDAG-Systems International." https://www.dywidag-systems.com/emea/projects/project-details/article/innovative-ats-hybrid-wind-tower-germany.html (October 19, 2015).

Schaumann, P, and M Seidel. 2000. "Failure Analysis of Bolted Steel Flanges." *Proceedings of the 7th International Symposium on Structural Failure and Plasticity (Implast 2000)* (Implast): 1–6.

Shakya, Anil. "Wind Load Assessment for Steel Lattice." : 1–7.

"SPECIFIC ACTION OF STRESSES - 14014_74." http://navyaviation.tpub.com/14014/css/14014_74.htm (October 21, 2015).

Standard, European. 2004. "S355 European Standard Steel." 1(7): 1–7.

"Steel Grades according to American Standards - A36, A572, A588, A709, A913, A992." : 992.

"Stress Strain Diagram For Ductile And Brittle Materials - Transtutors." http://www.transtutors.com/homework-help/mechanical-engineering/simple-stresses-and-strain/stress-strain-diagram-for-ductile-and-brittle-materials.aspx (October 19, 2015).

"The Inside of a Wind Turbine | Department of Energy." http://energy.gov/eere/wind/inside-wind-turbine-0 (October 19, 2015).

"Theory -8." https://courses.cit.cornell.edu/virtual_lab/chalktalks/theory/8.shtml (October 21, 2015).

"Torsion (mechanics) - Wikipedia, the Free Encyclopedia." https://en.wikipedia.org/wiki/Torsion_(mechanics) (January 9, 2016).

Travanty, By Frank. 2001. "Tower and Antenna Wind Loading as a." : 23–33.

US DOE. 2014. "2013 Wind Technologies Market Report (Presentation)." (August). http://energy.gov/sites/prod/files/2014/08/f18/2013 Wind Technologies Market Report Presentation.pdf.

Verma, Ankit. 2011. "Adhesive Bonded Towers for Wind Turbines. Design, Optimization and Cost Analysis." (November): 83.

"Wind Basics - Hill Country Wind Power." http://www.hillcountrywindpower.com/wind-basics.php (December 13, 2015).

"Wind Farm | Riley Group." http://www.riley-group.com/wind-farm/ (October 19, 2015).

"Wind Turbine Risks to Seabirds: New Tool Maps Birds' Sensitivity to Offshore Farms (Constantine Alexander's Blog)." http://www.constantinealexander.net/2014/11/wind-turbine-risks-to-seabirds-new-tool-maps-birds-sensitivity-to-offshore-farms.html (October 19, 2015).

"WindAction | Wind Turbines and Public Safety: Setbacks Matter." http://www.windaction.org/posts/31986-wind-turbines-and-public-safety-setbacks-matter#.Vmmqf_mrTIU (December 10, 2015).

9. APPENDIX

9.1. Experimental Load Input Data

Sensor No	Sensor Height	Ext. Des. Bending Moment	Partial Coefficient	Max. Char. Bending Moment	Max. Des. Torsion	Max. Des. Shear Force	Des. Normal Force Tower Top	Wind Speed
-	-	Mresd	γ_f	Mresc	M_{zd}	$F_{resp,d}$	F_{zc}	V
[#]	[m]	[kNm]	[-]	[kNm]	[kNm]	[kN]	[kN]	[m/s]
1	0	57898	1.35	-	-1069	-98	-1284.6	56.5
2	0.2	57702	1.35	-	-1069	-98	-1284.6	56.5
3	7.4	50667	1.35	-	-1069	-98	-1284.7	56.5
4	12.6	45684	1.35	-	-1069	-98	-1283.5	56.6
5	18.3	40242	1.35	-	-1069	-98	-1284.2	56.6
6	28.8	30562	1.35	-	-1069	-98	-1282.1	56.6
7	33	26818	1.35	-	-1069	-98	-1240.8	57.5
8	41.7	19392	1.35	-	-1069	-98	-1470.4	13.8
9	50.2	13008	1.35	-	-1069	-98	-1480.8	13.7
10	55.4	9418	1.35	-	-1069	-98	-1487.7	13.7
11	63	5539	1.35	-	-1015	-44	-1442.6	23.4

9.2. Interpolated Experimental Load Input Data

Cross Section Number	Level	Ext. Des. Bending Moment Interpolation	Normal Force Design	Max. Des. Torsion	Max. Des. Shear Force	Wind Speed
-	H	M_{resd}	F	M_{zd}	$F_{resp,d}$	V
(#)	[m]	[kNm]	[kN]	[kNm]	[kN]	[m/s]
38	63.000	5539.000	1443.000	-1015.000	-44	23.400
37	62.750	5666.599	1462.000	-1017.000	-45.776	23.081
36	62.600	5727.846	1465.000	-1018.000	-46.629	22.928
35	59.900	7097.746	1519.000	-1037.000	-65.67	19.502
34	57.600	8261.446	1559.000	-1053.000	-81.9	16.592
33	55.400	9427.665	1595.000	-1069.000	-98	13.700
32	53.100	11001.742	1615.000	-1069.000	-98	13.700
31	50.200	12977.623	1644.000	-1069.000	-98	13.700
30	47.400	15122.982	1671.000	-1069.000	-98	13.733
29	44.500	17270.259	1700.000	-1069.000	-98	13.767
28	41.600	19419.314	1730.000	-1069.000	-98	13.961
27	38.800	21857.091	1691.000	-1069.000	-98	28.306
26	35.900	24293.160	1656.000	-1069.000	-98	42.642
25	33.100	26728.376	1624.000	-1069.000	-98	56.973
24	33.075	26753.983	1623.000	-1069.000	-98	57.123
23	33.000	26818.000	1631.000	-1069.000	-98	57.500
22	32.900	26884.857	1642.000	-1069.000	-98	57.484
21	32.895	26911.600	1643.000	-1069.000	-98	57.478
20	30.850	28734.571	1695.000	-1069.000	-98	57.039
19	28.800	30557.543	1748.000	-1069.000	-98	56.601
18	26.700	32442.686	1783.000	-1069.000	-98	56.600
17	23.900	35042.457	1834.000	-1069.000	-98	56.600
16	21.100	37640.385	1886.000	-1069.000	-98	56.600
15	18.300	40235.547	1939.000	-1069.000	-98	56.600
14	15.400	42920.037	1996.000	-1069.000	-98	56.600
13	12.685	45602.847	2053.000	-1069.000	-98	56.600
12	12.655	45631.490	2053.000	-1069.000	-98	56.600
11	12.560	45722.331	2069.000	-1069.000	-98	56.599
10	12.465	45813.366	2085.000	-1069.000	-98	56.597
9	12.435	45842.114	2085.000	-1069.000	-98	56.597
8	10.300	47868.854	2132.000	-1069.000	-98	56.556
7	7.400	50676.771	2199.000	-1069.000	-98	56.500
6	5.800	52142.396	2240.000	-1069.000	-98	56.500
5	2.900	55005.250	2321.000	-1069.000	-98	56.500
4	0.300	57594.521	2393.000	-1069.000	-98	56.500
3	0.270	57633.604	2395.000	-1069.000	-98	56.500
2	0.200	57702.000	2417.000	-1069.000	-98	56.500
1	0.000	57898.000	2423.000	-1069.000	-98	56.500

9.3. Load Input Data

Cross Section Number	Level	Mean Diameter	Thickness	Dimensionless Length Parameter	Cross Section Area	Moment of Inertia	Ext. Des. Bending Moment	Normal Force Design	Max. Des. Torsion	Max. Des. Shear Force	Wind Speed	Drag Coefficient	Wind Pressure		Section Length Buckling	Load Case
-	H	D_{mi}	t_i	ω	A	I	M_{resd}	F_{zd}	M_z	$F_{res\ p,d}$	V	k_w	q_{wmax}	q_{eq}	L	-
(#)	[m]	[m]	[mm]	[-]	[m2]	[m4]	[kNm]	[kN]	[kNm]	[kN]	[m/s]	[-]	[kN/m2]	[kN/m2]	[m]	[-]
38	63.000	2.300	130	197.814	0.9393	0.6231	5539.0	1443	-1015	-44.00	23.4	0.65	335.381	0.436	30000	-
37	62.750	2.300	20	197.814	0.1445	0.0956	5666.6	1462	-1017	-45.78	23.081	0.65	326.299	0.424	30000	-
36	62.600	2.300	20	197.814	0.1445	0.0956	5727.8	1465	-1018	-46.63	22.928	0.65	321.987	0.419	30000	-
35	59.900	2.600	15	214.834	0.1225	0.1035	7097.7	1519	-1037	-65.67	19.502	0.65	232.951	0.303	30000	-
34	57.600	2.600	15	214.834	0.1225	0.1035	8261.4	1559	-1053	-81.90	16.592	0.65	168.618	0.219	30000	-
33	55.400	2.700	15	210.819	0.1272	0.1159	9427.7	1595	-1069	-98.00	13.7	0.65	114.960	0.149	30000	-
32	53.100	2.700	15	210.819	0.1272	0.1159	11001.7	1615	-1069	-98.00	13.7	0.65	114.960	0.149	30000	-
31	50.200	2.800	15	207.020	0.1319	0.1293	12977.6	1644	-1069	-98.00	13.7	0.65	114.960	0.149	30000	-
30	47.400	2.800	15	207.020	0.1319	0.1293	15123.0	1671	-1069	-98.00	13.733	0.65	115.515	0.150	30000	-
29	44.500	3.000	15	200.000	0.1414	0.1590	17270.3	1700	-1069	-98.00	13.767	0.65	116.087	0.151	30000	-
28	41.600	3.000	18	182.574	0.1696	0.1909	19419.3	1730	-1069	-98.00	13.961	0.65	119.382	0.155	30000	-
27	38.800	3.000	18	182.574	0.1696	0.1909	21857.1	1691	-1069	-98.00	28.306	0.65	490.753	0.638	30000	-
26	35.900	3.000	18	182.574	0.1696	0.1909	24293.2	1656	-1069	-98.00	42.642	0.65	1113.733	1.448	30000	-
25	33.100	3.100	18	179.605	0.1753	0.2106	26728.4	1624	-1069	-98.00	56.973	0.65	1988.128	2.585	30000	-
24	33.075	3.100	170	179.605	1.6556	1.9948	26754.0	1623	-1069	-98.00	57.123	0.65	1998.610	2.598	30000	-
23	33.000	3.100	170	122.371	1.6556	1.9948	26818.0	1631	-1069	-98.00	57.5	0.65	2025.078	2.633	20440	-
22	32.900	3.100	18	122.371	0.1753	0.2106	26884.9	1642	-1069	-98.00	57.484	0.65	2023.951	2.631	20440	-
21	32.895	3.100	18	122.371	0.1753	0.2106	26911.6	1643	-1069	-98.00	57.478	0.65	2023.529	2.631	20440	-
20	30.850	3.100	18	122.371	0.1753	0.2106	28734.6	1695	-1069	-98.00	57.039	0.65	1992.737	2.591	20440	-
19	28.800	3.500	20	109.256	0.2199	0.3368	30557.5	1748	-1069	-98.00	56.601	0.65	1962.250	2.551	20440	-
18	26.700	3.500	20	109.256	0.2199	0.3368	32442.7	1783	-1069	-98.00	56.6	0.65	1962.181	2.551	20440	-
17	23.900	3.500	20	109.256	0.2199	0.3368	35042.5	1834	-1069	-98.00	56.6	0.65	1962.181	2.551	20440	-
16	21.100	3.500	20	109.256	0.2199	0.3368	37640.4	1886	-1069	-98.00	56.6	0.65	1962.181	2.551	20440	-
15	18.300	3.500	20	109.256	0.2199	0.3368	40235.5	1939	-1069	-98.00	56.6	0.65	1962.181	2.551	20440	-
14	15.400	3.600	20	107.728	0.2262	0.3664	42920.0	1996	-1069	-98.00	56.6	0.65	1962.181	2.551	20440	-
13	12.685	3.750	20	105.552	0.2356	0.4142	45602.8	2053	-1069	-98.00	56.6	0.65	1962.181	2.551	20440	-
12	12.655	3.750	190	105.552	2.2384	3.9448	45631.5	2053	-1069	-98.00	56.6	0.65	1962.181	2.551	20440	-
11	12.560	3.750	190	59.519	2.2384	3.9448	45722.3	2069	-1069	-98.00	56.599	0.65	1962.111	2.551	12360	-
10	12.465	3.750	23	59.519	0.2710	0.4763	45813.4	2085	-1069	-98.00	56.597	0.65	1961.973	2.551	12360	-
9	12.435	3.750	25	57.088	0.2945	0.5177	45842.1	2085	-1069	-98.00	56.597	0.65	1961.973	2.551	12360	-
8	10.300	3.750	25	57.088	0.2945	0.5177	47868.9	2132	-1069	-98.00	56.556	0.65	1959.131	2.547	12360	-
7	7.400	3.750	30	52.114	0.3534	0.6213	50676.8	2199	-1069	-98.00	56.5	0.65	1955.253	2.542	12360	-
6	5.800	3.750	30	52.114	0.3534	0.6213	52142.4	2240	-1069	-98.00	56.5	0.65	1955.253	2.542	12360	-
5	2.900	3.750	30	52.114	0.3534	0.6213	55005.3	2321	-1069	-98.00	56.5	0.65	1955.253	2.542	12360	-
4	0.300	3.750	30	52.114	0.3534	0.6213	57594.5	2393	-1069	-98.00	56.5	0.65	1955.253	2.542	12360	-
3	0.270	3.750	200	52.114	2.3562	4.1535	57633.6	2395	-1069	-98.00	56.5	0.65	1955.253	2.542	12360	-
2	0.200	3.750	30	0.843	0.3534	0.6213	57702.0	2417	-1069	-98.00	56.5	0.65	1955.253	2.542	200	-
1	0.000	3.750	30	0.843	0.3534	0.6213	57898.0	2423	-1069	-98.00	56.5	0.65	1955.253	2.542	200	-

9.4. Stress Calculation

Cross Section Number	Level	Mean Radius	Thickness	Normal Stress	Bending Stress	Shear Stress Torsion	Shear Stress Force	Total Normal Stress	Total Shear Stress	Hoop Stress	Total Ref. Stress (Von Misses)
-	H	rmi	t	σ_n	σ_b	τ_{tors}	τ_{shear}	σ_z	$\sigma_{z\theta}$	σ_θ	σ_{ref}
(#)	[m]	[m]	[m]	[N/mm2]	[N/mm2]	[N/mm2]	[N/mm2]	[N/mm2]	[N/mm2]	[N/mm2]	[N/mm2]
38	63.000	1.150	0.13	10.0	67.8	-6.2	-0.61	77.8	-6.8	0.0251	78.68
37	62.750	1.150	0.02	10.1	69.4	-6.2	-0.63	79.5	-6.9	0.0244	80.36
36	62.600	1.150	0.02	10.1	70.1	-8.3	-0.65	80.3	-8.9	0.0241	81.72
35	59.900	1.300	0.015	12.4	90.1	-6.6	-1.07	102.5	-7.7	0.0262	103.39
34	57.600	1.300	0.015	12.7	104.9	-6.7	-1.34	117.7	-8.0	0.0190	118.46
33	55.400	1.350	0.015	12.5	111.0	-6.3	-1.54	123.5	-7.8	0.0135	124.26
32	53.100	1.350	0.015	12.7	129.5	-6.3	-1.54	142.2	-7.8	0.0135	142.85
31	50.200	1.400	0.015	12.5	142.0	-5.8	-1.49	154.5	-7.3	0.0139	154.98
30	47.400	1.400	0.015	12.7	165.5	-5.8	-1.49	178.1	-7.3	0.0140	178.59
29	44.500	1.500	0.015	12.0	164.5	-4.3	-1.39	176.5	-5.6	0.0151	176.79
28	41.600	1.500	0.018	10.2	154.5	-4.3	-1.16	164.6	-5.4	0.0129	164.91
27	38.800	1.500	0.018	10.0	173.8	-4.3	-1.16	183.8	-5.4	0.0532	184.02
26	35.900	1.500	0.018	9.8	193.2	-4.3	-1.16	203.0	-5.4	0.1207	203.13
25	33.100	1.550	0.018	9.3	199.0	-0.5	-1.12	208.3	-1.6	0.2226	208.19
24	33.075	1.550	0.17	9.3	199.2	-0.5	-1.12	208.5	-1.6	0.2237	208.37
23	33.000	1.550	0.17	9.3	199.7	-4.0	-1.12	209.0	-5.1	0.2267	209.06
22	32.900	1.550	0.018	9.4	200.2	-4.0	-1.12	209.5	-5.1	0.2266	209.62
21	32.895	1.550	0.018	9.4	200.4	-4.0	-1.12	209.8	-5.1	0.2265	209.82
20	30.850	1.550	0.018	9.7	214.0	-3.6	-1.12	223.6	-4.7	0.2231	223.66
19	28.800	1.750	0.02	7.9	160.6	-2.8	-0.89	168.6	-3.7	0.2232	168.57
18	26.700	1.750	0.02	8.1	170.5	-2.8	-0.89	178.6	-3.7	0.2232	178.63
17	23.900	1.750	0.02	8.3	184.2	-2.8	-0.89	192.5	-3.7	0.2232	192.52
16	21.100	1.750	0.02	8.6	197.8	-2.8	-0.89	206.4	-3.7	0.2232	206.41
15	18.300	1.750	0.02	8.8	211.5	-2.8	-0.89	220.3	-3.7	0.2232	220.28
14	15.400	1.800	0.02	8.8	213.2	-2.7	-0.87	222.0	-3.5	0.2296	221.96
13	12.685	1.875	0.02	8.7	208.6	-0.3	-0.83	217.4	-1.1	0.2391	217.25
12	12.655	1.875	0.19	8.7	208.8	-0.3	-0.83	217.5	-1.1	0.2391	217.38
11	12.560	1.875	0.19	7.6	182.2	-2.1	-0.72	189.8	-2.9	0.2079	189.79
10	12.465	1.875	0.023	7.7	182.6	-2.0	-0.72	190.2	-2.7	0.2079	190.20
9	12.435	1.875	0.025	7.1	168.2	-2.0	-0.67	175.3	-2.6	0.1913	175.27
8	10.300	1.875	0.025	7.2	175.7	-1.6	-0.67	182.9	-2.3	0.1910	182.86
7	7.400	1.875	0.03	6.2	155.4	-1.6	-0.55	161.6	-2.2	0.1589	161.57
6	5.800	1.875	0.03	6.3	159.9	-1.6	-0.55	166.2	-2.2	0.1589	166.18
5	2.900	1.875	0.03	6.6	168.7	-1.6	-0.55	175.2	-2.2	0.1589	175.18
4	0.300	1.875	0.03	6.8	176.6	-0.3	-0.55	183.4	-0.8	0.1589	183.29
3	0.270	1.875	0.2	1.0	176.7	-1.6	-0.55	177.7	-2.2	0.1589	177.69
2	0.200	1.875	0.03	6.8	176.9	-1.6	-0.55	183.8	-2.2	0.1589	183.72
1	0.000	1.875	0.03	6.9	177.5	-1.6	-0.55	184.4	-2.2	0.1589	184.34

9.5. Meridional Buckling Stress

Cross Section Number	Level		Mean Radius	Thickness	Dimensionless Length Parameter	Correction Factor	Elastic Critical Meridional Buckling Stress	Characteristic Imperfection Amplitude	Elastic Imperfection Reduction Factor	Plastic Limit Relative Slenderness	Relative Slenderness	Buckling Reduction Factor	Characteristic Yield Strength	Meridional Characteristic Buckling Stress	Partial Factor	Meridional Design Buckling Stress
-	H		r_{mi}	t_i	ω	C_x	$\sigma_{x,Rcr}$	Δw_k	α_x	$\bar{\lambda}_p$	$\bar{\lambda}_x$	χ_x	f_{yk}	$\sigma_{x,Rk}$	γ_{M1}	$\sigma_{x,Rd}$
(#)	[m]		[mm]	[mm]	[-]	[-]	[N/mm2]	[-]	[-]	[-]	[-]	[-]	[N/mm2]	[N/mm2]	[-]	[N/mm2]
38	63.000		1150.000	20.000	197.814	0.804	1776.454	6.066	0.462	1.074	0.441	0.835	345.000	288.021	1.200	240.018
37	62.750		1150.000	20.000	197.814	0.804	1776.454	6.066	0.462	1.074	0.441	0.835	345.000	288.021	1.200	240.018
36	62.600		1150.000	20.000	197.814	0.804	1776.454	6.066	0.462	1.074	0.441	0.835	345.000	288.021	1.200	240.018
35	59.900		1300.000	15.000	214.834	0.868	1272.566	5.586	0.425	1.030	0.521	0.768	345.000	265.041	1.200	220.867
34	57.600		1300.000	15.000	214.834	0.868	1272.566	5.586	0.425	1.030	0.521	0.768	345.000	265.041	1.200	220.867
33	55.400		1350.000	15.000	210.819	0.877	1238.274	5.692	0.421	1.026	0.528	0.762	345.000	262.815	1.200	219.013
32	53.100		1350.000	15.000	210.819	0.877	1238.274	5.692	0.421	1.026	0.528	0.762	345.000	262.815	1.200	219.013
31	50.200		1400.000	15.000	207.020	0.885	1205.335	5.797	0.417	1.021	0.535	0.755	345.000	260.575	1.200	217.146
30	47.400		1400.000	15.000	207.020	0.885	1205.335	5.797	0.417	1.021	0.535	0.755	345.000	260.575	1.200	217.146
29	44.500		1500.000	15.000	200.000	0.900	1143.450	6.000	0.410	1.013	0.549	0.742	345.000	256.065	1.200	213.388
28	41.600		1500.000	18.000	182.574	0.887	1352.738	6.573	0.428	1.035	0.505	0.781	345.000	269.361	1.200	224.468
27	38.800		1500.000	18.000	182.574	0.887	1352.738	6.573	0.428	1.035	0.505	0.781	345.000	269.361	1.200	224.468
26	35.900		1500.000	18.000	182.574	0.887	1352.738	6.573	0.428	1.035	0.505	0.781	345.000	269.361	1.200	224.468
25	33.100		1550.000	18.000	179.605	0.894	1319.444	6.681	0.425	1.031	0.511	0.775	345.000	267.438	1.200	222.865
24	33.075		1550.000	18.000	179.605	0.894	1319.444	6.681	0.425	1.031	0.511	0.775	345.000	267.438	1.200	222.865
23	33.000		1550.000	18.000	122.371	0.939	1384.820	6.681	0.425	1.031	0.499	0.784	345.000	270.481	1.200	225.401
22	32.900		1550.000	18.000	122.371	0.939	1384.820	6.681	0.425	1.031	0.499	0.784	345.000	270.481	1.200	225.401
21	32.895		1550.000	18.000	122.371	0.939	1384.820	6.681	0.425	1.031	0.499	0.784	345.000	270.481	1.200	225.401
20	30.850		1550.000	18.000	122.371	0.939	1384.820	6.681	0.425	1.031	0.499	0.784	345.000	270.481	1.200	225.401
19	28.800		1750.000	20.000	109.256	0.950	1379.531	7.483	0.424	1.029	0.500	0.783	345.000	270.074	1.200	225.062
18	26.700		1750.000	20.000	109.256	0.950	1379.531	7.483	0.424	1.029	0.500	0.783	345.000	270.074	1.200	225.062
17	23.900		1750.000	20.000	109.256	0.950	1379.531	7.483	0.424	1.029	0.500	0.783	345.000	270.074	1.200	225.062
16	21.100		1750.000	20.000	109.256	0.950	1379.531	7.483	0.424	1.029	0.500	0.783	345.000	270.074	1.200	225.062
15	18.300		1750.000	20.000	109.256	0.950	1379.531	7.483	0.424	1.029	0.500	0.783	345.000	270.074	1.200	225.062
14	15.400		1800.000	20.000	107.728	0.954	1346.073	7.589	0.421	1.026	0.506	0.777	345.000	268.224	1.200	223.520
13	12.685		1875.000	20.000	105.552	0.958	1298.653	7.746	0.417	1.021	0.515	0.769	345.000	265.458	1.200	221.215
12	12.655		1875.000	20.000	105.552	0.958	1298.653	7.746	0.417	1.021	0.515	0.769	345.000	265.458	1.200	221.215
11	12.560		1875.000	20.000	63.827	0.988	1338.864	7.746	0.417	1.021	0.508	0.775	345.000	267.425	1.200	222.854
10	12.465		1875.000	23.000	59.519	0.985	1534.573	8.307	0.430	1.037	0.474	0.804	345.000	277.220	1.200	231.016
9	12.435		1875.000	25.000	57.088	0.983	1664.504	8.660	0.438	1.047	0.455	0.819	345.000	282.586	1.200	235.489
8	10.300		1875.000	25.000	57.088	0.983	1664.504	8.660	0.438	1.047	0.455	0.819	345.000	282.586	1.200	235.489
7	7.400		1875.000	30.000	52.114	0.978	1987.559	9.487	0.455	1.066	0.417	0.850	345.000	293.221	1.200	244.351
6	5.800		1875.000	30.000	52.114	0.978	1987.559	9.487	0.455	1.066	0.417	0.850	345.000	293.221	1.200	244.351
5	2.900		1875.000	30.000	52.114	0.978	1987.559	9.487	0.455	1.066	0.417	0.850	345.000	293.221	1.200	244.351
4	0.300		1875.000	30.000	52.114	0.978	1987.559	9.487	0.455	1.066	0.417	0.850	345.000	293.221	1.200	244.351
3	0.270		1875.000	18.000	67.279	0.990	1207.818	7.348	0.406	1.008	0.534	0.752	345.000	259.309	1.200	216.091
2	0.200		1875.000	30.000	0.843	2.101	4270.556	9.487	0.455	1.066	0.284	0.942	345.000	324.868	1.200	270.723
1	0.000		1875.000	30.000	0.843	2.101	4270.556	9.487	0.455	1.066	0.284	0.942	345.000	324.868	1.200	270.723

9.6. Circumferential Buckling Stress

Cross Section Number	Level	H	Mean Radius	Thickness	Dimensionless Length Parameter	Dimensionless Length Parameter by External Pressure Buckling Factor	Correction Factor	Elastic Critical Circumferential Buckling Stresses	Drag Coefficient	Equivalent Axisymmetric Wind Pressure	Plastic Limit Relative Slenderness	Relative Slenderness	Buckling Reduction Factor	Characteristic Yield Strength	Circumferential Characteristic Buckling Stress	Partial Factor	Circumferential Design Buckling Stress
-	-	H	r_{mi}	t_i	ω	ω/C_θ	$C_{\theta E}$	$\sigma_{\theta,Ecr}$	k_{wi}	q_{eq}	λ_p	λ_θ	χ_θ	f_{yk}	$\sigma_{\theta,Rk}$	γ_{M1}	$\sigma_{\theta,Rd}$
(#)		[m]	[mm]	[mm]	[-]	[-]	[-]	[N/mm2]	[-]	[N/mm2]	[-]	[-]	[-]	[N/mm2]	[N/mm2]	[-]	[N/mm2]
	38	63.000	1150.000	20.000	197.814	197.814	1.500	22.127	0.490	0.001	1.275	3.949	0.042	345.000	14.383	1.200	11.985
	37	62.750	1150.000	20.000	197.814	197.814	1.500	22.127	0.490	0.001	1.275	3.949	0.042	345.000	14.383	1.200	11.985
	36	62.600	1150.000	20.000	197.814	197.814	1.500	22.127	0.490	0.001	1.275	3.949	0.042	345.000	14.383	1.200	11.985
	35	59.900	1300.000	15.000	214.834	214.834	1.500	15.298	0.496	0.001	1.275	4.749	0.029	345.000	9.944	1.200	8.287
	34	57.600	1300.000	15.000	214.834	214.834	1.500	15.298	0.496	0.001	1.275	4.749	0.029	345.000	9.944	1.200	8.287
	33	55.400	1350.000	15.000	210.819	210.819	1.500	15.979	0.497	0.001	1.275	4.647	0.030	345.000	10.387	1.200	8.655
	32	53.100	1350.000	15.000	210.819	210.819	1.500	15.979	0.497	0.001	1.275	4.647	0.030	345.000	10.387	1.200	8.655
	31	50.200	1400.000	15.000	207.020	207.020	1.500	16.865	0.498	0.001	1.275	4.523	0.032	345.000	10.962	1.200	9.135
	30	47.400	1400.000	15.000	207.020	207.020	1.500	16.865	0.498	0.001	1.275	4.523	0.032	345.000	10.962	1.200	9.135
	29	44.500	1500.000	15.000	200.000	200.000	1.500	19.263	0.500	0.001	1.275	4.232	0.036	345.000	12.521	1.200	10.434
	28	41.600	1500.000	18.000	182.574	182.574	1.500	21.804	0.498	0.001	1.275	3.978	0.041	345.000	14.173	1.200	11.811
	27	38.800	1500.000	18.000	182.574	182.574	1.500	21.804	0.498	0.001	1.275	3.978	0.041	345.000	14.173	1.200	11.811
	26	35.900	1500.000	18.000	182.574	182.574	1.500	21.804	0.498	0.001	1.275	3.978	0.041	345.000	14.173	1.200	11.811
	25	33.100	1550.000	18.000	179.605	179.605	1.500	23.167	0.499	0.001	1.275	3.859	0.044	345.000	15.059	1.200	12.549
	24	33.075	1550.000	18.000	179.605	179.605	1.500	23.167	0.499	0.001	1.275	3.859	0.044	345.000	15.059	1.200	12.549
	23	33.000	1550.000	18.000	122.371	122.371	1.501	27.502	0.507	0.001	1.275	3.542	0.052	345.000	17.876	1.200	14.897
	22	32.900	1550.000	18.000	122.371	122.371	1.501	27.502	0.507	0.001	1.275	3.542	0.052	345.000	17.876	1.200	14.897
	21	32.895	1550.000	18.000	122.371	122.371	1.501	27.502	0.507	0.001	1.275	3.542	0.052	345.000	17.876	1.200	14.897
	20	30.850	1550.000	18.000	122.371	122.371	1.501	27.502	0.507	0.001	1.275	3.542	0.052	345.000	17.876	1.200	14.897
	19	28.800	1750.000	20.000	109.256	109.256	1.501	30.314	0.510	0.001	1.275	3.374	0.057	345.000	19.704	1.200	16.420
	18	26.700	1750.000	20.000	109.256	109.256	1.501	30.314	0.510	0.001	1.275	3.374	0.057	345.000	19.704	1.200	16.420
	17	23.900	1750.000	20.000	109.256	109.256	1.501	30.314	0.510	0.001	1.275	3.374	0.057	345.000	19.704	1.200	16.420
	16	21.100	1750.000	20.000	109.256	109.256	1.501	30.314	0.510	0.001	1.275	3.374	0.057	345.000	19.704	1.200	16.420
	15	18.300	1750.000	20.000	109.256	109.256	1.501	30.314	0.510	0.001	1.275	3.374	0.057	345.000	19.704	1.200	16.420
	14	15.400	1800.000	20.000	107.728	107.728	1.501	29.890	0.511	0.001	1.275	3.397	0.056	345.000	19.429	1.200	16.190
	13	12.685	1875.000	20.000	105.552	105.552	1.501	29.286	0.513	0.001	1.275	3.432	0.055	345.000	19.036	1.200	15.863
	12	12.655	1875.000	20.000	105.552	105.552	1.501	29.286	0.513	0.001	1.275	3.432	0.055	345.000	19.036	1.200	15.863
	11	12.560	1875.000	20.000	63.827	63.827	1.502	48.431	0.528	0.001	1.275	2.669	0.091	345.000	31.480	1.200	26.234
	10	12.465	1875.000	23.000	59.519	59.519	1.503	59.727	0.526	0.001	1.275	2.403	0.113	345.000	38.823	1.200	32.352
	9	12.435	1875.000	25.000	57.088	57.088	1.503	67.685	0.525	0.001	1.275	2.258	0.128	345.000	43.995	1.200	36.662
	8	10.300	1875.000	25.000	57.088	57.088	1.503	67.685	0.525	0.001	1.275	2.258	0.128	345.000	43.995	1.200	36.662
	7	7.400	1875.000	30.000	52.114	52.114	1.504	88.974	0.522	0.001	1.275	1.969	0.168	345.000	57.833	1.200	48.194
	6	5.800	1875.000	30.000	52.114	52.114	1.504	88.974	0.522	0.001	1.275	1.969	0.168	345.000	57.833	1.200	48.194
	5	2.900	1875.000	30.000	52.114	52.114	1.504	88.974	0.522	0.001	1.275	1.969	0.168	345.000	57.833	1.200	48.194
	4	0.300	1875.000	30.000	52.114	52.114	1.504	88.974	0.522	0.001	1.275	1.969	0.168	345.000	57.833	1.200	48.194
	3	0.270	1875.000	18.000	67.279	67.279	1.502	41.351	0.530	0.001	1.275	2.888	0.078	345.000	26.878	1.200	22.399
	2	0.200	1875.000	30.000	0.843	0.843	7.224	26482.803	0.945	0.002	1.275	0.114	1.000	345.000	345.000	1.200	287.500
	1	0.000	1875.000	30.000	0.843	0.843	7.224	26482.803	0.945	0.002	1.275	0.114	1.000	345.000	345.000	1.200	287.500

9.7. Shear Buckling Stress

Cross Section Number	Level	Mean Radius	Thickness	Dimensionless Length Parameter	Correction Factor	Elastic Critical Shear Buckling Stress	Plastic Limit Relative Slendernes	Relative Slenderness	Buckling Reduction Factor	Characteristic Yield Strength	Shear Characteristic Buckling Stress	Partial Factor	Shear Design Buckling Stress
-	H	r_{mi}	ti	ω	C_τ	$\tau_{x\theta,Rcr}$	$\bar{\lambda}_p$	$\bar{\lambda}_\tau$	χ_τ	f_{yk}	$\tau_{x\theta,Rk}$	γ_{M1}	$\tau_{x\theta,Rd}$
(#)	[m]	[mm]	[mm]	[-]	[-]	[N/mm2]	[-]	[-]	[-]	[N/mm2]	[N/mm2]	[-]	[N/mm2]
38	63.000	1150.000	20.000	197.814	1.000	194.753	1.275	1.011	0.581	345.000	115.666	1.200	96.388
37	62.750	1150.000	20.000	197.814	1.000	194.753	1.275	1.011	0.581	345.000	115.666	1.200	96.388
36	62.600	1150.000	20.000	197.814	1.000	194.753	1.275	1.011	0.581	345.000	115.666	1.200	96.388
35	59.900	1300.000	15.000	214.834	1.000	123.987	1.275	1.267	0.405	345.000	80.668	1.200	67.224
34	57.600	1300.000	15.000	214.834	1.000	123.987	1.275	1.267	0.405	345.000	80.668	1.200	67.224
33	55.400	1350.000	15.000	210.819	1.000	120.527	1.275	1.286	0.393	345.000	78.342	1.200	65.285
32	53.100	1350.000	15.000	210.819	1.000	120.527	1.275	1.286	0.393	345.000	78.342	1.200	65.285
31	50.200	1400.000	15.000	207.020	1.000	117.284	1.275	1.303	0.383	345.000	76.234	1.200	63.529
30	47.400	1400.000	15.000	207.020	1.000	117.284	1.275	1.303	0.383	345.000	76.234	1.200	63.529
29	44.500	1500.000	15.000	200.000	1.000	111.369	1.275	1.337	0.363	345.000	72.390	1.200	60.325
28	41.600	1500.000	18.000	182.574	1.000	139.876	1.275	1.193	0.456	345.000	90.800	1.200	75.666
27	38.800	1500.000	18.000	182.574	1.000	139.876	1.275	1.193	0.456	345.000	90.800	1.200	75.666
26	35.900	1500.000	18.000	182.574	1.000	139.876	1.275	1.193	0.456	345.000	90.800	1.200	75.666
25	33.100	1550.000	18.000	179.605	1.000	136.478	1.275	1.208	0.446	345.000	88.783	1.200	73.986
24	33.075	1550.000	18.000	179.605	1.000	136.478	1.275	1.208	0.446	345.000	88.783	1.200	73.986
23	33.000	1550.000	18.000	122.371	1.000	165.342	1.275	1.098	0.522	345.000	103.880	1.200	86.566
22	32.900	1550.000	18.000	122.371	1.000	165.342	1.275	1.098	0.522	345.000	103.880	1.200	86.566
21	32.895	1550.000	18.000	122.371	1.000	165.342	1.275	1.098	0.522	345.000	103.880	1.200	86.566
20	30.850	1550.000	18.000	122.371	1.000	165.342	1.275	1.098	0.522	345.000	103.880	1.200	86.566
19	28.800	1750.000	20.000	109.256	1.000	172.206	1.275	1.075	0.537	345.000	106.899	1.200	89.083
18	26.700	1750.000	20.000	109.256	1.000	172.206	1.275	1.075	0.537	345.000	106.899	1.200	89.083
17	23.900	1750.000	20.000	109.256	1.000	172.206	1.275	1.075	0.537	345.000	106.899	1.200	89.083
16	21.100	1750.000	20.000	109.256	1.000	172.206	1.275	1.075	0.537	345.000	106.899	1.200	89.083
15	18.300	1750.000	20.000	109.256	1.000	172.206	1.275	1.075	0.537	345.000	106.899	1.200	89.083
14	15.400	1800.000	20.000	107.728	1.000	168.606	1.275	1.087	0.529	345.000	105.339	1.200	87.782
13	12.685	1875.000	20.000	105.552	1.000	163.522	1.275	1.104	0.517	345.000	103.048	1.200	85.873
12	12.655	1875.000	20.000	105.552	1.000	163.522	1.275	1.104	0.517	345.000	103.048	1.200	85.873
11	12.560	1875.000	20.000	63.827	1.000	210.285	1.275	0.973	0.607	345.000	120.867	1.200	100.722
10	12.465	1875.000	23.000	59.519	1.000	250.426	1.275	0.892	0.663	345.000	131.989	1.200	109.991
9	12.435	1875.000	25.000	57.088	1.000	277.936	1.275	0.847	0.694	345.000	138.176	1.200	115.147
8	10.300	1875.000	25.000	57.088	1.000	277.936	1.275	0.847	0.694	345.000	138.176	1.200	115.147
7	7.400	1875.000	30.000	52.114	1.000	349.078	1.275	0.755	0.756	345.000	150.632	1.200	125.527
6	5.800	1875.000	30.000	52.114	1.000	349.078	1.275	0.755	0.756	345.000	150.632	1.200	125.527
5	2.900	1875.000	30.000	52.114	1.000	349.078	1.275	0.755	0.756	345.000	150.632	1.200	125.527
4	0.300	1875.000	30.000	52.114	1.000	349.078	1.275	0.755	0.756	345.000	150.632	1.200	125.527
3	0.270	1875.000	18.000	67.279	1.000	184.336	1.275	1.039	0.561	345.000	111.816	1.200	93.180
2	0.200	1875.000	30.000	0.843	8.428	23129.495	1.275	0.093	1.000	345.000	199.186	1.200	165.988
1	0.000	1875.000	30.000	0.843	8.428	23129.495	1.275	0.093	1.000	345.000	199.186	1.200	165.988

9.8. SRF Buckling Calculation

Cross Section Number	Yielding Strength Design	Total Ref. Stress	SRF Yielding	Meridional Design Buckling Stress	Total Normal Stress	SRF Meridional Buckling	Circumferential Design Buckling Stress	Hoop Stress	SRF Circumferential Buckling	Shear Design Buckling Stress	Total Shear Stress	SRF Shear Buckling	Interaction Parameter			SRF Interaction	Stress Reserve Factor (Ultm.)
-	f_{yd}	σ_{ref}	SRF	$\sigma_{x,Rd}$	σ_z	SRF	$\sigma_{\theta,Rd}$	σ_θ	SRF	$\tau_{x\theta,Rd}$	$\tau_{x\theta}$	SRF	k_x	k_σ	Interact Utility	SRF	SRF_U
(#)	[N/mm2]	[N/mm2]	[-]	[N/mm2]	[N/mm2]	[-]	[N/mm2]	[N/mm2]	[-]	[N/mm2]	[N/mm2]	[-]	[-]	[-]	[-]	[-]	[-]
38	287.500	78.677	3.654	240.018	77.798	3.085	11.985	0.0251	478.084	96.388	6.821	14.132	1.697	1.669	0.160	6.256	3.085
37	287.500	80.362	3.578	240.018	79.492	3.019	11.985	0.0244	491.390	96.388	6.858	14.056	1.697	1.669	0.165	6.043	3.019
36	295.833	81.723	3.620	240.018	80.262	2.990	11.985	0.0241	497.970	96.388	8.918	10.809	1.697	1.669	0.175	5.725	2.990
35	295.833	103.388	2.861	220.867	102.547	2.154	8.287	0.0262	315.730	67.224	7.657	8.780	1.590	1.582	0.327	3.055	2.154
34	295.833	118.462	2.497	220.867	117.653	1.877	8.287	0.0190	436.191	67.224	8.023	8.378	1.590	1.582	0.402	2.488	1.877
33	295.833	124.261	2.381	219.013	123.525	1.773	8.655	0.0135	643.515	65.285	7.832	8.335	1.580	1.577	0.440	2.274	1.773
32	295.833	142.852	2.071	219.013	142.214	1.540	8.655	0.0135	643.515	65.285	7.832	8.335	1.580	1.577	0.541	1.850	1.540
31	295.833	154.982	1.909	217.146	154.468	1.406	9.135	0.0139	654.921	63.529	7.334	8.663	1.570	1.573	0.619	1.615	1.406
30	295.833	178.594	1.656	217.146	178.148	1.219	9.135	0.0140	651.778	63.529	7.334	8.663	1.570	1.573	0.766	1.305	1.219
29	295.833	176.795	1.673	213.388	176.533	1.209	10.434	0.0151	691.412	60.325	5.637	10.701	1.551	1.566	0.770	1.299	1.209
28	295.833	164.909	1.794	224.468	164.650	1.363	11.811	0.0129	913.219	75.666	5.406	13.997	1.610	1.604	0.622	1.608	1.363
27	295.833	184.021	1.608	224.468	183.809	1.221	11.811	0.0532	222.152	75.666	5.406	13.997	1.610	1.604	0.739	1.352	1.221
26	295.833	203.134	1.456	224.468	202.978	1.106	11.811	0.1207	97.889	75.666	5.406	13.997	1.610	1.604	0.865	1.156	1.106
25	287.500	208.186	1.381	222.865	208.279	1.070	12.549	0.2226	56.384	73.986	1.575	46.980	1.601	1.599	0.899	1.112	1.070
24	287.500	208.370	1.380	222.865	208.464	1.069	12.549	0.2237	56.088	73.986	1.575	46.980	1.601	1.599	0.901	1.110	1.069
23	287.500	209.060	1.375	225.401	208.987	1.079	14.897	0.2267	65.713	86.566	5.097	16.982	1.615	1.636	0.895	1.118	1.079
22	287.500	209.620	1.372	225.401	209.547	1.076	14.897	0.2266	65.749	86.566	5.097	16.982	1.615	1.636	0.899	1.113	1.076
21	295.833	209.825	1.410	225.401	209.752	1.075	14.897	0.2265	65.763	86.566	5.097	16.982	1.615	1.636	0.900	1.111	1.075
20	295.833	223.659	1.323	225.401	223.622	1.008	14.897	0.2231	66.779	86.566	4.704	18.403	1.615	1.636	0.996	1.004	1.004
19	295.833	168.573	1.755	225.062	168.563	1.335	16.420	0.2232	73.565	89.083	3.700	24.074	1.613	1.644	0.633	1.580	1.335
18	295.833	178.634	1.656	225.062	178.630	1.260	16.420	0.2232	73.567	89.083	3.700	24.074	1.613	1.644	0.694	1.440	1.260
17	295.833	192.522	1.537	225.062	192.527	1.169	16.420	0.2232	73.567	89.083	3.700	24.074	1.613	1.644	0.783	1.278	1.169
16	295.833	206.406	1.433	225.062	206.418	1.090	16.420	0.2232	73.567	89.083	3.700	24.074	1.613	1.644	0.875	1.143	1.090
15	295.833	220.282	1.343	225.062	220.300	1.022	16.420	0.2232	73.567	89.083	3.700	24.074	1.613	1.644	0.971	1.029	1.022
14	295.833	221.961	1.333	223.520	221.992	1.007	16.190	0.2296	70.523	87.782	3.521	24.932	1.604	1.640	0.994	1.006	1.006
13	287.500	217.246	1.323	221.215	217.357	1.018	15.863	0.2391	66.335	85.873	1.110	77.397	1.592	1.634	0.973	1.028	1.018
12	287.500	217.377	1.323	221.215	217.488	1.017	15.863	0.2391	66.335	85.873	1.110	77.397	1.592	1.634	0.974	1.027	1.017
11	287.500	189.787	1.515	222.854	189.827	1.174	26.234	0.2079	126.158	100.722	2.853	35.305	1.601	1.684	0.776	1.289	1.174
10	287.500	190.201	1.512	231.016	190.248	1.214	32.352	0.2079	155.594	109.991	2.685	40.971	1.646	1.720	0.728	1.373	1.214
9	295.833	175.273	1.688	235.489	175.310	1.343	36.662	0.1913	191.657	115.147	2.627	43.837	1.671	1.741	0.612	1.634	1.343
8	295.833	182.855	1.618	235.489	182.907	1.287	36.662	0.1910	191.935	115.147	2.304	49.976	1.671	1.741	0.657	1.523	1.287
7	295.833	161.569	1.831	244.351	161.604	1.512	48.194	0.1589	303.366	125.527	2.193	57.237	1.722	1.786	0.491	2.035	1.512
6	295.833	166.178	1.780	244.351	166.214	1.470	48.194	0.1589	303.366	125.527	2.193	57.237	1.722	1.786	0.516	1.939	1.470
5	295.833	175.183	1.689	244.351	175.221	1.395	48.194	0.1589	303.366	125.527	2.193	57.237	1.722	1.786	0.565	1.771	1.395
4	287.500	183.290	1.569	244.351	183.364	1.333	48.194	0.1589	303.366	125.527	0.819	153.205	1.722	1.786	0.610	1.639	1.333
3	287.500	177.691	1.618	216.091	177.729	1.216	22.399	0.1589	140.992	93.180	2.193	42.488	1.565	1.658	0.738	1.354	1.216
2	295.833	183.721	1.610	270.723	183.761	1.473	287.500	0.1589	1809.720	165.988	2.193	75.686	1.887	2.000	0.482	2.076	1.473
1	295.833	184.339	1.605	270.723	184.379	1.468	287.500	0.1589	1809.720	165.988	2.193	75.686	1.887	2.000	0.485	2.063	1.468
			1.323			1.007			56.088			8.335				1.004	1.004

9.9. Fatigue Details

Sensor No	Sensor Height	Experimental Fatigue Equivalent Moment	Equivalent Cycles
-	-	$\Delta M_{x'y.eq}$	n_{eq}
[#]	[m]	[kNm]	[#]
1	0	12329	1.00E+07
2	0.2	12281	1.00E+07
3	7.4	10601	1.00E+07
4	12.6	9424	1.00E+07
5	18.3	8181	1.00E+07
6	28.8	6225	1.00E+07
7	33	5536	1.00E+07
8	41.7	4239	1.00E+07
9	50.2	3200	1.00E+07
10	55.4	2886	1.00E+07
11	63	3024	1.00E+07

Cross Section Number	Level	Interpolation Fatigue Equivalent Moment
-	H	$\Delta M_{x'y.eq}$
[#]	[m]	[kNm]
38	63.000	3024.000
37	62.750	3019.461
36	62.630	3017.282
35	59.946	2968.546
34	57.666	2927.146
33	55.386	2886.845
32	53.106	3024.522
31	50.244	3197.343
30	47.384	3544.215
29	44.525	3893.685
28	41.668	4243.771
27	38.812	4669.544
26	35.958	5095.020
25	33.105	5520.347
24	33.075	5524.819
23	33.000	5536.000
22	32.925	5548.304
21	32.895	5553.225
20	30.850	5888.702
19	28.805	6224.180
18	26.760	6605.023
17	23.940	7130.349
16	21.122	7655.302
15	18.307	8179.696
14	15.495	8792.687
13	12.685	9405.464
12	12.655	9412.006
11	12.560	9433.054
10	12.465	9454.557
9	12.435	9461.347
8	10.320	9940.069
7	7.390	10603.333
6	5.890	10956.333
5	2.960	11637.000
4	0.310	12255.333
3	0.270	12264.667
2	0.200	12281.000
1	0.000	12329.000

Endurance Number of Cycles	Detail Category													
N	36σ	40σ	45σ	50σ	56σ	63σ	71σ	80σ	90σ	100σ	112σ	125σ	140σ	160σ
[#]	[MPa]	[MPa]	[MPa]	[MPa]	[MPa]	[MPa]	[MPa]	[MPa]	[MPa]	[MPa]	[MPa]	[MPa]	[MPa]	[MPa]
1.00E+04	136.5809	151.7565	170.7261	189.6957	212.4592	239.0166	269.3679	303.5131	341.4522	379.3914	424.9183	474.2392	531.1479	607.0262
2.00E+06	36	40	45	50	56	63	71	80	90	100	112	125	140	160
5.00E+06	26.532	29.48	33.165	36.85	41.272	46.431	52.327	58.96	66.33	73.7	82.544	92.125	103.18	117.92
1.00E+08	14.566068	16.18452	18.207585	20.23065	22.658328	25.490619	28.727523	32.36904	36.41517	40.4613	45.316656	50.576625	56.64582	64.73808
1.09E+08	14.566068	16.18452	18.207585	20.23065	22.658328	25.490619	28.727523	32.36904	36.41517	40.4613	45.316656	50.576625	56.64582	64.73808

9.10. Fatigue Calculation 1

Cross Section Number	Level	Mean Diameter	Thickness	Section Modulus		Thickness Reduction Factor	Detail Category 71-80-90 In Terms of Cycle								Detail Category		Stress Concentration Factor	Fatigue Equivalent Moment		Bending Stress Range	Design Bending Stress Range	Torsion Stress Range	Design Torsion Stress Range	
							$\Delta\sigma_{fat71}$				$\Delta\sigma_{fat80}$				$\Delta\sigma_{fat90}$											
-	H	Dmi	ti	Wbending	Wtorsion	Cred	5*10^6	1*10^7	10^8		5*10^6	1*10^7	10^8		5*10^6	1*10^7	10^8	2*10^6	2*10^6	SCF	ΔM_y	ΔM_z	$\Delta\sigma_l$	$\Delta\sigma_{Ld}$	$\Delta\tau_t$	$\Delta\tau_{t,d}$	
(#)	[m]	[m]	[m]	[m3]	[m3]	[-]	[Mpa]	[Mpa]	[Mpa]		[Mpa]	[Mpa]	[Mpa]		[Mpa]	[Mpa]	[Mpa]	[Mpa]	[Mpa]	[-]	[kNm]	[kNm]	[Mpa]	[Mpa]	[Mpa]	[Mpa]	
38	63.000	2.300	0.13	5.129E-01	1.026E+00	0.72	52.31	51.07	28.74		58.94	57.55	32.39		66.31	64.74	36.43	71.00	71.00	1.00	3024.00	-1015.00	5.90	7.46	0.49	0.63	32.47
37	62.750	2.300	0.02	8.239E-02	1.648E-01	1.00	52.31	51.07	28.74		58.94	57.55	32.39		66.31	64.74	36.43	71.00	80.00	1.00	3019.46	-1017.00	36.65	46.36	3.09	3.90	36.58
36	62.600	2.300	0.02	8.239E-02	1.648E-01	1.00	52.31	51.07	28.74		58.94	57.55	32.39		66.31	64.74	36.43	71.00	80.00	1.00	3017.28	-1018.00	36.62	46.33	3.09	3.91	36.58
35	59.900	2.600	0.015	7.919E-02	1.584E-01	1.00	52.31	51.07	28.74		58.94	57.55	32.39		66.31	64.74	36.43	71.00	80.00	1.00	2968.55	-1037.00	37.49	47.42	3.27	4.14	36.58
34	57.600	2.600	0.015	7.919E-02	1.584E-01	1.00	52.31	51.07	28.74		58.94	57.55	32.39		66.31	64.74	36.43	71.00	80.00	1.00	2927.15	-1053.00	36.97	46.76	3.32	4.21	36.58
33	55.400	2.700	0.015	8.541E-02	1.708E-01	1.00	52.31	51.07	28.74		58.94	57.55	32.39		66.31	64.74	36.43	71.00	71.00	1.00	2886.85	-1069.00	33.80	42.76	3.13	3.96	32.47
32	53.100	2.700	0.015	8.541E-02	1.708E-01	1.00	52.31	51.07	28.74		58.94	57.55	32.39		66.31	64.74	36.43	71.00	71.00	1.00	3024.52	-1069.00	35.41	44.80	3.13	3.96	32.47
31	50.200	2.800	0.015	9.187E-02	1.837E-01	1.00	52.31	51.07	28.74		58.94	57.55	32.39		66.31	64.74	36.43	71.00	71.00	1.00	3197.34	-1069.00	34.80	44.02	2.91	3.68	32.47
30	47.400	2.800	0.015	9.187E-02	1.837E-01	1.00	52.31	51.07	28.74		58.94	57.55	32.39		66.31	64.74	36.43	71.00	80.00	1.00	3544.22	-1069.00	38.58	48.80	2.91	3.68	36.58
29	44.500	3.000	0.015	1.055E-01	2.110E-01	1.00	52.31	51.07	28.74		58.94	57.55	32.39		66.31	64.74	36.43	71.00	80.00	1.00	3893.69	-1069.00	36.91	46.69	2.53	3.20	36.58
28	41.600	3.000	0.018	1.265E-01	2.530E-01	1.00	52.31	51.07	28.74		58.94	57.55	32.39		66.31	64.74	36.43	71.00	71.00	1.00	4243.77	-1069.00	33.55	42.44	2.11	2.67	32.47
27	38.800	3.000	0.018	1.265E-01	2.530E-01	1.00	52.31	51.07	28.74		58.94	57.55	32.39		66.31	64.74	36.43	71.00	80.00	1.00	4669.54	-1069.00	36.92	46.70	2.11	2.67	36.58
26	35.900	3.000	0.018	1.265E-01	2.530E-01	1.00	52.31	51.07	28.74		58.94	57.55	32.39		66.31	64.74	36.43	71.00	80.00	1.00	5095.02	-1069.00	40.28	50.96	2.11	2.67	36.58
25	33.100	3.100	0.018	1.351E-01	2.702E-01	1.00	52.31	51.07	28.74		58.94	57.55	32.39		66.31	64.74	36.43	80.00	90.00	1.00	5520.35	-1069.00	40.87	51.70	1.98	2.50	41.16
24	33.075	3.100	0.17	1.220E+00	2.440E+00	0.68	52.31	51.07	28.74		58.94	57.55	32.39		66.31	64.74	36.43	71.00	71.00	1.00	5524.82	-1069.00	4.53	5.73	0.22	0.28	32.47
23	33.000	3.100	0.17	1.220E+00	2.440E+00	0.68	52.31	51.07	28.74		58.94	57.55	32.39		66.31	64.74	36.43	71.00	71.00	1.00	5536.00	-1069.00	4.54	5.74	0.22	0.28	32.47
22	32.900	3.100	0.018	1.351E-01	2.702E-01	1.00	52.31	51.07	28.74		58.94	57.55	32.39		66.31	64.74	36.43	80.00	90.00	1.00	5548.30	-1069.00	41.07	51.96	1.98	2.50	41.16
21	32.895	3.100	0.018	1.351E-01	2.702E-01	1.00	52.31	51.07	28.74		58.94	57.55	32.39		66.31	64.74	36.43	80.00	90.00	1.00	5553.23	-1069.00	41.11	52.01	1.98	2.50	41.16
20	30.850	3.100	0.018	1.351E-01	2.702E-01	1.00	52.31	51.07	28.74		58.94	57.55	32.39		66.31	64.74	36.43	80.00	90.00	1.00	5888.70	-1069.00	43.59	55.15	1.98	2.50	41.16
19	28.800	3.500	0.02	1.913E-01	3.827E-01	1.00	52.31	51.07	28.74		58.94	57.55	32.39		66.31	64.74	36.43	71.00	71.00	1.00	6224.18	-1069.00	32.53	41.15	1.40	1.77	32.47
18	26.700	3.500	0.02	1.913E-01	3.827E-01	1.00	52.31	51.07	28.74		58.94	57.55	32.39		66.31	64.74	36.43	71.00	71.00	1.00	6605.02	-1069.00	34.52	43.67	1.40	1.77	32.47
17	23.900	3.500	0.02	1.913E-01	3.827E-01	1.00	52.31	51.07	28.74		58.94	57.55	32.39		66.31	64.74	36.43	71.00	80.00	1.00	7130.35	-1069.00	37.27	47.14	1.40	1.77	36.58
16	21.100	3.500	0.02	1.913E-01	3.827E-01	1.00	52.31	51.07	28.74		58.94	57.55	32.39		66.31	64.74	36.43	71.00	80.00	1.00	7655.30	-1069.00	40.01	50.61	1.40	1.77	36.58
15	18.300	3.500	0.02	1.913E-01	3.827E-01	1.00	52.31	51.07	28.74		58.94	57.55	32.39		66.31	64.74	36.43	80.00	90.00	1.00	8179.70	-1069.00	42.75	54.08	1.40	1.77	41.16
14	15.400	3.600	0.02	2.025E-01	4.049E-01	1.00	52.31	51.07	28.74		58.94	57.55	32.39		66.31	64.74	36.43	80.00	90.00	1.00	8792.69	-1069.00	43.43	54.94	1.32	1.67	41.16
13	12.685	3.750	0.02	2.197E-01	4.395E-01	1.00	52.31	51.07	28.74		58.94	57.55	32.39		66.31	64.74	36.43	80.00	90.00	1.00	9405.46	-1069.00	42.81	54.15	1.22	1.54	41.16
12	12.655	3.750	0.19	2.002E+00	4.005E+00	0.67	52.31	51.07	28.74		58.94	57.55	32.39		66.31	64.74	36.43	71.00	71.00	1.00	9412.01	-1069.00	4.70	5.95	0.13	0.17	32.47
11	12.560	3.750	0.19	2.002E+00	4.005E+00	0.67	52.31	51.07	28.74		58.94	57.55	32.39		66.31	64.74	36.43	71.00	71.00	1.00	9433.05	-1069.00	4.71	5.96	0.13	0.17	32.47
10	12.465	3.750	0.023	2.525E-01	5.050E-01	1.00	52.31	51.07	28.74		58.94	57.55	32.39		66.31	64.74	36.43	71.00	80.00	1.00	9454.56	-1069.00	37.45	47.37	1.06	1.34	36.58
9	12.435	3.750	0.025	2.743E-01	5.486E-01	1.00	52.31	51.07	28.74		58.94	57.55	32.39		66.31	64.74	36.43	71.00	71.00	1.00	9461.35	-1069.00	34.49	43.63	0.97	1.23	32.47
8	10.300	3.750	0.025	2.743E-01	5.486E-01	1.00	52.31	51.07	28.74		58.94	57.55	32.39		66.31	64.74	36.43	71.00	80.00	1.00	9940.07	-1069.00	36.24	45.84	0.97	1.23	36.58
7	7.400	3.750	0.03	3.287E-01	6.575E-01	0.96	52.31	51.07	28.74		58.94	57.55	32.39		66.31	64.74	36.43	71.00	71.00	1.00	10603.33	-1069.00	32.26	40.80	0.81	1.03	32.47
6	5.800	3.750	0.03	3.287E-01	6.575E-01	0.96	52.31	51.07	28.74		58.94	57.55	32.39		66.31	64.74	36.43	71.00	71.00	1.00	10956.33	-1069.00	33.33	42.16	0.81	1.03	32.47
5	2.900	3.750	0.03	3.287E-01	6.575E-01	0.96	52.31	51.07	28.74		58.94	57.55	32.39		66.31	64.74	36.43	71.00	71.00	1.00	11637.00	-1069.00	35.40	44.78	0.81	1.03	32.47
4	0.300	3.750	0.03	3.287E-01	6.575E-01	0.96	52.31	51.07	28.74		58.94	57.55	32.39		66.31	64.74	36.43	71.00	80.00	1.00	12255.33	-1069.00	37.28	47.16	0.81	1.03	36.58
3	0.270	3.750	0.2	2.103E+00	4.206E+00	0.66	52.31	51.07	28.74		58.94	57.55	32.39		66.31	64.74	36.43	71.00	71.00	1.00	12264.67	-1069.00	5.83	7.38	0.13	0.16	32.47
2	0.200	3.750	0.03	3.287E-01	6.575E-01	0.96	52.31	51.07	28.74		58.94	57.55	32.39		66.31	64.74	36.43	71.00	80.00	1.00	12281.00	-1069.00	37.36	47.26	0.81	1.03	36.58
1	0.000	3.750	0.03	3.287E-01	6.575E-01	0.96	52.31	51.07	28.74		58.94	57.55	32.39		66.31	64.74	36.43	71.00	80.00	1.00	12329.00	-1069.00	37.50	47.44	0.81	1.03	36.58

9.11. Fatigue Calculation 2

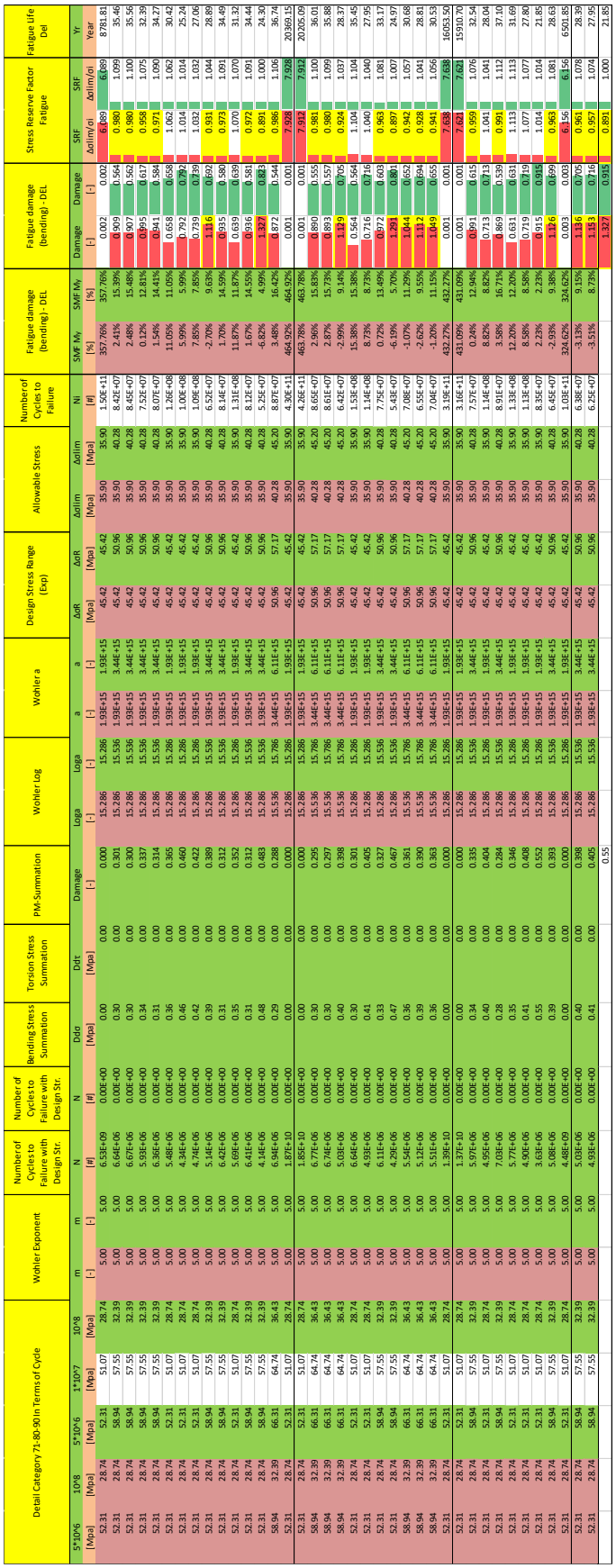

9.12. Flange Failure Modes 1

		Bottom Flange	Bottom Middle	Middle Top	
Minor Sheet Thickness	t_{smin}	30	20	18	[mm]
Major Sheet Thickness	t_{smaj}	30	20	18	[mm]
Sheet Material	-			[-]	
Outer Flange Diameter	D_o	3780	3770	3118	[mm]
Flange Width	W_f	200	190	170	[mm]
Inner Flange Diameter	D_i	3380	3390	2778	[mm]
Thickness-width ratio	Rtw	2.86	2.00	1.70	[-]
Flange Thickness	t_f	70	95	100	[mm]
Bolt Circle Diameter	D_{bc}	3455	3529	2982	[mm]
Quality of bolt		10.9	10.9	10.9	[-]
Bolt Size		M36	M36	M36	mm
Number of Bolts	n		160	144	96 [#]
Hole size	dH		42	39	39 [mm]
Distance Between Bolts	c		68	79	98 [mm]
Flange Level	hf		0.2	12.56	33 [m]
Pre-stress Force	Fv		510	510	510 [kN]
Normal force-Design	Fz,fl		1783	1498	1147 [kN]
Max. bending moment-Design	Mres		57702	45722.33	26818 [kNm]

3565

			Bottom	Bottom Middle 1	Top Middle 1	
Min. Allow. Force Failure Mode		A	1176	588	588	[kN]
Min. Allow. Force Failure Mode		B	1072	425	378	[kN]
Min. Allow. Force Failure Mode		C	-	-	-	[kN]
Min. Allow. Force Failure Mode		D	416	450	671	[kN]
Min. Allow. Force Failure Mode		E	735	1657	1993	[kN]
	$Z_{U,min}$	Minumum Allowable Seg. Force	Min. ZU	416	425	378 [kN]
		Eurocode Restriction 1		ok	ok	ok
		Eurocode Restriction 2		ok	ok	ok
Bolt Force Mode A-B		Segment Force	Z	384.68	338.68	360.46 [kN]
		Minumum Allowable Seg. Force	Zall	416	425	378 [kN]
		Extreme	SRF	1.08	1.25	1.05
Flange Bending Mode C-D-E		Segment Force	Z	384.68	338.68	360.46 [kN]
		Allowable Segment Force - Bolt	Zall	416	450	671 [kN]
		Extreme	SRF	1.08	1.33	1.86

9.13. Flange Failure Modes 2

Bold Size		36	36	36	36 [-]
Bold Quality		10.9	10.9	10.9	10.9 [-]
Ultimate tensile stress	f_{ub}	1000	1000	1000	[N/mm2]
Ultimate tensile force	G_{ub}	817	817	817	[kN]
Characteristic Yield Stress Bolt	f_{yk}	900	900	900	[N/mm2]
Characteristic Yield Strength Bolt	$F_{t,R}$	735	735	735	[kN]
Pre-stress force -char.	F_{vc}	510	510	510	[kN]
Pre-stress/yield force ratio	R_v	69%	69%	69%	%
Pre-stress force - design	F_{vd}	510	510	510	[kN]
Young Modulus - bolt	E	210000	210000	210000	[N/mm2]
Shaft Diameter	d	36	36	36	[mm]
Contact Surface Diameter	d_w	57	57	57	[mm]
Height Triangle on the thread	H	3.46	3.46	3.46	[mm]
Basic Minor Diameter	d_1	31.67	31.67	31.67	[mm]
Middle Diameter	d_2	33.40	33.40	33.40	[mm]
Core Diameter	d_3	31.09	31.09	31.09	[mm]
Stress Area	A_s	816.7	816.7	816.7	[mm2]
Shaft Area	A_N	1018	1018	1018	[mm2]
Bolt Length	l	245	245	205	[mm]
Thread Length	l_{thr}	48	48	48	[mm]
	Ftrd	668.22759	668.2276	668.2276	
Yield Stress - flange - character	$f_{y,k,fl}$	290	290	290	
Yield Stress - flange - design	$f_{y,d,fl}$	264	264	264	
Partial Safety Coef. -yield. -fl.	γ_M	1.1	1.1	1.1	
Arc Length Between Bolts (m)	c_m	74	82	101	
Mean Radious	r_{mi}	1875	1875	1550	[mm]
Number of Bolts	n	160	144	96	[#]
Flange Neck Thickness	t_{neck}	30	20	18	[mm]
Plastic Moment Resistance	$M_{PL,3,L}$	4.37E+06	2.16E+06	2.17E+06	[Nmm]
Segment Force	Z	384.68	338.6839	360.457	[kN]
Plastic Shear Force Resistance	$N_{PL,3}$	582	431	481	
Plastic Moment Resistance	$M_{P,L,3,M/N}$	2.46E+06	8.27E+05	9.52E+05	[Nmm]
Distance (D_{DC}-D_I)	a	37.5	139	102	[mm]
Distance (D_m-D_{DC})	b	147.5	55.25	59	[mm]
Radious from Bolt Center	r_{bc}	1727.5	1819.75	1491	[mm]
Arc Length Between Bolt Cn (m)	c	68	79	98	
Plastic Moment Resistance	$M_{PL,2}$	2.19E+07	4.72E+07	6.43E+07	
Plastic Moment Resistance	$M'_{PL,2}$	8.34E+06	2.40E+07	3.86E+07	
Washer Thickness	t_w	6	6	6	[mm]
Washer Outer Diameter	D_w	66	66	66	[mm]
Washer Inner Diameter	d_w	37	37	37	[mm]
	$\Delta M_{PL,2}$	15877.087	7718.029	7718.029	
Plastic Moment Resistance	$M_{PL,3,T}$	2.38E+07	4.87E+07	6.69E+07	[Nmm]
Segment Force	Z	384.68	338.6839	360.457	[kN]
Plastic Shear Force Resistance	$V_{PL,3}$	785	1183	1544	
Plastic Moment Resistance	$M_{P,L,3,M/V}$	2.24E+07	4.87E+07	6.69E+07	[Nmm]
	b'_E	120.5	29	32.75	